SCHOOL OF CHEMISTRY

CARDIFF UNIVERSITY

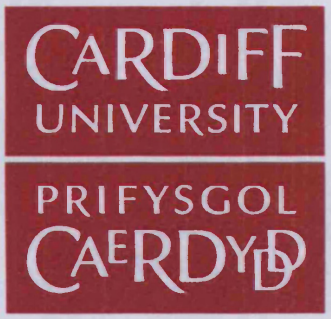

Phthalocyanine Dimers and PIMs Based on Hexaphenylbenzene

Thesis submitted for the degree of Doctor of Philosophy by:

Rhys Bryan Short

Supervisor: Neil B. McKeown

2010

ProQuest LLC
789 East Eisenhower Parkway
P.O. Box 1346
Ann Arbor, MI 48106-1346

Acknowledgments

First of all I would like to thank my supervisor Neil McKeown for the constant help and support throughout the project. Secondly, Lino and Grazia, who have been amazing from day one to submission date. Not just with great ideas and help in the lab with any problems, but great friends outside! Also my lab colleagues and friends Alex 'egg', Jono, Kadhum, Mo, Alaa, Viley, Rupert, Mathew, Julia and Richard.

Thanks to all the friends I have met on the way, especially in the 'reading' room. Namely, Ian, Jess, Andy, Mike, Kev, Laura, Vin the list goes on!).

Thank you to all the staff at Cardiff who have been essential in me getting to this point, Rob, Robin, Benson and Dave for all their spectroscopy expertise. Gaz, Jamie, Alun, Mal and Sham for making sure everything was always available and working.

Lastly but most importantly my parents, who without their love and support throughout my life I would not be where I am today! Thank you for everything!!

Abbreviations

APCI	Atmospheric pressure chemical ionisation
Å	Angstrom
Ar	Unspecified aryl substituent
atm	atmosphere
BET	Brunauer, Emmett, and Teller
br	Broad
calc.	Calculated
CAN	Cerium(IV) Ammonium Nitrate
COF	Covalent-Organic-Frameworks
DMAE	N,N-dimethylaminoethanol
DCM	Dichloromethane
DMF	*N,N*–Dimethylformamide
EI	Electron Impact
Eq	Equivalent
ES	Electrospray
Et	Ethyl
EtOH	Ethanol
g	Grams
GPC	Gel Permeation Chromatography
Hr/s	Hour/s
HATN	Hexachloro-hexaAzaTriNaphthylene
HRMS	High Resolution Mass Spectrometry
Hz	Hertz
IR	Infra Red
IUPAC	International Union of Pure and Applied Chemistry

J	Coupling constant (in Hz)
lit.	Literature
LRMS	Low Resolution Mass Spectrometry
m	Multiplet
MALDI-TOF	Matrix assisted laser desorption/ionisation – time of flight
MALDI-MS	Matrix assisted laser desorption/ionisation – mass spectrometry
MeOH	Methanol
min	Minute(s)
mmol	Millimole(s)
M*n*	Number-average molecular weight
MOF	Metal Organic Framework
m.p.	Melting point
M*w*	Mass-average molecular weight
NMR	Nuclear Magnetic Resonance
OMe	Methoxy
OMIM	Organic Molecules of Intrinsic Microporosity
Pc	Phthalocyanine
Ph	Phenyl
PIM	Polymers of Intrinsic Microporosity
q	quartet
r.t.	room temperature
s	singlet
t	triplet
TGA	Thermo-Gravimetric Analysis
THF	Tetrahydrofuran
TLC	Thin Layer Chromatography
UV	Ultraviolet

Abstract

The first part of the work, described in Chapter One, concentrates on the attempted synthesis of discrete, water-soluble phthalocyanine dimers, which were of interest as model compounds for studies into the photochemical stability of phthalocyanine dyes. The phthalocyanines were linked together by two different bridges derived from diethyl 3,3-bis(4-(3,4-dicyanophenoxy)phenyl)pentanedioate and 1,2-di(4'-(3'',4''-dicyano)phenoxy)-3,4,5,6-tetraphenyl-benzene. The formation of the dimers using 4-(2,6-di-*iso*-propylphenoxy)phthalonitrile was possible, as determined by mass spectrometry and visible absorption spectroscopy of the crude product mixture, but their isolation proved extremely difficult and so this work was abandoned to concentrate on the work described in chapters 3-4.

After an introduction to the research area of organic microporous materials (Chapter 2) and a statement of the new aims and objectives, the second part of the work, described in Chapter 3, concerns the use of hexaphenylbenzene as a structural unit for the synthesis of polymers of intrinsic microporosity, PIMs. Even though hexaphenylbenzene does not have a site of contortion, typical of PIMs, it was thought that the rigidity and non-planarity of this unit due to the lack of rotational freedom of the benzene rings would hinder efficient packing of the polymer in the solid state and induce intrinsic microporosity. A number of different hexaphenylbenzene-based monomers suitable for use in the type of polymerisation reactions used to make PIMs due to their catechol units were synthesised. It was discovered that the position of the catechol substituents in relation to one another had a significant effect on the molecular mass and hence physical properties of the polymer, in particular its ability to form self-standing films. It can be concluded that placing the catechol units on opposite sides of the hexaphenylbenzene unit (para-substitution) suppressed cyclic oligomer formation and allowed the preparation of polymers of high molecular mass with good film-forming properties. In addition, the microporosity of this polymer was greater than that obtained from the monomer in which the catechol units were placed adjacent to one another (ortho-substitution). The

resulting self-standing films allowed the measurement of gas permeation through this polymer, which showed encouraging performance.

The crystal packing properties of the monomers and a [2+2] cyclic oligomer isolated from the polymerisation reaction using the monomer with adjacent catechol units on the hexaphenylbenzene core are described in Chapter 4. The macrocyclic [2+2] cyclic oligomer is highly fluorescent and its binding with nitrobenzene, as a model for small nitrated aromatic compounds, was investigated in the context of its possible use as a sensor. However, studies offered no evidence of selective binding.

Finally, Chapter 5 offers suggestions on the concept of using hexaphenylbenzene units in flow chemistry.

Table of contents

Chapter 1

1.1 Phthalocyanines

Phthalocyanines are 18-π electron aromatic macrocycles, consisting of four isoindole units connected by nitrogen atoms. Their structure is closely related to the naturally occurring porphyrin ring system, the differences being the four benzo-subunits and the nitrogen atoms at each of the meso positions.[1] (**Figure 1.1.1**).

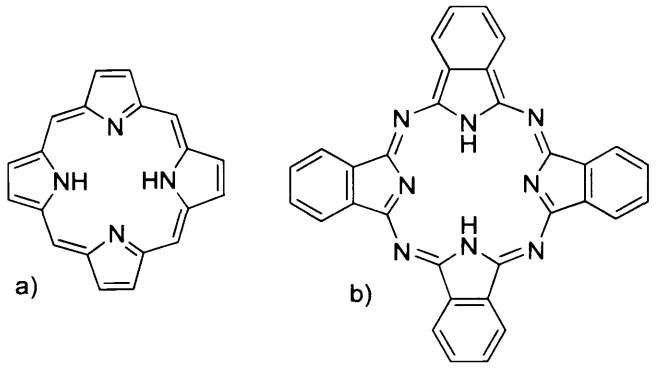

Figure 1.1.1 The structure of a simple porphyrin, porphine (a). The structure of a phthalocyanine (b).

The name phthalocyanine, was given to this class of compound by Reginald P. Linstead. It comes from a combination of the prefix phthal, from the Greek for naphtha (rock oil), and the Greek for cyanine (blue). He was the first academic to investigate the structure of phthalocyanines after their accidental discovery in 1928 at the Grangemouth plant of Scottish Dyes Ltd, during the industrial preparation of phthalimide from phthalic anhydride and ammonia. The glass-lined reaction vessel had cracked exposing the outer steel vessel to the reaction, resulting in the formation of an iron containing blue impurity.[2,3] Imperial Chemical Industries (ICI), which had purchased Scottish Dyes in 1928 were interested in the structure of this substance which showed high stability as an insoluble pigment, and could therefore be sold. The preparation and the properties of the substance were investigated by Linstead and a patent was submitted in 1928.[4] Previously, what appears to be metal free[5] and copper phthalocyanines[6] had been reported in 1907 and 1927, respectively, but it was only after the third accidental discovery that there was sufficient interest to elucidate the structure of these highly coloured by-products. After a series of investigations, in 1934 Linstead published six

papers where the structure of Pc and the synthesis of some of its metal derivatives were described.[7,8,9,10,11,12] The proposed structure was confirmed by means of X-ray diffraction techniques by Robertson in 1936.[13] Pcs, especially the copper derivative, were soon exploited as pigments and dyes,[1] but more recently they have been investigated as molecular materials and their synthesis and study have developed into a fascinating area of research.[14]

1.2 Phthalocyanine synthesis

1.2.1 Metal free phthalocyanines

Metal free Pc can be synthesised starting from different 1,2-disubstituted benzene precursors but are most commonly synthesised from phthalonitrile[1,15] (**Scheme 1.2.1.1**).

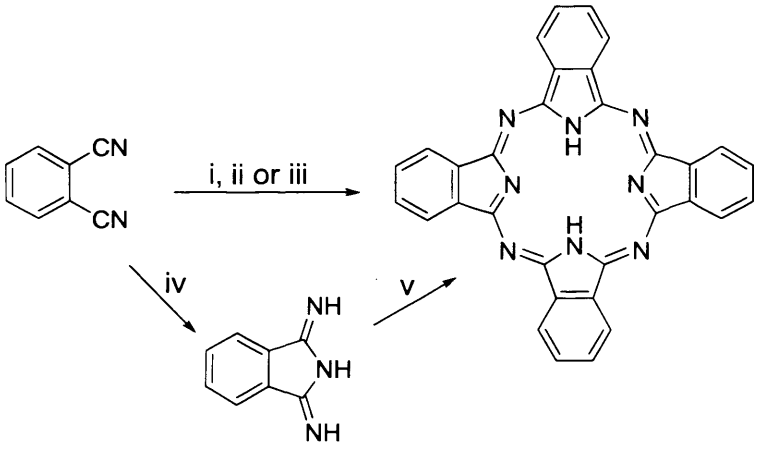

Scheme 1.2.1.1. Synthetic routes to metal free **Pc**. Reagents and conditions: i) lithium, refluxing pentanol, aqueous hydrolysis. ii) Heat with DBU or DBN or NH_3 in refluxing pentanol or heat in DMAE. iii) Fuse with hydroquinone. iv) NH_3, refluxing MeOH, NaOMe. v) Reflux in a high boiling point alcohol.

Phthalonitrile cyclotetramerisation to form Pc can be performed by heating the phthalonitrile in a solvent such as n-pentan-1-ol in the presence of a base,[16] or in a basic solvent such as N,N-dimethylaminoethanol (DMAE).[17] Lithium, sodium, or magnesium alkoxides, generally formed *in situ* by the addition of the metal to a primary alcohol (e.g. n-pentan-1-ol) can be used as a base to form the respective alkali metal Pcs, which can be easily converted into the metal free phthalocyanine by acid work-up.[18] Phthalonitrile cyclotetramerisation can be achieved without solvent at high temperatures (> 180 °C) above which the phthalonitrile melts and in the presence of a reducing agent. Finally, phthalonitrile can be converted by NH_3 in diiminoisoindoline which under relatively mild conditions condenses to form Pc.[1]

1.2.2 Metal-containing phthalocyanine

It is possible to place around seventy different elements in the central cavity of Pc[1,19] which can strongly influence its physical properties. Metal Pcs are generally prepared from the precursor using the metal salt as a template for the cyclotetramerisation (**Scheme1.2.2.1**).

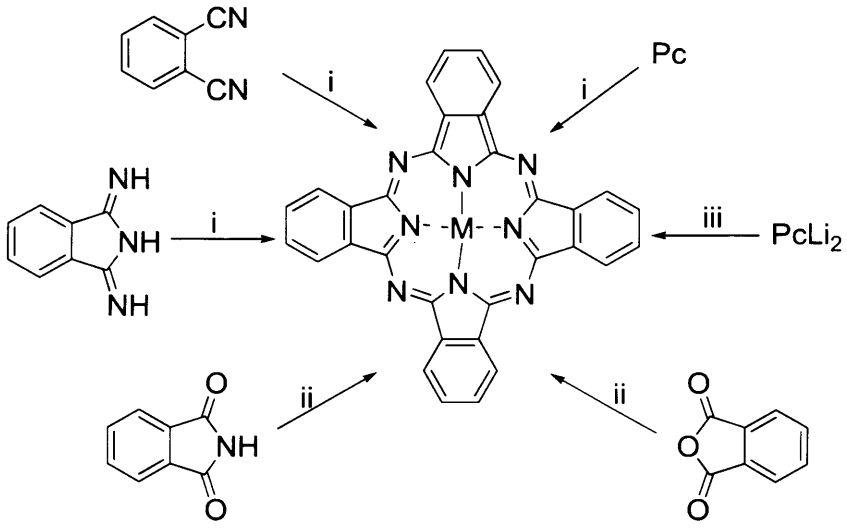

Scheme 1.2.2.1. Synthetic routes to **MPc**. Reagents and conditions: i) Heat with metal salt. ii) Heat with metal salt and urea. iii) Heat in ethanol with metal salt.

When phthalic anhydride [20]or phthalimide[21] are used, in the synthesis, it is necessary to add a source of nitrogen, usually urea. In the majority of cases, the metallation can be achieved also by refluxing Pc or $PcLi_2$ in the presence of the metal salt.[1,10,22] The presence of the metal cation allows the possibility of axial substitution, which could enhance the solubility and reduce the Pcs co-facial aggregation due to the strong π-π interaction. Along with the axial sites being a good place for substitution, there are another 16 possible sites of substitution present in the phthalocyanine ring. In general the substituents are introduced in the phthalonitrile precursors before the cyclotetramerisation reaction. Incorporation of substituents, both in axial and in the ring, not only can increase its solubility, but can also allow the physical properties to be changed.[19]

1.3 Applications of phthalocyanine as materials

Since their discovery phthalocyanines have always been used as green or blue pigments. Since then phthalocyanines have been studied as molecular materials due to their optical and electronic properties,[1] which is due to their electronic delocalization.[19] The symmetry in phthalocyanines and planarity enables them to be used in supramolecular and polymer chemistry.[19] More recently phthalocyanines have been used as photoconductor,[23] and in molecular electronics,[24] cancer therapy,[25] and catalysis applications.[26]

1.4 Phthalocyanine dimers

Phthalocyanine dimers were first described by Leznoff *et al*, in 1984, where the proposed idea was to use dimeric phthalocyanines in the reduction of oxygen to hydrogen peroxide.[27] Binuclear porphyrins had been used for this purpose, however they lose catalytic activity over a period of time. Therefore Leznoff *et al* developed the idea of using binuclear phthalocyanines which are more thermally and photochemically stable. A series of different

binuclear phthalocyanines were synthesised from a mixed condensation of bisphthalonitrile or its isoindoline derivative with a simple phthalonitrile.[23]

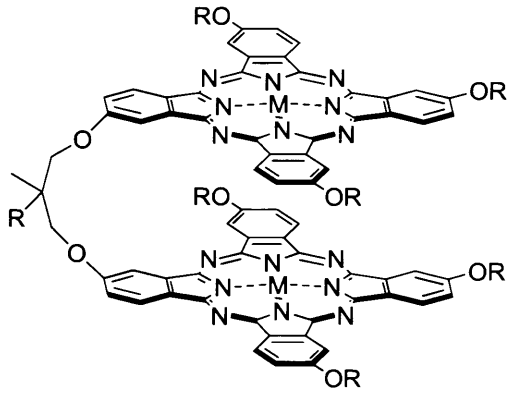

Figure 1.4.1. General structure of binuclear phthalocyanines synthesised by Leznoff.[23]

They found that the binuclear phthalocyanines, or "clamshell" species, can be either in a closed or open conformation with or without Pc-Pc interactions. Most of the phthalocyanines were found to be in the closed form which shows a double π---π^* band in the visible adsorption spectrum near 650 nm (Q band),[23] characteristic of aggregation. The independence from concentration shows that the aggregation is intramolecular as opposed to the intermolecular.

In another paper, Leznoff investigated a series of dimers with naphthalene and anthracene linkages, in an attempt to understand their exchange interactions and capacity to form mixed-valence species[28] (**Figure 1.4.2**).

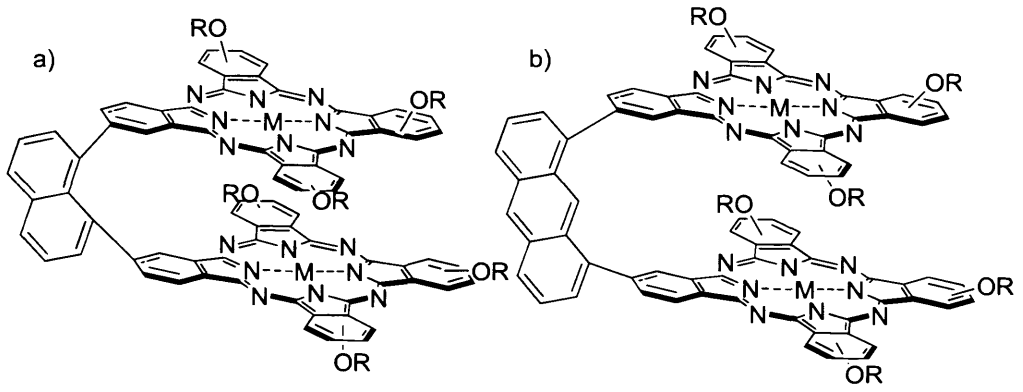

Figure 1.4.2. Napthalene (a) and anthracene (b) linked cofacial binuclear Pcs (only syn conformation shown)

They found a strong interaction between the two halves of the dimer by electronic absorption. Interestingly, when these dimers were adsorbed on a surface they acted as electrocatalysts for the reduction of dioxygen, and were more effective than the corresponding monomeric structures.

Work on the synthesis of alkynyl phthalocyanines using palladium coupling reactions has been reported by Cook *et al.*[29] These molecules can be reacted further to give 'dinuclear' phthalocyanines linked by an alkynyl chain. They exploited the use of the palladium coupled reactions to synthesise a series of complicated phthalocyanine compounds. The first step was aimed to obtain diethynylated and monoethynylated phthalocyanines. Their approach has been to produce unsymmetrical phthalocyanine, where three of the benenzoid rings have the same substituents and the fourth is different. Generally the fourth ring contains either bromine or both bromine and another site for coupling which were, then, subjected to Sonogashira and Stille couplings to give a series of ethynylated Pcs (**Figure 1.4.3**).

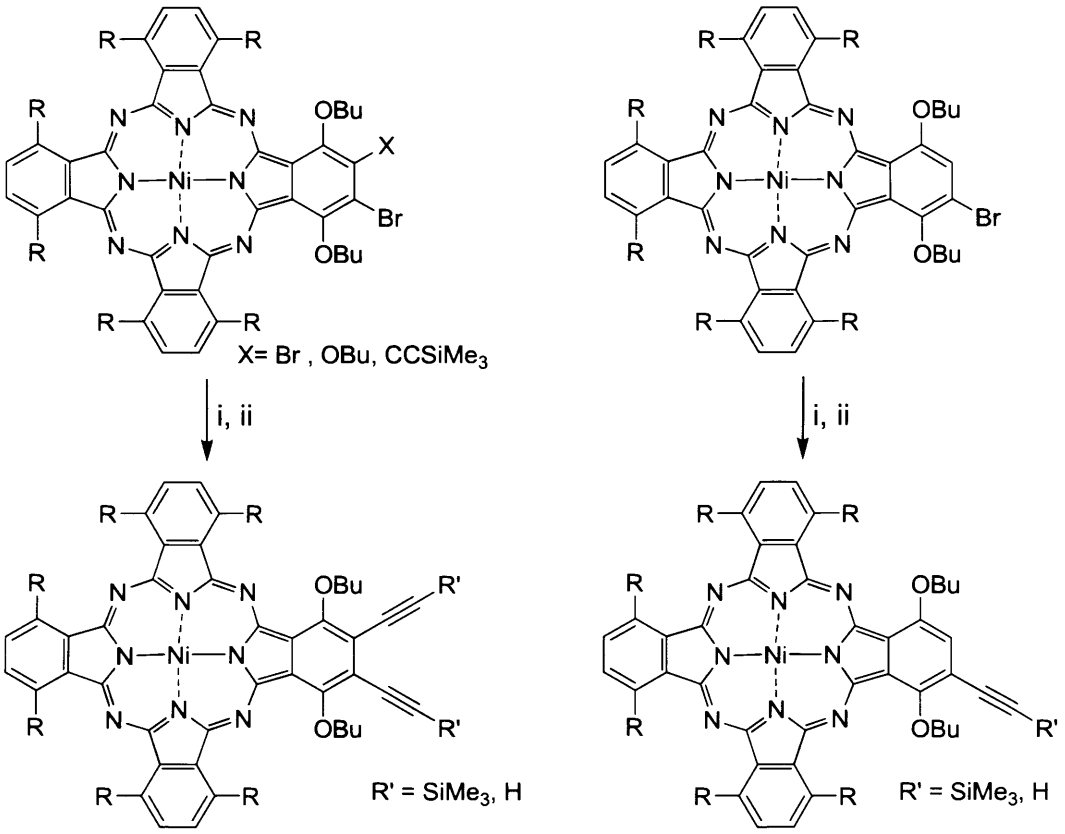

Figure 1.4.3. Synthesis of diethynlated and monoethynlated Pcs. Reagents and conditions; i. HCC-$SiMe_3$. $[Pd(PPh_3)_2Cl_2]$, Ph_3P, CuI. ii. HCC-$SnBu_3$. $[Pd(PPh_3)_4]$.

After the synthesis of these phthalocyanine monomers, they were coupled in the presence of a copper salt in pyridine (or a solvent containing pyridine) to give a series of different Pc dimers (**Figure 1.4.4**).

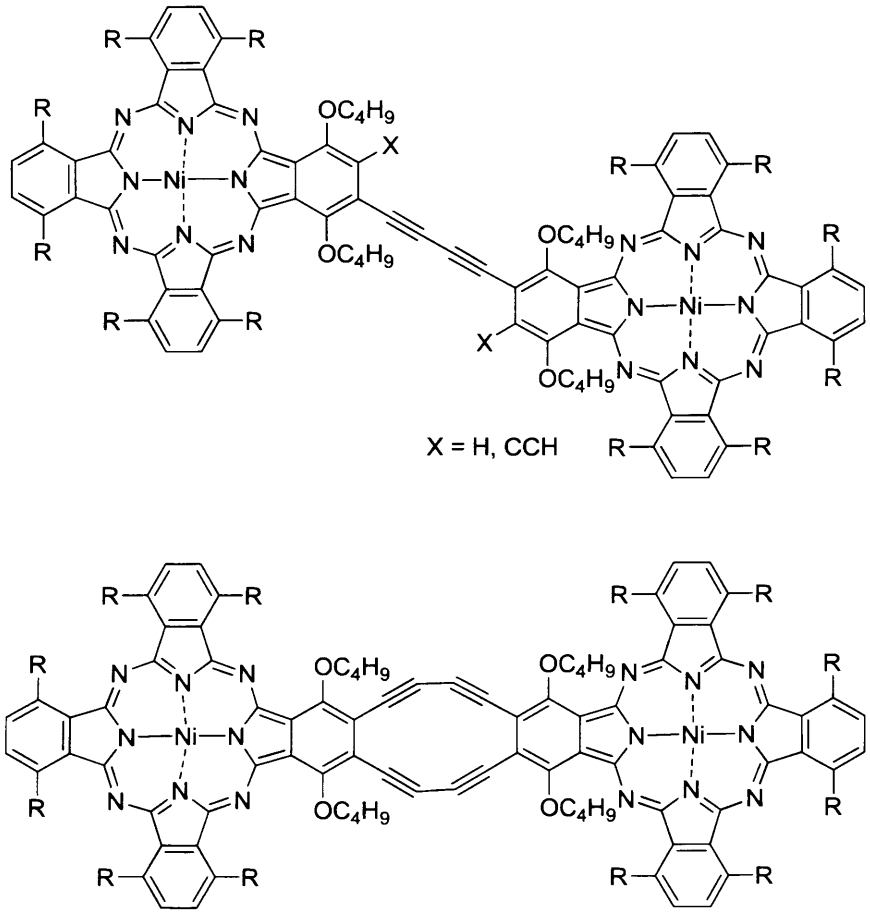

Figure 1.4.4. Synthesised Pc dimers by Cook, all R = decyl.

Both these compounds showed a split in the Q-band at 823 and 691 nm which is an indication of the exciton coupling of the metal centres. Cook also found that when heating these compounds to around 110 °C they enter the liquid crystal phase. However, if these were heated further irreversible oligomerisation occurred most likely due to the alkynyl chains.[25]

1.5 Project aim

As noted in the introductory section, phthalocyanines are one of the major classes of blue colourants. Although generally stable, prolonged exposure to light tends to fade phthalocyanines especially those water-soluble derivatives used as dyes for ink-jet printing. The decomposition of phthalocyanines in light is usually due to the formation of singlet oxygen due to the interaction of atmospheric oxygen to the photochemically excited state of the macrocycle. For phthalocyanine pigments (i.e. insoluble microcrystals) this process is hindered by intermolecular coupling of the excited states of neighbouring molecules, which inhibits the interaction with molecular oxygen. The original aim of this PhD project was to prepare discrete, water-soluble phthalocyanine oligomers as it has long been established that when phthalocyanines are bound together via a flexible linking group they possess an enhanced tendency to aggregate (intramolecular aggregation).[30] It was planned to design and prepare such oligomers to ensure that only *intramolecular* aggregation can occur, even in aqueous media, where cofacial intermolecular interactions between the hydrophobic aromatic macrocycles is prevalent. This was to be achieved by preparing oligomers with very bulky linkers to act as steric blocking groups to prevent intermolecular aggregation (**Figure 1.5.1**).

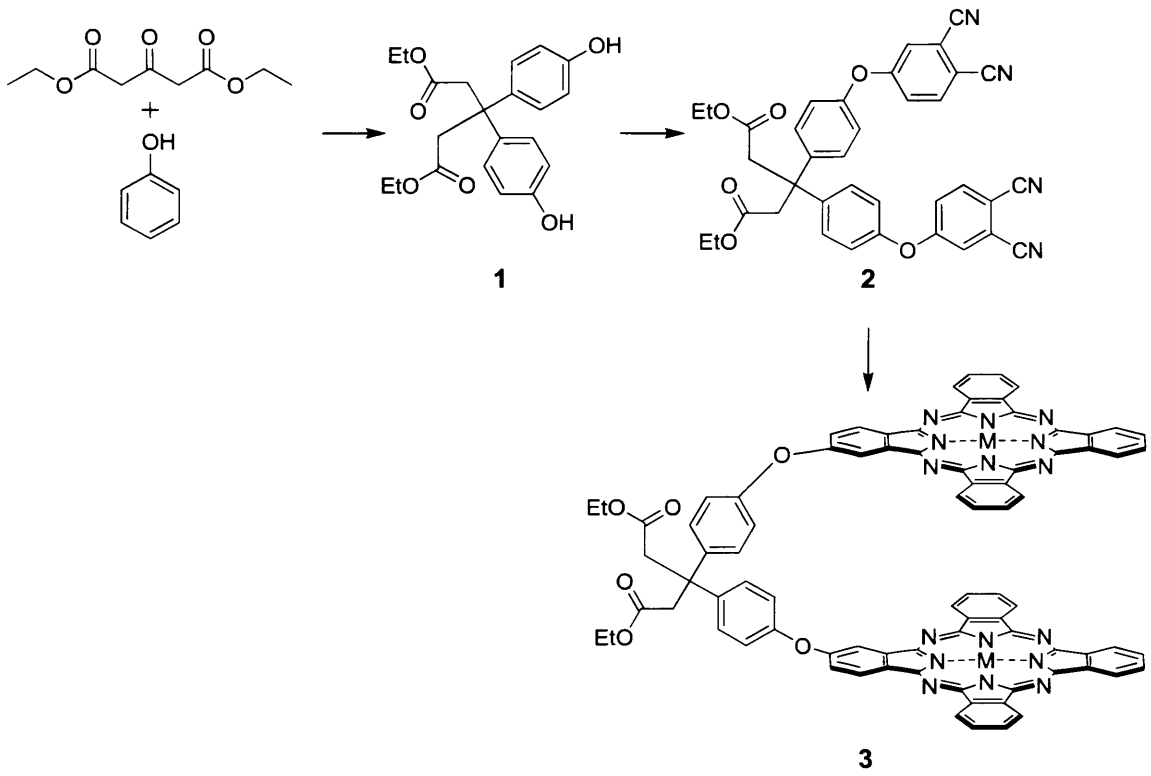

Figure 1.5.1. Initial plan for synthesis of phthalocyanine dimer **3**

Once dimer **3** was produced, the ester groups were to be converted into bulkier groups, using Grignard reactions involving large aromatic moieties, to stop intermolecular aggregation. It was anticipated that a series of such dimers would provide useful model compounds for the study of photochemical decomposition.

1.6 Synthesis of phthalonitrile precursors

The first step to produce the target novel phthalocyanine dimers was to synthesise the precursor phthalonitriles and bisphthalonitriles that contain the reactive linking group for the addition of large groups.

Two different phthalonitriles were prepared, both containing *iso*-propyl groups, which would aid the solubility of the resulting phthalocyanines for purification and characterisation. Ultimately, water-soluble phthalocyanines were required but these initial studies focused on the methodology of dimer formation. The first phthalonitrile of interest was prepared in reasonable yield (63%) by the reaction of 4-nitrophthalonitrile and 2,6-di-*iso*-propylphenol to give 4-(2,6-di-*iso*-propylphenoxy)phthalonitrile **4** as outlined in (**Scheme 1.6.1**).[27]

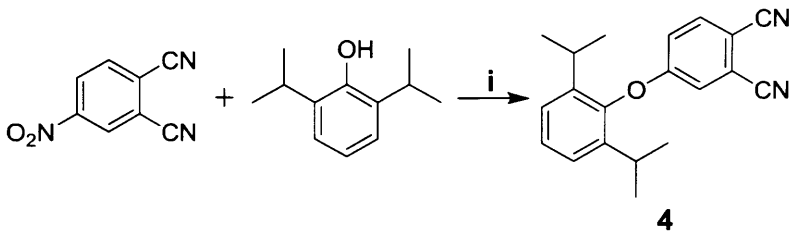

4

Scheme 1.6.1. Synthesis of 4-(2,6-di-*iso*-propylphenoxy)phthalonitrile **4**. Reactions and condition: i. K_2CO_3, DMF 100 °C

The second required phthalonitrile contains two 2,6-di-*iso*-propylphenyl groups. For its preparation, the precursor, 4,5-dichlorophthalonitrile **8**, was synthesised from 4,5-dichlorophthalic acid and then reacted with 2,6-di-*iso*-propylphenol to give 4,5-bis(2,6-di-*iso*-propylphenoxy)phthalonitrile[31] **9**, as outlined is (**Scheme 1.6.2**).

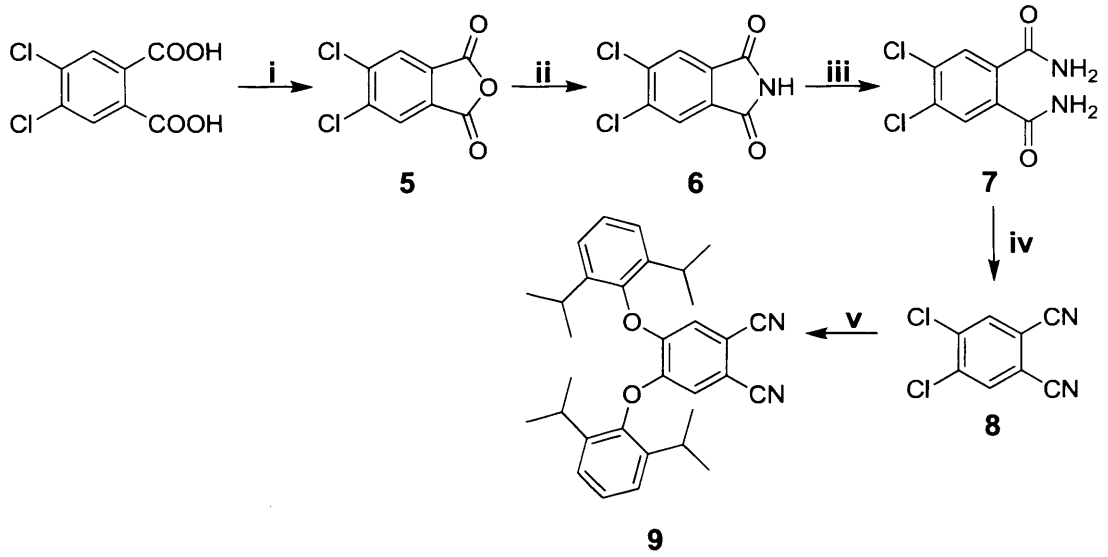

Scheme 1.6.2. Synthesis of bis(2,6-di-*iso*-propylphenoxy)phthalonitrile **9**. Reactions and condition: i. Acetic anhydride, reflux; ii. Formamide, reflux; iii. NH_4OH, 24hrs; iv. $SOCl_2$, 4,5-dichlorobenzene-1,2-diamide, 0 °C, 20 hrs; v. K_2CO_3, DMF 100 °C

After the synthesis of these two precursors, the work focussed on the preparation of the required bisphthalonitriles to provide the bridge for the phthalocyanine dimers. This was most likely due to steric hindrance around the dimer formation.

1.7 Bisphthalonitrile synthesis

The critical precursor for the first desired bisphthalonitrile was formed by a reaction between phenol and diethyl 3-oxopentanedioate, which eventually, proceeded smoothly to give **1** in good yield (62%) (**Scheme 1.7.1**).

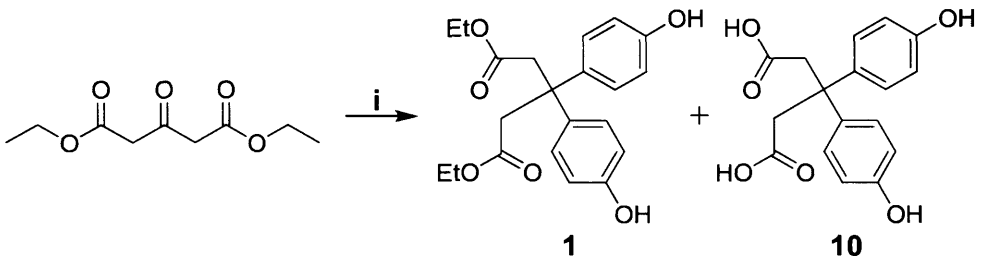

Scheme 1.7.1. Synthesis of diethyl 3,3-bis(4-hydroxyphenyl)pentanedioate. Reactions and condition: i. H_2SO_4, Phenol, 1 hr, RT.

The first attempt to prepare this compound consisted of reacting the two starting materials in 20 ml of H_2SO_4, monitoring the consumption of diethyl 3-oxopentanedioate by TLC. Upon work up, it was noted that the two ester groups had been hydrolysed to carboxylic acid. This unwanted reaction caused a problem in view of the need for the retention of the ester groups for the addition of the Grignard reactions in the later stages of the dimeric phthalocyanine synthesis, so the reaction conditions and duration were modified in order to prevent hydrolysis and these were closely monitored (**Table 1.7.2**).

Vol of H_2SO_4 (ml)	Time / hrs	Yield of **1**	Yield of **10**
20	4	0 %	72 %
20	2	8 %	57 %
20	1	22 %	41 %
10	1	47 %	30%
5	1	62 %	11 %

Table 1.7.2. Experimental conditions for optimisation study for yield of ester product. (1g of diethyl 3-oxopentanedioate was used at room temperature)

From **Table 1.7.2** it can be concluded that 5 ml of H_2SO_4 and a reaction time of 1 hr produced the highest yield of ester product, and gave the lowest amount of conversion to the acid byproduct. After the isolation of the product and its purification by flash chromatography, the

next step was to react it with 4-nitrophthalonitrile (**Scheme 1.7.3**) in order to form the bisphthalonitrile precursor **2**.

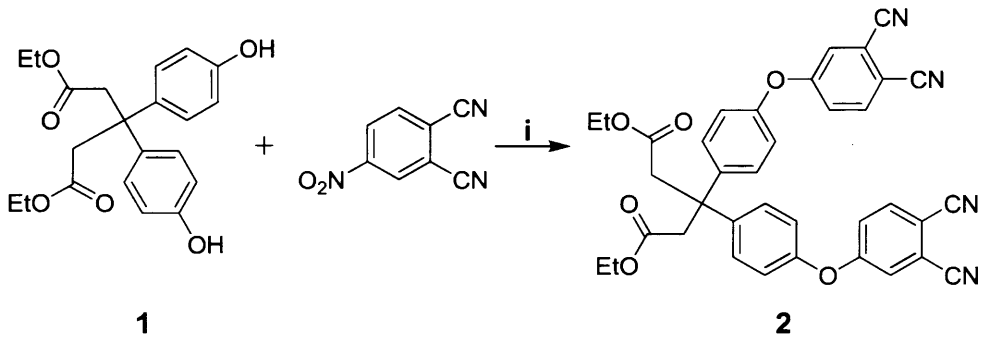

Scheme 1.7.3. Synthesis of bisphthalonitrile **2**. Reagents and conditions: i. K_2CO_3, DMF, 100°C

Following the successful synthesis of the first bisphthalonitrile, it was decided to attempt the synthesis of a further example, this time based on a dihydroxyhexaphenylbenzene molecule previously reported in the literature.[32] It was anticipated that a linking group based on the bulky hexaphenylbenzene unit would provide sufficient steric hinderance to prevent phthalocyanine intermolecular cofacial self-assembly. The first step in this synthesis involved the formation of the tetraphenylcyclopentadione precursor and this was achieved in good yield (83%) by using a double aldol condensation reaction between 1,3-diphenylpropan-2-one and 1,2-bis(4-methoxyphenyl)ethane-1,2-dione with KOH as the base (**Scheme 1.7.4**).

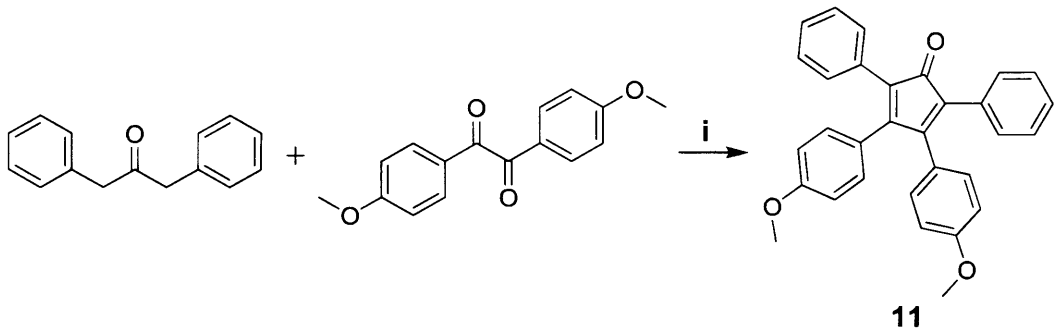

Scheme 1.7.4. Synthesis of **11**. Reagents and conditions: i. EtOH, KOH, 80 °C.

The required dimethoxy-hexaphenylbenzene precursor was prepared from **13** by the Diels-Alder reaction with the commercial diphenylacetylene. This reaction involved the loss of CO as a byproduct to form **12**, which was then demethylated using BBr_3, to achieve the dihydroxyhexaphenylbenzene monomer **13**. This was then reacted with 4-nitrophthalonitrile, to afford the second bisphthalonitrile **14** in good yield (62%) as shown below (**Scheme 1.7.5**).

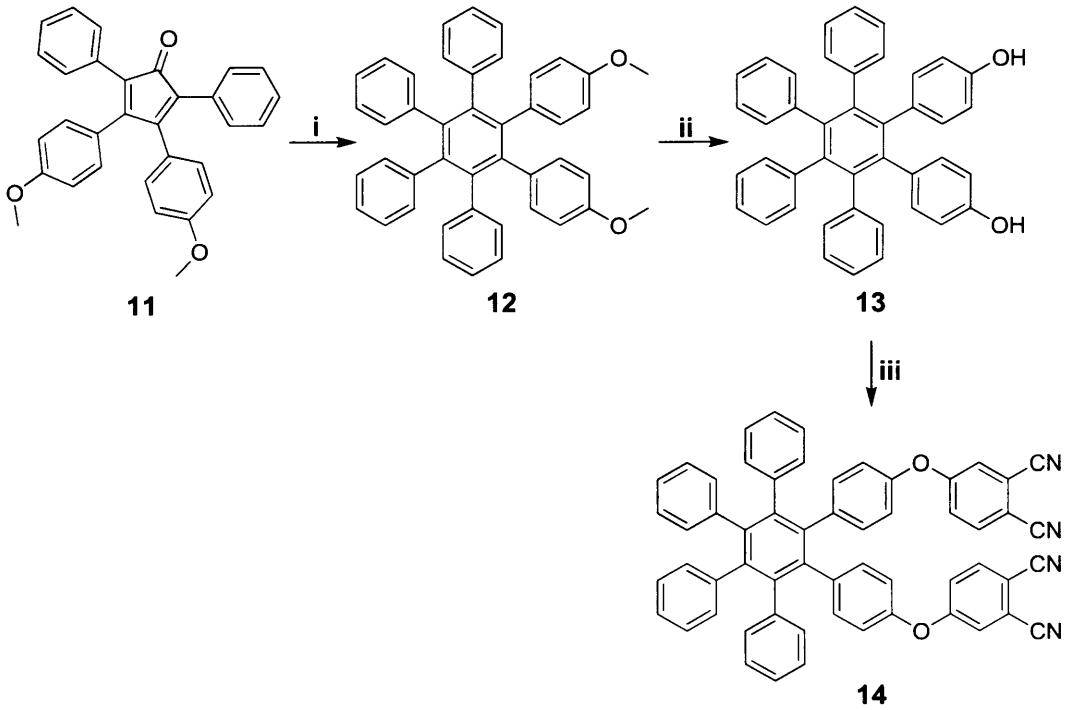

Scheme 1.7.5. Synthesis of bisphthalonitrile **14**. Reagents and conditions: i. Ph_2O, diphenylacetylene, reflux; ii. BBr_3, DCM; iii. K_2CO_3, DMF, 120°C, 4-nitrophthalonitrile.

After the successful synthesis of the two bisphthalonitriles, the next step was to react them with the previously prepared phthalonitriles **4** and **9**, to form the phthalocyanine dimers.

1.8 Synthesis of Dimers

The first series of phthalocyanine dimers was synthesised using a Zn^{2+} cation template. This metal cation differs from that used routinely for the phthalocyanines that are found in blue inks and dyes which contain Cu^{2+}, but the use of this diamagnetic cation allowed the characterization of the products by NMR, which would otherwise be difficult because of the paramagnetism of Cu^{2+}. The first attempted dimer synthesis involved reacting 3,3-bis(4-(3,4-dicyanophenoxy)phenyl)pentanedioate **2** with 4-(2,6-diisopropylphenoxy)phthalonitrile **4** in refluxing 1-methyl-2-pyrrolidine with zinc acetate (**Scheme 1.8.1**).

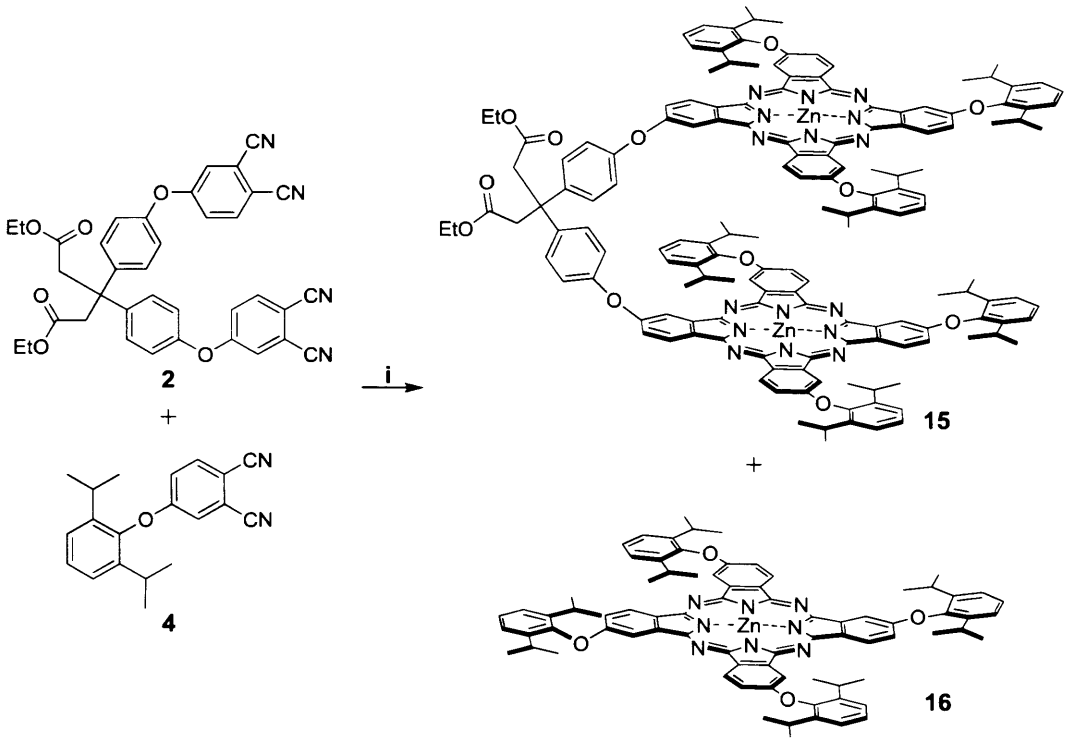

Scheme 1.8.1. Synthesis of dimer 1, **15**. Reagents and conditions: i. **2**, **4**, 1-methyl-2-pyrrolidone, $Zn(OAc)_2$, 165 °C, 15 hrs.

After isolation of the crude product, the work focussed on the difficult and laborious purification of the dimer. As the phthalonitrile **4** is used in great excess, the product mixture

contained a large amount of symmetrical phthalocyanine **16**, which since both it and the desired dimer has similar polarity made purification very difficult. Flash chromatography was the first technique used to separate the dimer from the symmetrical monomer. The separation provided two major fractions, one of which ^{1}H NMR showed to be composed solely of symmetrical Pc **16**, the second fraction, showed evidence of the esters within the bridging unit, although the integration of the peaks indicated that the phthalocyanine dimer had not been isolated purely, but as a mixture that also contained symmetrical Pc **16**. Column chromatography was repeated several times, using solvents of different polarities as eluent but, unfortunately, a mixture was obtain each time as shown by NMR. Analysis of the mixture by MALDI-TOF mass spectrometry showed the presence of the dimer and byproducts (**Figure 1.8.2**).

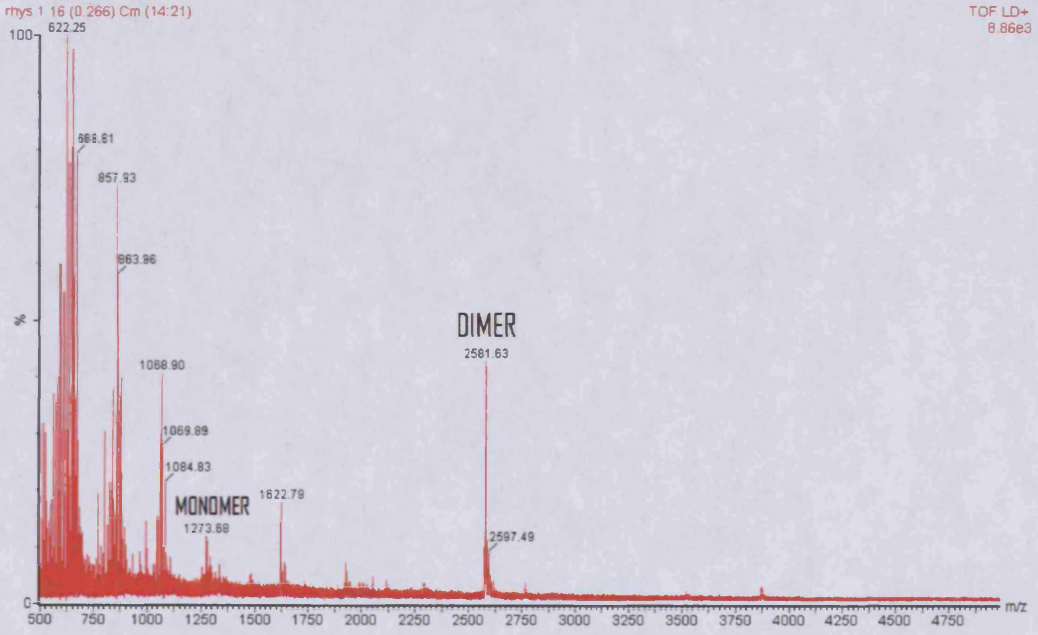

Figure 1.8.2. MALDI spectrum of dimer **15**.

Further confirmation of the presence of the phthalocyanine dimer, **15,** was obtained from UV-

visible adsorption spectroscopy which showed splitting of the Q-band consistent with cofacial aggregation as might be expected for a covalently linked phthalocyanine dimer (**Figure 1.8.3**).[23]

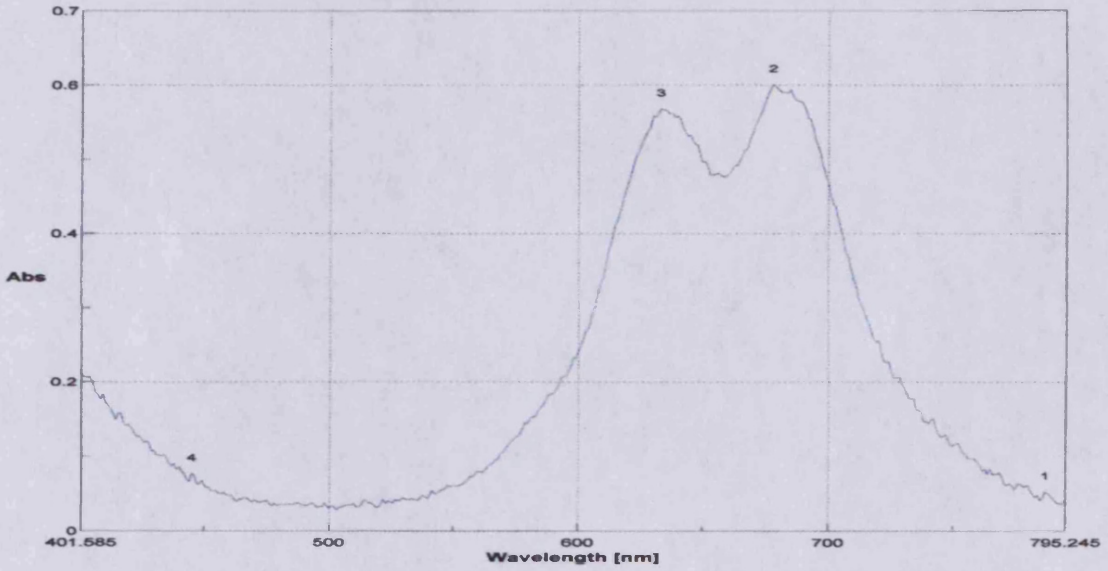

Figure 1.8.3. UV spectrum of dimer **15**.

Due to the difficulties in the purification of the first phthalocyanine dimer, it was decided to switch focus to reactions involving the second bisphthalonitrile in the hope of achieving a better and easier isolation of the resulting dimer. The synthesis is shown below (**Scheme 1.8.4**).

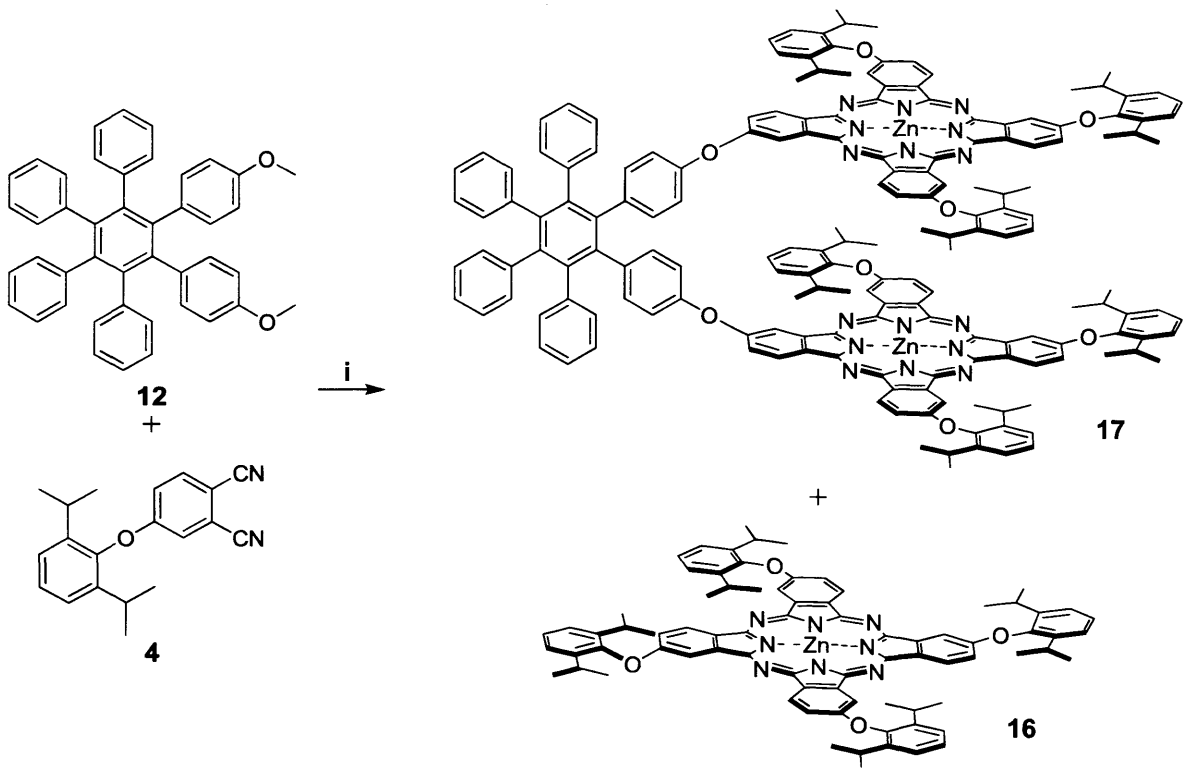

Scheme 1.8.4. Synthesis of dimer, **17**. Reagents and conditions. i., 1-methyl-2-pyrrolidone, $Zn(OAc)_2$, 165 °C, 15 hrs.

The resulting crude product mixture was first subjected to flash chromatography, using eluents of differing polarity, to attempt the separation of the dimer from the symmetrical phthalocyanine **16**, formed in relatively large quantities because of the excess of the phthalonitrile **4** used in the reaction. Unfortunately, as in the attempted preparation of dimer **15**, the separation between the desired dimer and the symmetric phthalocyanine monomer proved very difficult. The MALDI-TOF spectrum of the dimer-containing fraction obtained after exhaustive column chromatography is shown below (**Figure 1.8.5**).

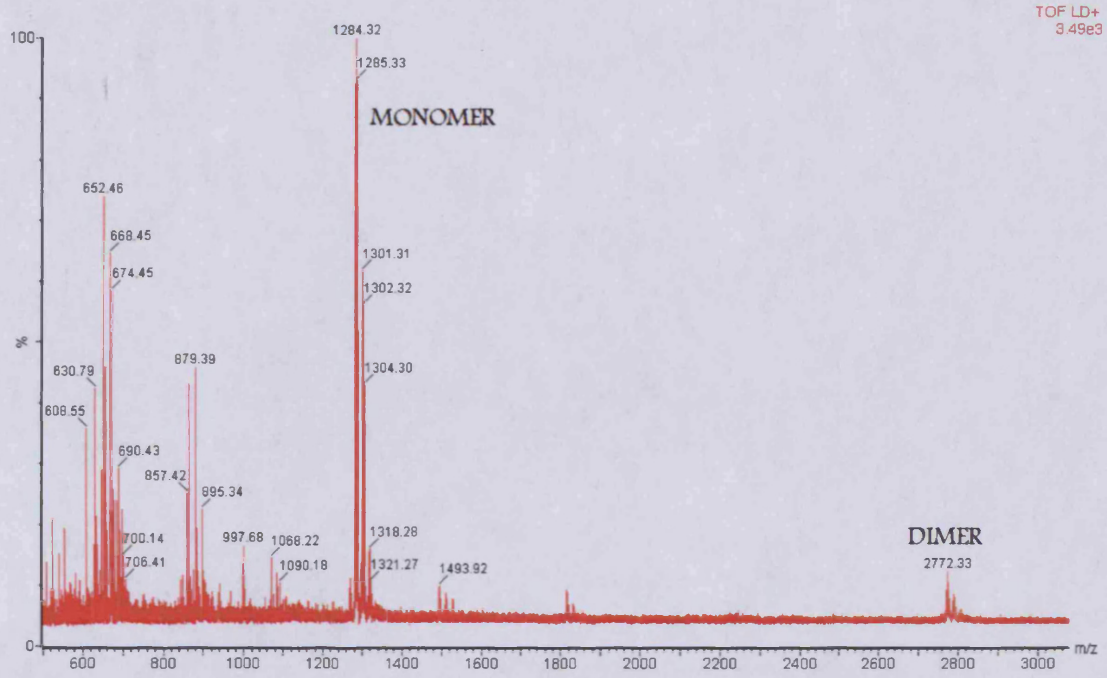

Figure 1.8.5. MALDI of second dimer, **17.**

The failure of these two different attempts at making dimers may be due to the strong tendency of phthalocyanines to aggregate, which makes them very difficult to separate from each other. In view of this, further chromatographic separations were attempted with the addition of pyridine and 4,4'-bipyridine which it was hoped would act as axial ligands, creating steric hindrance that would reduce aggregation and allow a better separation. This tactic was thought particularly promising for 4,4'bipyridine as this bidentate ligand should preferentially bind to the dimer and block the possible π-π stacking binding site of the dimer for the monomeric phthalocyanine (**Figure 1.8.6**). Unfortunately, even the use of these ligands did not have a beneficial effect on the purification of the dimer.

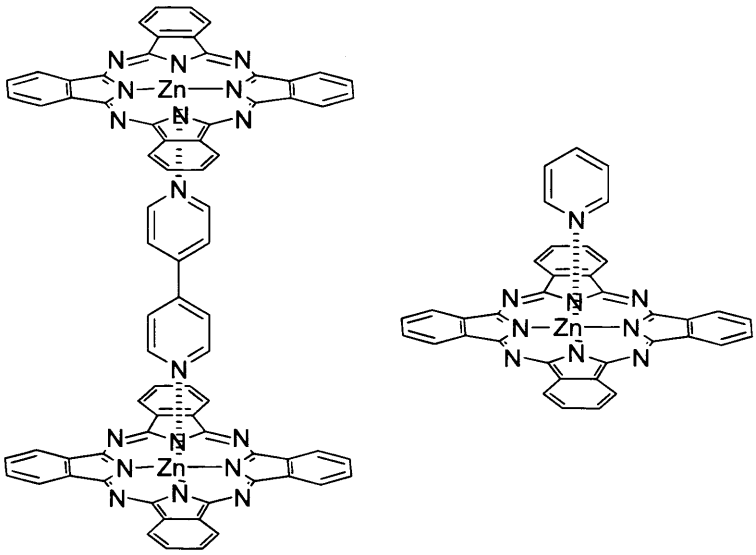

Figure 1.8.6. Diagram of how 4,4'-bipyridine and pyridine could block off the axial sites of the dimer

A further idea to obtain a bridged phthalocyanine dimer was to use unsubstituted phthalonitrile in the reaction with the bisphthalonitriles so that the resulting symmetrical byproduct was the unsubstituted and highly insoluble zinc phthalocyanine, which, it was hoped, could then be removed from the more soluble dimer. (**Scheme 1.8.7**).

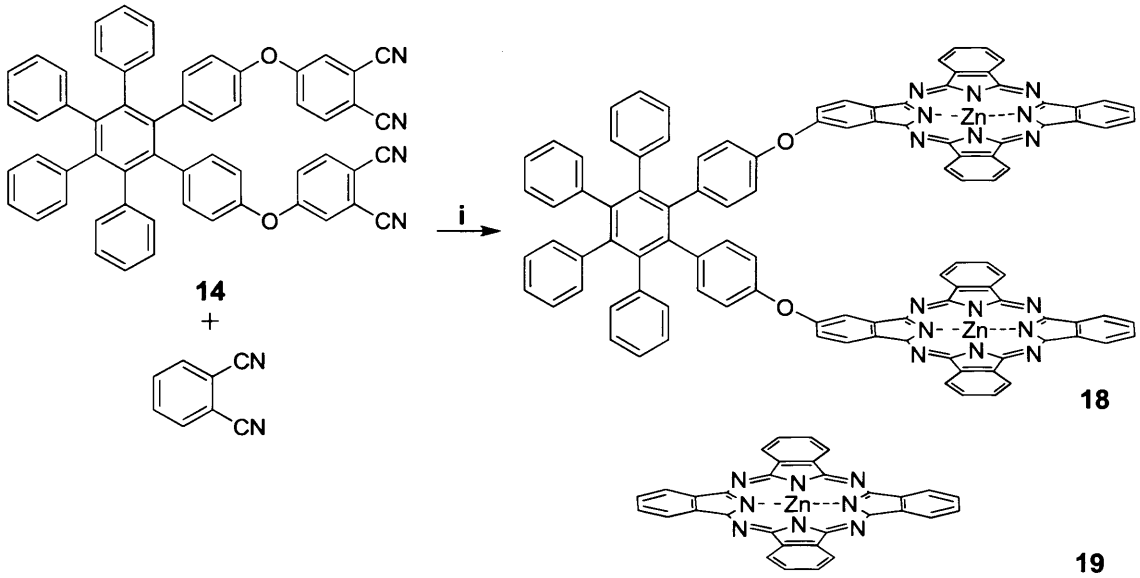

Scheme 1.8.7. Synthesis of Dimer 3, **18.** Reagents and conditions: i. **14**, phthalonitrile, 1-methyl-2-pyrrolidone, Zn acetate, 165 °C, 15 hrs.

Unsubstituted phthalocyanines are notoriously insoluble in most organic solvents, due to their tendency to form stable crystals with strong intermolecular interactions. It was anticipated that the unsymmetrical dimer that contained a bulky linking group would be more soluble and that this difference could be exploited to separate it from the monomer. The apparatus used for this kind of separation is the Soxhlet condenser; this enables hot solvent to be continuously passed through the mixture of compounds, previously placed in a thimble-shaped filter. Unfortunately, both the dimeric and monomeric phthlalocyanine were sufficiently soluble to dissolve in hot THF. MALDI-TOF spectroscopy (**Figure 1.8.8**) confirmed that a mixture of dimeric and monomeric phthalocyanine was obtained and so this method was abandoned.

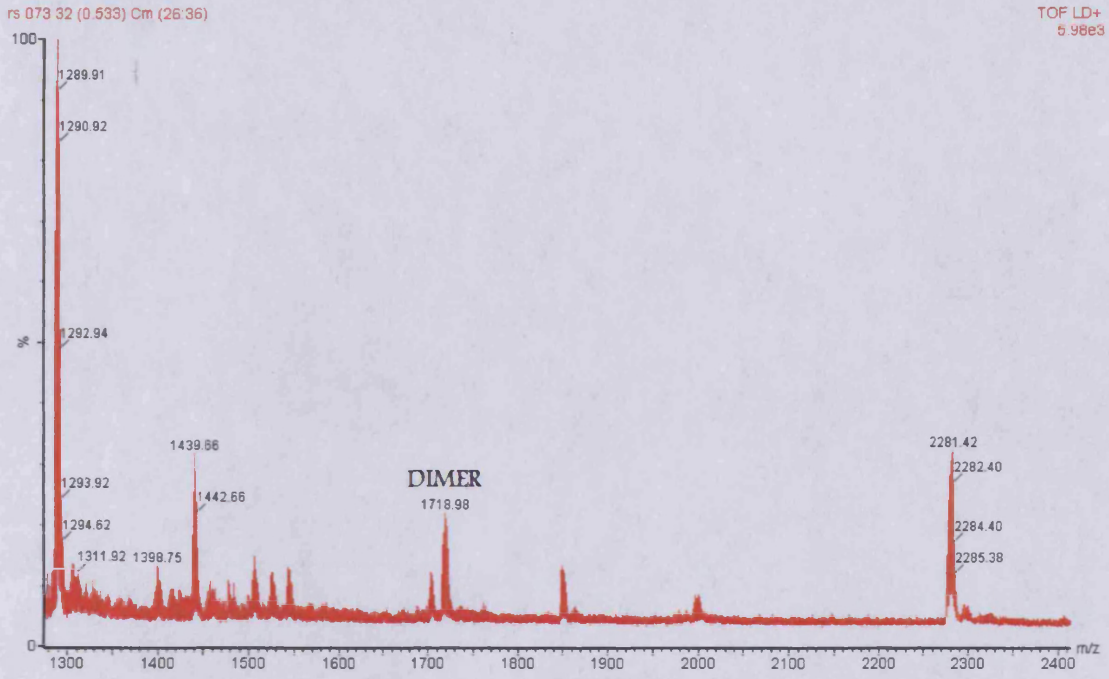

Figure 1.8.8. MALDI spectrum of the mixture of dimer **18** and monomer **19**.

Attempts using bis(2,6-di-*iso*-propylphenoxy)phthalonitrile **9** to make a phthalocyanine dimer was attempted, with both the synthesised bridges **2** and **14.** However only the monomer was present in both cases, this was most likely due to steric hindrance in forming the dimer. The *iso-propyl* groups take up a large area, and fitting them all in a small space on forming the dimers, most probably proved unfavourable.

Due to the challenging nature of this work and the changing priorities of the industrial sponsors of the project (Fuji Photo Film Ltd., Blackley, Manchester), the focus of the PhD programme changed to the study of microporous polymers as described in the following chapters of this thesis.

Chapter 2

Chapter 2 Introduction to Microporous materials

2.1. Microporosity.

A pore, which can be widely defined as a limited space or spatial confinement, is one of the most ancient concepts. The understanding, design, and manipulation of pores have significantly advanced science and technology, and are playing increasingly important roles in new technologies.[33] Of particular interest is the fact that porous materials have higher surface areas than non-porous materials. According to the International Union of Pure and Applied Chemistry (IUPAC), pores can be assigned to one of three classes[34]: channels and pores with diameters less than 2 nm are commonly known as micropores, and these generally represent the largest portion of the material's surface area, whereas, pores with diameters between 2 and 50 nm are known as mesopores and pores with diameters greater than 50 nm are defined as macropores. In the past decades, the study of microporous materials has become of increasing importance in chemistry, leading to the diversification and further improvement of this class of solids for established and new applications. There are, in fact, many areas of current academic and industrial activity where the use of high surface area materials may have significant impact, mainly for energy storage and separations technologies, including nanostructured materials for highly selective adsorption/separation processes,[35,36] for instance H_2O, H_2S, or CO_2 removal from natural gas, high capacity gas storage of H_2 and CH_4[37] for fuel storage applications and high selectivity/high permeability gas separations such as O_2 enrichment[38] and H_2 separation and recovery.

2.2 Measurements of microporosity by gas adsorption.

Gas sorption (both adsorption and desorption) at the clean surface of dry solid powders is the most established method for determining the surface area of microporous materials as well

as the pore size distribution. Due to the weak interactions involved between gas molecules and the surface, adsorption is a reversible phenomenon. Gas physisorption is non-selective, so it starts filling the surface step by step (or layer by layer) depending on the available solid surface and the relative pressure. Filling the first layer enables the measurement of the surface area of the material, because the amount of gas adsorbed when the mono-layer is saturated is proportional to the entire surface area of the sample. In a gas sorption experiment, the material is first heated and degassed by vacuum to remove adsorbed molecules. Then controlled doses of an inert gas, such as nitrogen are introduced and the gas is adsorbed, or alternatively, withdrawn and desorbed. The sample material is placed in a vacuum chamber at a constant and very low temperature, usually at the temperature of liquid nitrogen (77K), and subjected to a range of pressures, to generate adsorption and desorption isotherms. For a conventional volumetric analysis, the gas sorption by the material (adsorbent) is determined by the pressure variations on introduction of a known quantity of gas (adsorbate). Knowing the area occupied by one adsorbate molecule, σ (for example, σ = 16.2 Å^2 for nitrogen), and using an adsorption model, the total surface area of the material can be determined. The most widely used model is the BET (Brunauer, Emmett, and Teller)[39] equation for multilayer adsorption:

$$\frac{P}{n(P-P_0)} = \frac{1}{cn_m} + \frac{c-1}{cn_m}\frac{P}{P_0}$$

In which, P, P_0, c, n, n_m are the adsorption pressure, the saturation vapour pressure, a constant, the amount adsorbed (moles per gram of adsorbent) at the relative pressure P/P_0, and the monolayer capacity (moles of molecules needed to make a monolayer coverage on the surface of one gram of adsorbent), respectively. Through the slope and intercept of a plot of $P/[n(P_0-P)]$ against (P/P_0), n_m can be resolved. The specific surface area, S, can then be derived:

$$S = N_A n_m \sigma$$

In Eq. 2, N_A is Avogadro's number. The specific surface area that can be determined by gas sorption ranges from 0.01 to over 5000 m^2/g. In addition, the determination of pore size and pore size distribution of porous materials can be made from the adsorption/desorption isotherm using an assessment model, based on the shape and structure of the pores. The range of pore sizes that can be measured using gas sorption is from a few Ångstroms up to about half a micron. The complete adsorption/desorption analysis is called an adsorption isotherm. The IUPAC classification of adsorption isotherms[30] is illustrated in **Figure 2.2.1** associated with microporous (type I), nonporous or macroporous (types II, III, and VI) or mesoporous (types IV and V) materials.

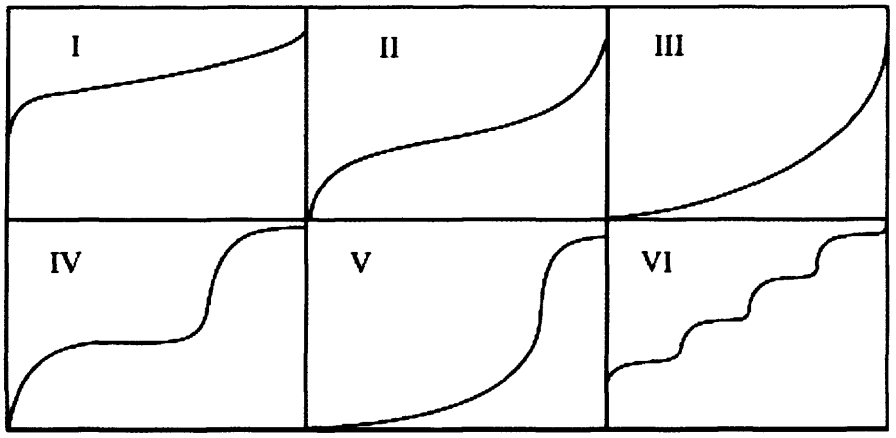

Figure 2.2.1. Type I is microporous. Type II, III, VI is a material wihout pores. Type IV, V is mesoporous. (Axis $x = V_{ads}\ ccg^{-1}$, $y = P/Po$)

The differences between types II and III isotherms and between types IV and V isotherms arise from the relative strengths of the fluid-solid and fluid-fluid attractive interactions: types II and IV are associated with stronger fluid-solid interactions and types III and V are associated with weaker fluid-solid interactions. The hysteresis loops usually exhibited by types IV and V isotherms are associated with capillary condensation in the mesopores. The type VI isotherm represents adsorption on nonporous or macroporous solids where stepwise multilayer adsorption occurs. Adsorption by mesopores is dominated by capillary condensation, whereas filling of micropores (type I) is controlled by stronger interactions between the adsorbate

molecules and pore walls.[30] It is noteworthy that this nomenclature addresses pore width but not pore shape, and pore shape and hysteresis can be important in some circumstances, such as when dealing with shape selective molecular sieve behaviour or, as in some of the materials presented in the thesis, due to welling on adsorption of nitrogen. Studying microporous materials we are, of course, interested in isotherms type I in which at low pressures there can be a great quantity of nitrogen adsorbed for an almost imperceptible increase of P/P_0 ratio.

2.3 Zeolites

A zeolite is a crystalline, hydrated aluminosilicate of alkali and alkaline earth cations having an infinite, open, three-dimensional structure with a surface area per gram of material that can range from 400 to 700 m^2/g. They were discovered in 1755 by a Swedish mineralogist Axel Cronstedt. They have a variety of applications including water softening,[40] detergents,[41] and converting crude oil into gasoline and other fuels.[42,43] Zeolites are able to lose and gain water reversibly and to exchange extra-framework cations, both of these exchanges do not bring about any structural changes to the crystal. Zeolites contain large amounts of water, which form hydration spheres around the exchangeable cations, if this water is removed at high temperatures (350 – 400 °C) small molecules can pass through the entry channels, but larger molecules cannot. This is known as the 'molecular sieve' property of zeolites (**Figure 2.3.1**)

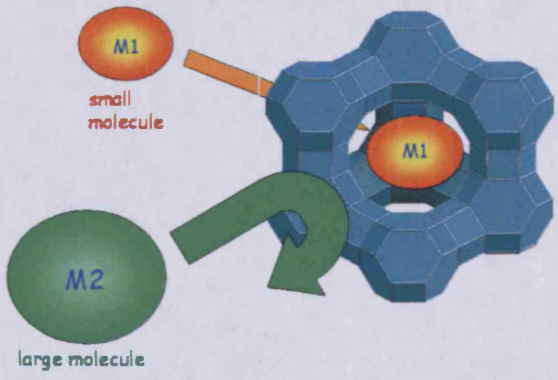

Figure 2.3.1. Showing molecular sieve model of zeolites.

The micropores in zeolites are of a uniform shape and size, this is different to activated carbon, and this allows zeolites to remove all of the gas from a system, such as H_2O in a refrigeration system.[44] Zeolites also absorb small polar molecules, e.g., CO_2, and have applications in the purification of methane.[45]

2.4 Activated Carbon

Activated carbons are highly adsorbent materials with a large number of different applications, these include filtration, purification, deodorization, decolourization and separation, and it is most commonly used to purify water.[46] The adsorbancy is due to their high porosity and surface area, which can be from 400 to 2500 m^2g^{-1}.[47] A variety of raw materials, including wood and coal, are used in activated carbon manufacture, this makes it cheap to manufacture. The large surface area of activated carbon is down to its structure, although not fully understood, it is agreed that it consists of a layered surface, in which flat sheets are broken and curved (**Figure 2.5.1**).

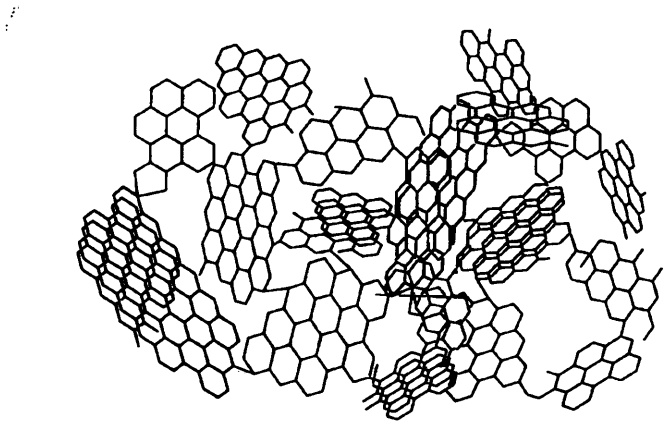

Figure 2.5.1. The amorphous structure of activated carbon.

However during the carbonisation of coals and wood, cross-linking occurs, which leads to extended graphitisation. The resulting network polymer, composed of randomly arranged

graphene sheets, is intrinsically microporous.[48] This gives rise to activated carbon with a number of different sized pores including micro-, meso- and macroporosity. The surface of activated carbon is very random and contains oxygen, nitrogen and polycyclic aromatic units that form graphene sheets.[49] It is this heterogeneous chemical nature of the surface, which allows activated carbons to adsorb a wide range of metal ions and organic compounds, but does not allow their use in a selective process.

2.5 Crystalline microporous materials

Crystals such as zeolites, are very ordered and have a well-defined pore size and shape. In terms of surface area, many of the largest reported are crystalline materials composed of organic components. For example, Metal-Organic-Frameworks, or MOFs, have attracted much attention in recent years due to the possibility of controlling the size and shape of the pores within the coordination framework. MOFs have some of the highest surface areas of all microporous materials with some BET surface areas in excess of 5000 m^2g^{-1},[50] with excellent potential for gas adsorption (e.g. methane adsorption = 240 cm^3/g at 298 K, 36 atm). There is also good potential for MOFs in hydrogen storage at 77 K (e.g., MOF-5 (**figure 2.5.1**); 5.1 wt.% at saturation and 7.5 wt.% for MOF-177 at 80 bar).[51]

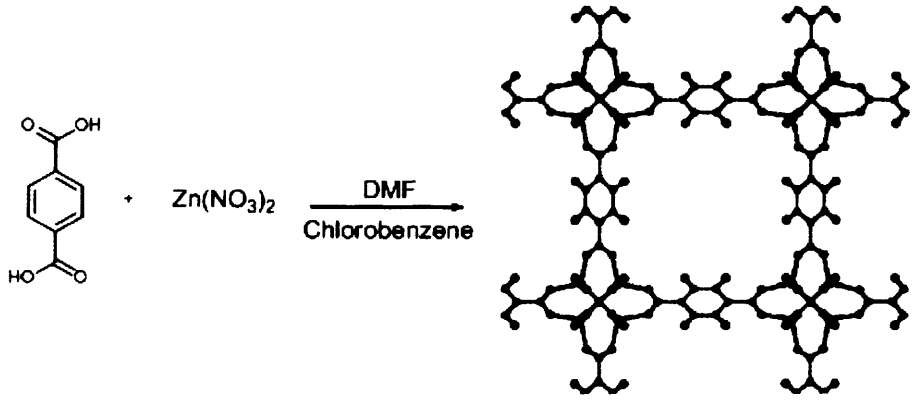

Figure 2.5.1. Synthesis of MOF-5

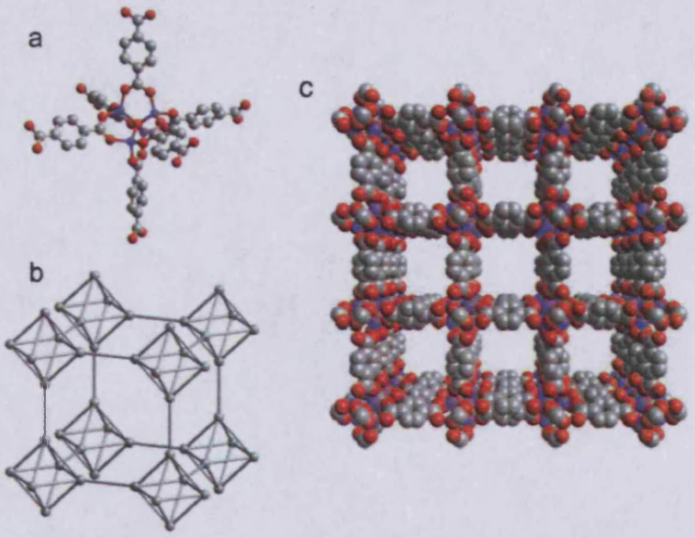

Figure 2.5.2. (a) Building unit present in crystals (MOF-5), where the carboxylate carbon atoms are in an octahedral geometry decorating (b) a primitive cubic lattice, and form (c) the most porous crystals known to date; structures were drawn using single-crystal X-ray diffraction data.[51]

Similarly, COFs (Covalent-Organic-Frameworks) are made up of purely light elements (H, B, C, O and N) which form strong covalent bonds. The thermodynamic nature of the assembly of these crystals favours the most stable configuration. The highest BET surface area of a COF yet reported is 4210 m^2/g (COF-103 as measured by N_2 adsorption at 77 K).[52] This COF had been formed using the condensation of *tetra*(4-(dihydroxy)borylphenyl)silane (**Scheme 2.5.3**)

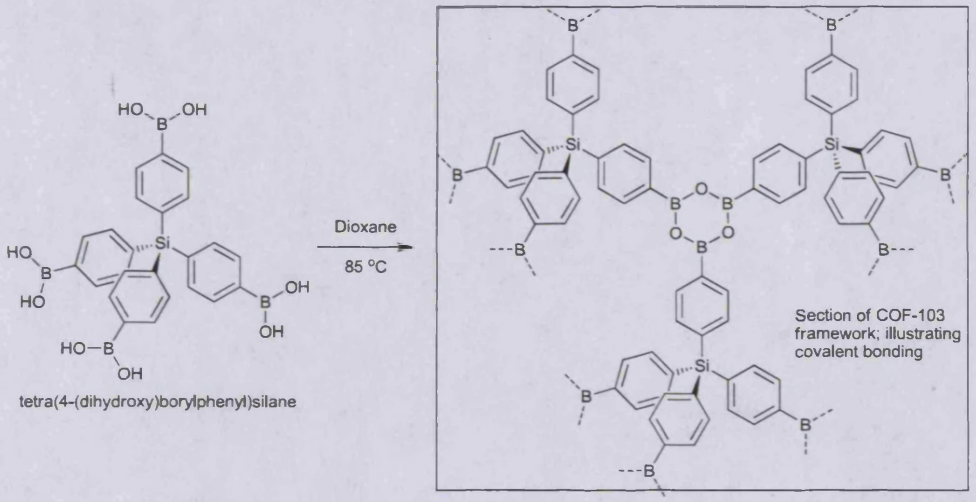

Scheme 2.5.3. COF-103 formation from condensation of tetra(4-(dihydroxy)borylphenyl)silane.

The Yaghi group have been able to prepare a range of different COFs, by using different boronic acids and co-crystals. Using these different starting materials they were able to design the size of the pore and cavity of the resulting COF (**Figure 2.5.4**).

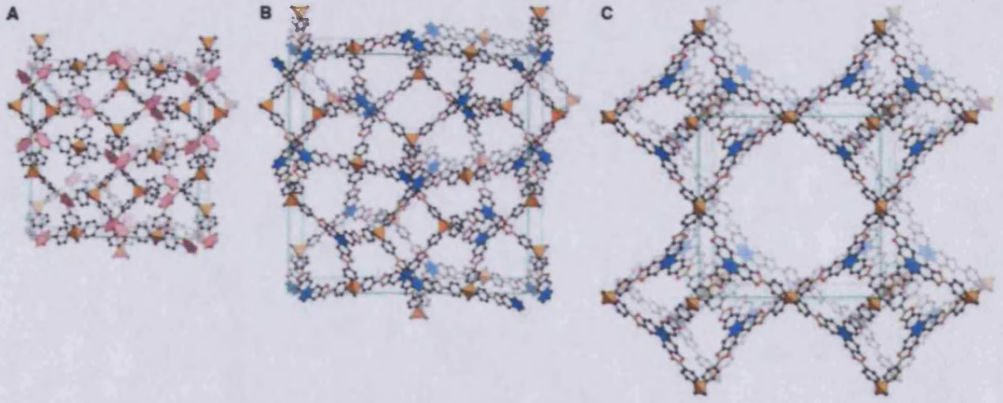

Scheme 2.5.4. Structure of crystalline products of COF-102 (A), COF-105 (B), and COF-108 (C), based on PXRD and modelling. Hydrogen atoms are omitted for clarity.[53]

The pores in COFs range from 8.9 Å to 29.6 Å. Indeed, the pores in COF-108 are so large it is classified as a mesoporous material. COFs are not the only purely organic crystalline structures that have been shown to be microporous. Recently there are examples of non-covalent crystals, which like COFs, keep their structure once any included solvent has been removed.[54] One such crystal, investigated by the McKeown group, is, 3,3',4,4'-tetra(trimethylsilylethynyl)biphenyl has a BET surface area of 278 m^2/g, with a typical type I microporous isotherm.[55]

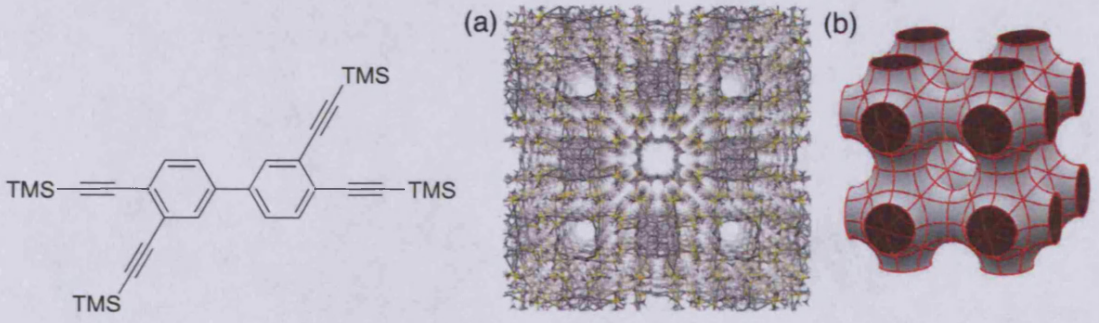

Figure 2.5.5. 3,3',4,4'-tetra(trimethylsilylethynyl)biphenyl (a) its crystal structure and (b) pore structure.

More recently, Cooper et al. have produced molecular cages that form microporous molecular crystals of various structures with BET surface areas up to 650 m^2/g.[56] Also the McKeown group have stabilised a phthalocyanine based clathrate using molecular 'wall-ties' (bidentate ligands which coordinate to two phthalocyanine metal sites) to produce a molecular crystal with permanent microporosity and BET surface areas in the range 850-1000 m^2/g.[57]

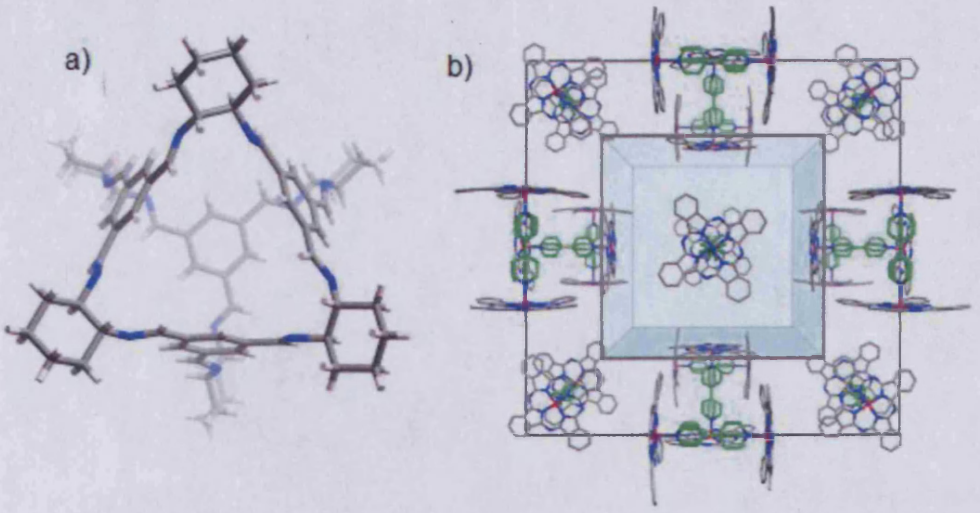

Figure 2.5.6 (a) Cooper's molecular cages[52] and (b) phthalocyanine nanoporous molecular crystals.[53]

2.6 Polymers of Intrinsic Microporosity

Polymers of Intrinsic Microporosity (PIMs) are macromolecules that are designed to pack space inefficiently due to their rigid and contorted structures. Over the past years, the McKeown group has developed the concept of PIMs by the synthesis of a diverse range of examples as described below.[58]

2.6.1 Phthalocyanine Network-PIMs.

The concept of PIMs originated from the idea of using extended aromatic components to mimic the graphene sheets of activated carbons within a rigid polymer network. Initially, the phthalocyanine[59] macrocycle was selected as the aromatic component due to its extended planarity (diameter ~ 1.5 nm) and range of useful properties. Previously prepared phthalocyanine network polymers[1] showed a strong tendency of the macrocycles to aggregate into columnar stacks, due to strong non-covalent interactions (primarily π–π interactions), resulting in nonporous solids.[60] Therefore, it was essential to use a highly rigid and nonlinear linking group between the phthalocyanine subunits that would ensure their space-inefficient

packing, thus preventing structural relaxation and consequent loss of microporosity. Perfectly suited to fulfil these requirements is a linking group derived from the commercially available 5,5',6,6'-tetrahydroxy-3,3,3',3'-tetramethyl-1,1'-spirobisindane (**20**, **Scheme 2.6.1.1**). The spiro-centre (the single tetrahedral carbon atom shared by two rings) of **20** provides the nonlinear shape, and the fused-ring structure the required rigidity. Phthalocyanine network polymers are generally prepared from a bis (phthalonitrile) precursor through a cyclotetramerisation reaction that is usually facilitated by a metal-ion template. Such a reaction using the bis (phthalonitrile) **21**, prepared from the dioxane-forming reaction between monomer **20** and 4,5-dichlorophthalonitrile **8**, gives network polymers as free-flowing, highly coloured powders.

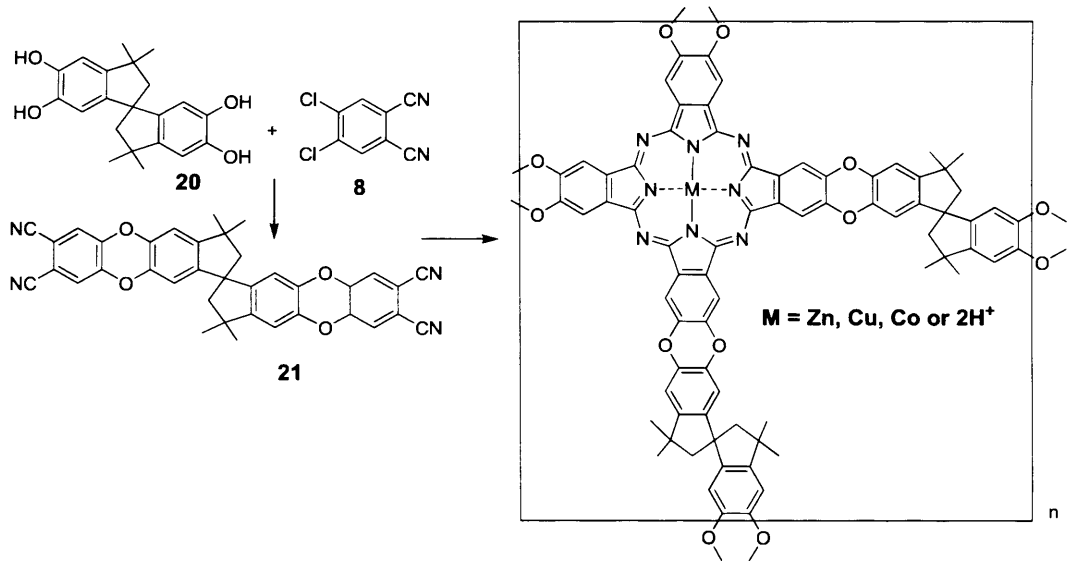

Scheme 2.6.1.1 Phthalocyanine network polymer formation.[56]

Spectroscopic (ESR, UV/visible absorption) and SAXS (Small Angle X-ray Scattering) analyses of the network polymers confirm that the spiro-cyclic crosslinks prevent a close packing of the phthalocyanine components, giving an amorphous microporous structure as depicted by the model shown below (**Figure 2.6.1.2**).

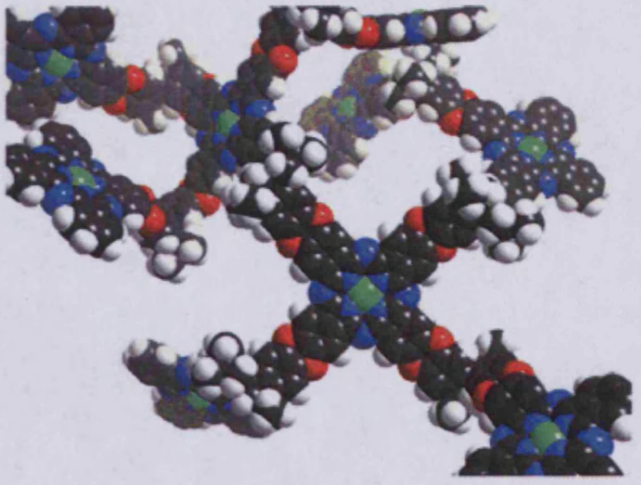

Figure 2.6.1.2. Molecular model of a phthalocyanine network polymer.[56]

Nitrogen adsorption measurements showed that these materials have high surface areas (in the range 500–1000 m^2/g) with very significant adsorption at low relative pressure ($P/P_0 < 0.01$) indicating microporosity.[61]

2.6.2 HATN network-PIM

This network-PIM was formed from the reaction between the spiro-cyclic monomer **20** and hexachlorohexaazatrinaphthylene[62] **21a** (**Scheme 2.6.2.1**). The important precursor, hexachlorohexaazatrinaphthylene **21a**, was readily prepared in good yield from the condensation reaction between hexaketonecyclohexane and 4,5-dichlorophenylene-1,2-diamine.[63]

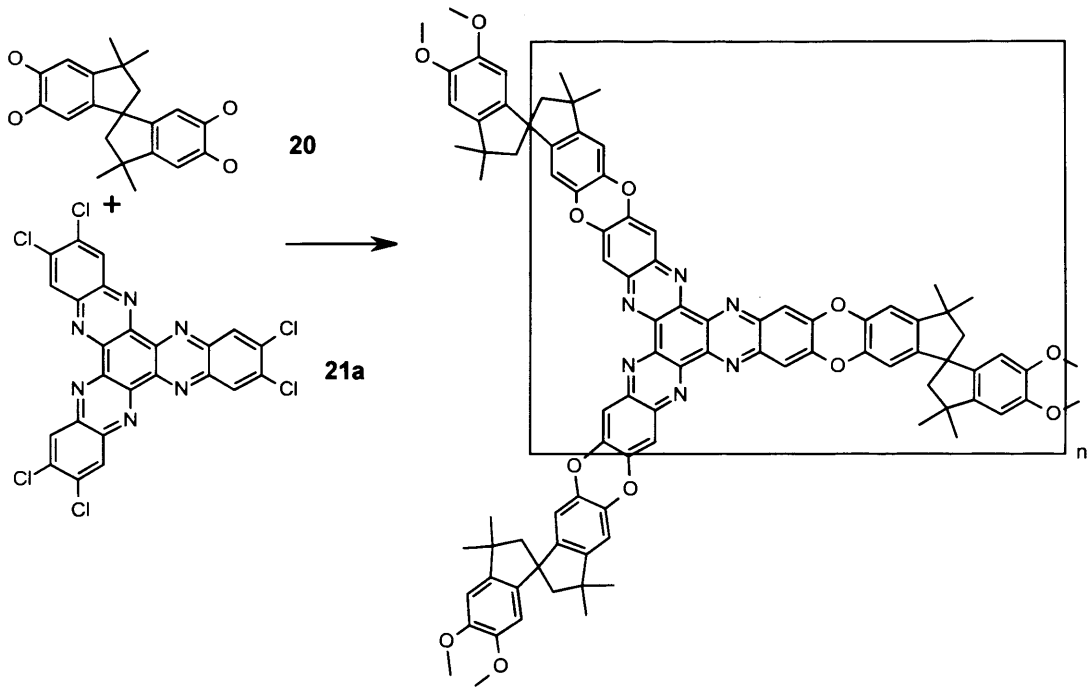

Scheme 2.6.2.1. HATN network polymer.

Nitrogen adsorption measurements give BET values for the surface area of this polymer in the range 750–850 m^2/g. The shape of the adsorption isotherms and their marked hysteresis are similar to those obtained from the phthalocyanine networks and are consistent with a wide distribution of pore size, spanning the microporous range. In addition, the HATN-network-PIM has in-built ligands for metal complexation and the Pd(II) loaded material is proving an excellent heterogeneous catalyst for Suzuki aryl–aryl coupling reactions.[64]

2.6.3 Cyclotricatechylene CTC network-PIM.

For hydrogen storage, PIMs may offer an attractive combination of properties including low intrinsic density (they are composed of only light elements C, H, N, O – a real advantage over MOF materials), chemical homogeneity (an advantage over MOFs), thermal and chemical stability, and synthetic reproducibility. Of particular interest is the potential to tailor the

micropore structure by choice of monomer precursors, for example, by the use of monomers that contain pre-formed cavities to provide sites of an appropriately small size for hydrogen adsorption.[65]

To investigate this possibility, the bowl-shaped receptor monomer, cyclotricatechylene (CTC)[66] **22** was incorporated within a network-PIM by using the usual benzodioxane-forming reaction between CTC and tetrafluoroterephthalonitrile **23**. **(Scheme 2.6.3.1)**

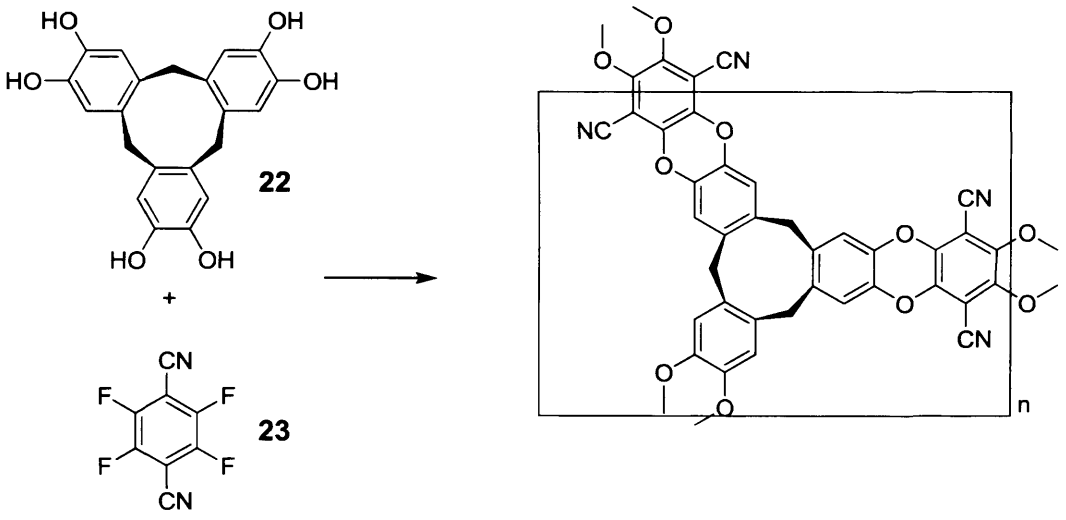

Scheme 2.6.3.1. CTC network polymer formation. [67]

The gas-adsorption properties of the resulting material, designated CTC-network-PIM were compared to those of HATN-network-PIM and the results are listed below (**Table 2.6.3.2**).

PIM	BET Area (m^2/g)	% mass H_2 (1 bar, 77K)	% mass H_2 (10 bar, 77 K)	H_2 per fused ring
HATN	820	1.37	1.56	0.43
CTC	830	1.43	1.70	0.56

Table 2.6.3.2. Gas adsorption data for HATN and CTC PIMs

The BET surface area of each PIM is in the region of 800 m^2/g as measured by nitrogen adsorption at 77 K. Analysis of the low-pressure nitrogen adsorption data by the Horvath–Kawazoe method indicates that in each case the pore size distribution is strongly biased towards pores in the range 0.6 – 0.7 nm. The particularly marked concentration of micropores of 0.6 nm diameter for the CTC-network-PIM appears related to the internal dimensions of the bowl-shaped CTC subunit and suggests that pore size distribution within PIMs can be tuned by the choice of monomer precursor.

2.6.4 Soluble-PIMs.[68]

Conventional microporous materials are held together by robust covalent bonds. However, for PIMs such a framework is not necessary to obtain microporosity as the intrinsic microporsity arises from the inefficient packing of the polymers chains. The relatively weak intermolecular interactions within PIMs can be reversibly disrupted by solvent to allow solution processing to provide a clear advantage over other microporous materials.

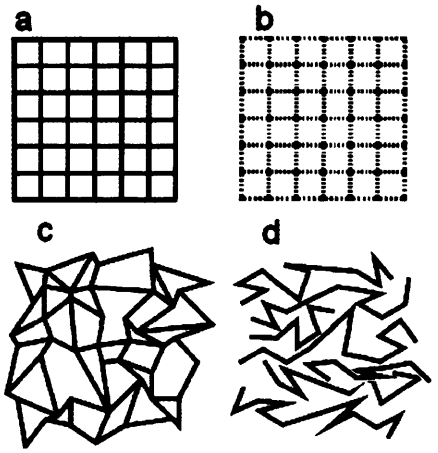

Figure 2.6.4.1. Two dimensional representations of microporous structures. a) Crystalline covalent network (e.g. zeolites or COF); b) nanoporous molecular crystal; c) amorphous polymer network or carbon; d) non-network polymer such as a PIM.

Generally, polymers pack space efficiently because the macromolecules can bend and twist to maximise intermolecular interactions. However, it has long been recognised that some polymers can possess large amounts of void space, which is usually referred to as free volume. In this context, are shown non-network polymers (**Figure 2.6.4.1**) derived from various combinations of bifunctional monomers (**Scheme 2.7.4.2** ; f_{av} = average functionality = 2) that previously proved successful in forming Network-PIMs. The reaction between the aromatic tetrol monomers **20, 24, 25** with the appropriate fluorine-containing compounds **23, 26** and **27** gave soluble PIMs **PIMS-1 – PIMS-6**. The combination of the fact that one of the two precursor monomers contains a "site of contortion" (*e.g.* **20**), with the planarity of the dibenzodioxane ring formed during the polymerization, inducing microporosity in this family of non-network polymers simply because their highly rigid and contorted molecular structures cannot fill space efficiently. In particular, the lack of rotational freedom along the polymer backbone ensures that the macromolecules cannot rearrange their conformation to collapse the open structure of the material, resulting in solids that possess high surface areas (500–780 m^2/g).

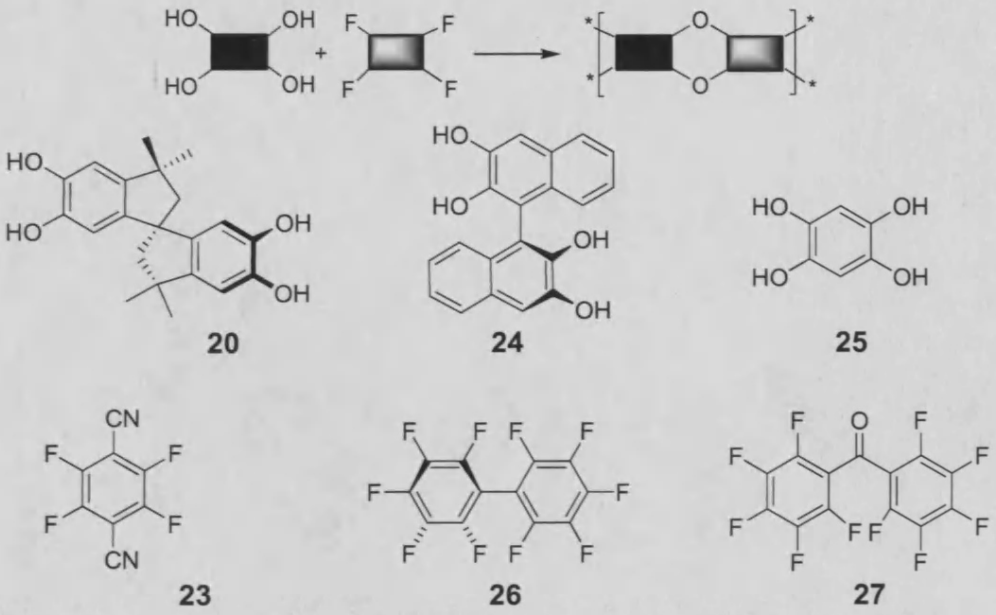

Scheme 2.6.4.2 . Different monomers

In addition, unlike conventional microporous materials, these PIMs are soluble and can be processed readily using solvent-based techniques. The two polymers derived from the reaction of **25** and **23** or **25** and **27** are likely to be linear (dibenzodioxane is planar)[69] and thus able to pack efficiently and these polymers proved to be highly insoluble, non-porous materials (BET surface area < 20 m^2/g). Surface area determination demonstrates that **PIMs 1–6** are microporous with high surface areas. Micropore analysis indicates a significant proportion of micropores with dimensions in the range 0.4–0.8 nm.[70]

2.6.5 PIMs derived from bis (phenazyl)-based monomers.

A large number of bis (catechol) monomers have been used for PIM synthesis but there are no readily available tetra-halide monomers that contain spiro-centres to provide a suitable site of contortion.[63] This was remedied by the simple synthesis of suitably reactive tetrachloride monomers based on phenazine units prepared directly from suitable bis(catechol) monomers such as **20** and 2,3,6,7-tetrahydroxy-9,10-dimethyl-9,10-ethanoanthracene **30**. This is achieved

by oxidation of the bis-catechol with nitric acid,[71] or more efficiently with CAN,[72] to produce the bisquinones **28** and **31** that, on reaction with 1,2-diamino-4,5-dichlorobenzene, provide the monomers **29** and **32** (**Scheme 2.6.5.1**).

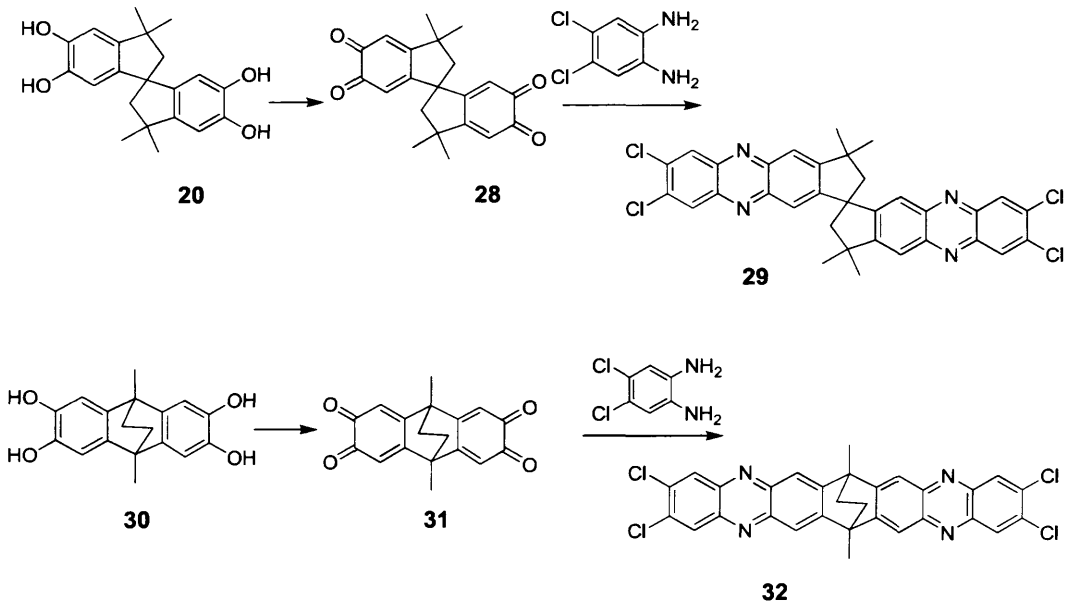

Scheme 2.6.5.1. Preparation of phenazine-baased halogenated monomers.

PIMs-**7**-**10** were prepared by the reactions between monomers **20** and **29**, **30** and **29**, **20** and **32**, and **30** and **32**, respectively (**Scheme 2.6.5.2**). PIMs-**7**-**9** are soluble in a range of organic solvents (especially $CHCl_3$), but PIM-**10** is soluble only in *m*-cresol and concentrated H_2SO_4.

GPC confirmed that the polymers possess reasonably high average molecular mass. For example, purified PIM-7 prepared under optimized reaction conditions has apparent average molecular masses of *M*n = 26000 and *M*w = 51000 g/mol, relative to polystyrene standards. Nitrogen adsorption isotherms measured at 77 K confirms that PIMs-**7**-**10** are microporous with BET analysis of the isotherms suggesting an apparent surface area for each polymer of more than 650 m^2/g.

2.6.6 Triptycene based PIMs.

The most microporous amorphous network reported to date prepared using the concept of intrinsic microporosity is that derived from 9,10-dimethyl-2,3,6,7,12,13-hexahydroxytriptycene, trip(Me)-PIM (**Scheme 2.6.6.1** apparent BET surface area = 1730 m^2/g).[73] Consideration of a molecular model of an ideal fragment of Trip(Et)-PIM reveals a possible explanation for the enhanced porosity. The triptycene component clearly provides the necessary nonlinearity required for microporosity, a role performed by the spirocentre in PIM-1 (**Scheme 2.6.4.2**) and the HATN-PIM (**Scheme 2.6.2.1**), or the bowl-shaped subunit in the CTC-network (**Scheme 2.6.3.1**). The shape of the triptycene monomer also constrains the growth of the polymer within the same plane to provide a rigid macromolecular structure with large concavities. The faces of the ribbonlike "struts" between the triptycenes are oriented perpendicular to the plane of the macromolecular growth. This arrangement blocks face-to-face association between these planar struts, leading to greater IM.

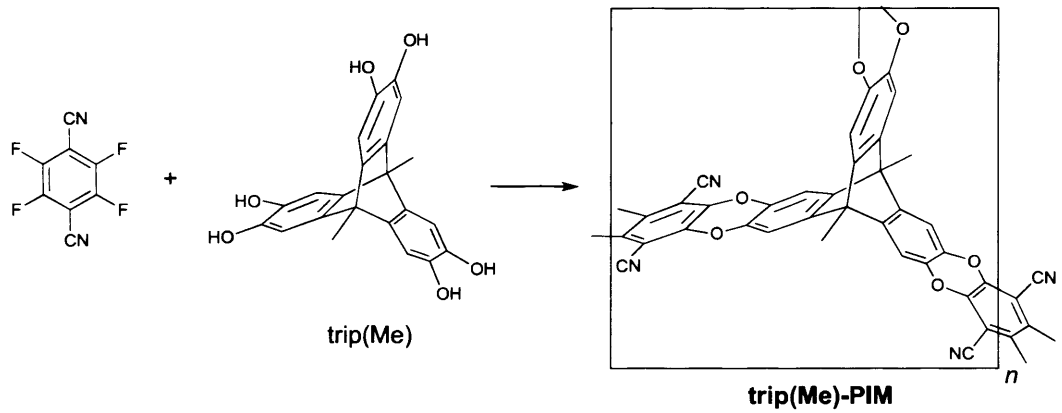

Scheme 2.6.6.1 Synthesis of trip(Me)-PIM

A series of triptycene based PIMs with different length side groups attached to the bridgehead positions was synthesised and reported, and showed successive decrease in surface area with increased alkyl chain length (**Table 2.6.6.2**).

				H_2 uptake, 77 K, mmol/g (%mass)	
Side chain	BET area; (m^2/g)	N_2 uptake; (mmol/g)	Density (mL/g)	1 bar	10 bar
Me	1760	42.2	1.67	8.90 (1.79)	15.6 (3.2)
Et	1416	39.5	1.40	8.33 (1.68)	13.7 (2.8)
Pr	1343	32.1	1.40	7.69 (1.55)	12.2 (2.5)
Bu	978	23.8	1.48	6.55 (1.32)	10.3 (2.1)
Pe	947	17.9	1.48	5.61 (1.13)	8.8 (1.8)
Oct	618	11.6	1.27	3.67 (0.74)	6.0 (1.2)

Table 2.6.6.2. Gas Adsorption Data for the Trip(R)-PIM series.

The adsorption isotherm displays remarkably distinct hysteresis extending to low partial pressures between the adsorption and desorption cycles. This indicates that there is activated adsorption arising either from a swelling of the polymer matrix or from the restricted access of nitrogen molecules to pores due to blocking at narrow openings. Analysis of the low-pressure nitrogen adsorption data by the Horvath–Kawazoe method[70] indicates that the pore size distribution within Trip-PIM is strongly biased towards sub-nanometre pores.[73] A requirement for the adsorption of gaseous probes, particularly those with low enthalpy of adsorption such as hydrogen, is multi-wall interactions. Smaller pore widths achieve this feat most effectively, as demonstrated by the ability of trip(Me)-PIMs to adsorb high amounts of hydrogen (up to 3.2 % mass, 77 K,

Table 2.6.6.2) at a relatively low pressure.

2.7 Highly permeable polymers for membrane applications

Gas separation membranes are increasingly being investigated for their possible use in natural gas purification, carbon dioxide capture or hydrogen recovery. A successful membrane must possess good selectivity for a particular gas and demonstrate good permeability (i.e. flux) to enable a small area of membrane to be used. However, membranes tend to have a combination of high permeability and low selectivity or *vice versa*. This trade off was quantified by Robeson,[74] using a double logarithmic plot of selectivity (as a ratio of permeability) against the permeability of the fastest gas species. Due to recent advances in polymer material the upper limit was redefined in 2008.[75] High permeability is linked to high free volume (i.e. space not occupied by the polymer molecules) but in addition it should contain pores of less than 1 nm, to ensure that the membrane behaves as a 'molecular sieve' by allowing smaller molecules to be transported faster than larger ones.

2.7.1 Substituted polyacetylenes.

These types of polymers (e.g. polytrimethylsilylpropyne – PTMSP; **Figure 2.7.1.1**) are prepared by chain polymensation of the acetylenic monomer using a transition metal catalyst.[76] The resulting double bonds can be in the cis or trans configuration and the bulky side chains restrict rotational freedom along the polymer backbone. The resulting rigid and contorted macromolecules do not allow the polymer to pack efficiently[77] and gives it a high free volume which in turn gives it a high permeability but due to the relatively large micropores created; these polymers provide low selectivity as discussed above.

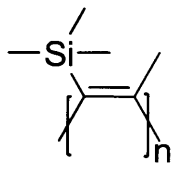

Figure 2.7.1.1. Poly(trimethylsilylpropyne) repeating unit.

2.7.2 Perfluoropolymers.

Of the commercially available perfluoropolymers Teflon AF2400 (**Figure 2.7.2.2**) has the highest permeability, particularly for oxygen and can be used for the separation of O_2 from N_2. Teflon AF polymers have lower densities than other polytetrafluroethylenes, which leads to their high free volume.

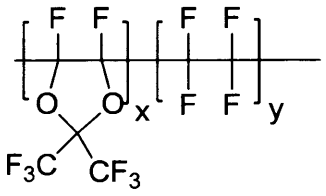

Scheme 2.7.2.1. Teflon AF2400 (x=0.87, y=0.13).

2.7.3 PIMs.

Membranes prepared from PIM-1 have high permeability even when compared to the highest of free volume polymers discussed above. Of particular interest is that they also demonstrate high selectivity for the separation of a number of commercially important gas pairs (e.g. O_2/N_2; CH_4/CO_2).[78.79] An advantage of PIMs is the possibility of altering the side groups to enhance performance.

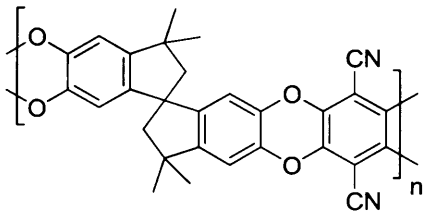

Scheme 2.7.3.1. Repeating unit of PIM-1 used in membrane fabrication.

2.8 Aims of revised project

Due to the difficulties encountered with the purification of the phthalocyanine dimers, as described in Chapter 1, it was decided to use some of the methodology previously used to prepare hexaphenylbenzene-based precursors for bridged phthalocyanines for the synthesis of novel monomers for Polymers of Intrinsic Microporosity (PIMs). Of particular interest are PIMs which are soluble in organic solvents which can be used to cast films for potential use as microporous membranes for gas separations. We hoped that, due to the very different structures of the proposed hexaphenylbenzene monomers, as compared to those used previously (e.g. spirobisindanes), that their gas permeability would be enhanced with respect to selectivity and/or permeability.

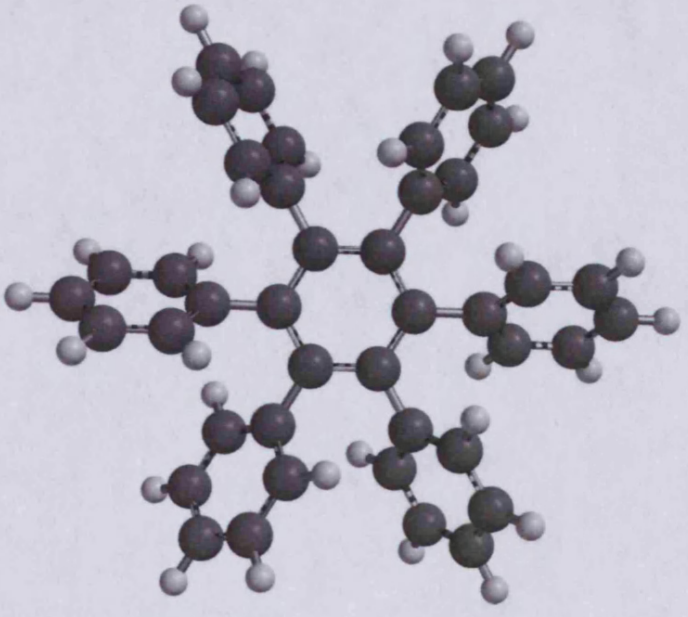

Figure 2.8.1. A molecular model of the 1,2,3,4,5,6-hexaphenylbenzene unit.

Hexaphenylbenzene is an interesting building unit for organic materials due to its rigidity,

which arises from the mutual steric interactions of the phenyl groups. These interactions results in a propeller-like shape. Derivatives of hexaphenylbenzene have been of considerable interest for a wide variety of applications in materials chemistry including: precursors to synthetic graphene fragments or use in organic electronics,[80] building blocks for crystal engineering[81,82,83] and proton-transport materials.[84] They have also been used extensively for making polymers of high glass-transition temperatures.[85,86]

Of immediate interest was PIM-like polymers derived from 1,2-bis(3',4'-dihydroxyphenyl)-3,4,5,6-tetraphenylbenzene, (**31; Figure 2.8.2**), similar to compound **14** that was used as a bridge for phthalocyanine dimers was suggested as a possible monomer. Although the hexaphenylbenzene unit possesses no spirocentre its rigidity and the steric hindrance due to the six aromatic rings that surround the central benzene may lead to inefficient packing and hence the desired microporosity.

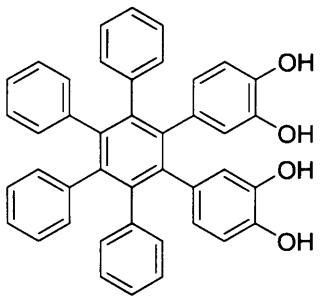

31

Figure 2.8.2. Biscatechol monomer **31** for making PIMs incorporating the hexaphenylbenzene unit.

Chapter 3

Chapter 3. Synthesis of hexaphenylbenzene-derived microporous materials.

3.1 Hexaphenylbenzene-based Organic Molecules of Intrinsic Microporosity (OMIM).

Thus far in the field of organic microporous materials it was believed that microporosity was a result of the packing inefficiency resulting from long-range rigid non-linear polymer chain entanglement or crystalline order. Work within the McKeown group by Dr. Kadhum Msayib and Mr. Jonathan Walker led to the discovery that the triptycene tetramer compound **OMIM-1** has an apparent BET surface area of 580 m^2/g. The result was surprising for such a small discrete molecule and it has prompted further work on this class of material termed Organic Molecules of Intrinsic Microporosity (OMIM). Hence it was of interest to make an OMIM in which the triptycenes are replaced by hexaphenylbenzene units to assess the utility of this component for the preparation of further microporous materials.

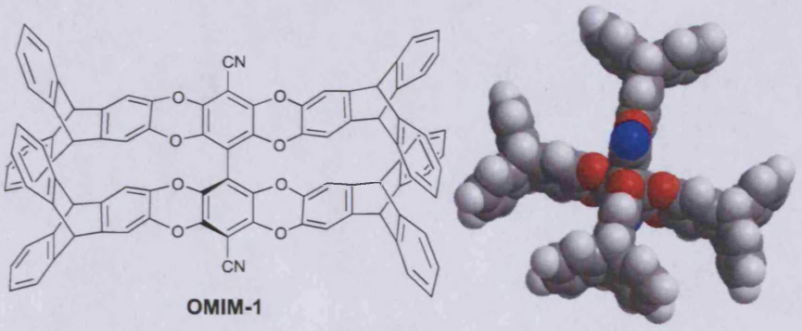

OMIM-1

Figure. 3.1.1 Chemical and space filling energy minimised structure of **OMIM-1**, which demonstrates an apparent BET surface area = 580 m^2/g (N_2, 77K).

The synthesis of the hexaphenylbenzene-based OMIM **34** required the synthesis of the monomer 1-(3',4'-dihydroxyphenyl)-2,3,4,5,6-pentaphenylbenzene, **33** that would then be reacted with 2,2',3,3',5,5',6,6'-octafluorobiphenyl-4,4'-dicarbonitrile **32** (**Figure 3.1.2**).

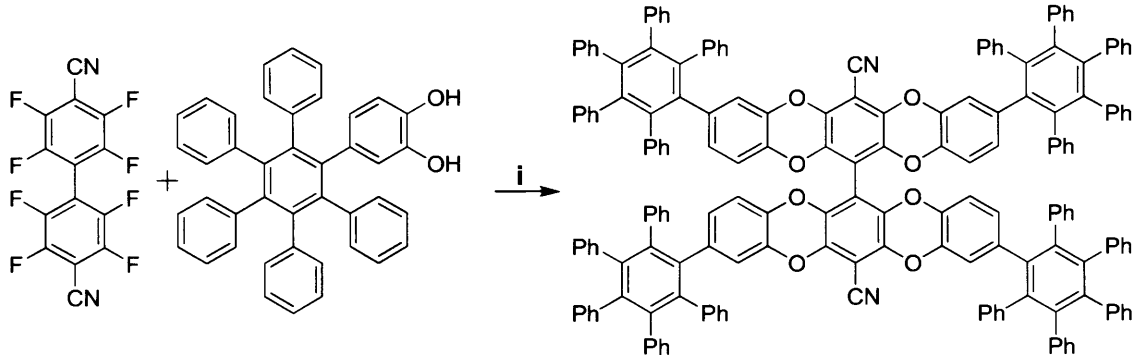

32 **33** **34**

Figure 3.1.2. Synthesis of the desired hexaphenylbenzene-containing monomer. Reagents and conditions. i. K_2CO_3, DMF, 120 °C, 18 hrs.

The synthesis of the desired monomer **33** is outlined in **Scheme 3.1.3**. Firstly, 1,2-dimethoxy-4-(phenylethynyl)benzene was synthesised using a palladium catalysed Sonogashira coupling between phenyl acetylene and 4-bromoveratrole. The resulting 1,2-dimethoxy-4-(phenylethynyl)benzene was then heated with 2,3,4,5-tetraphenylcyclopenta-2,4-dienone, in a Diels-Alder reaction to give 1-(3',4'-dimethoxyphenyl)-2,3,4,5,6-pentaphenylbenzene **36**. This was then demethylated using boron tribromide[87] to give monomer **33**.

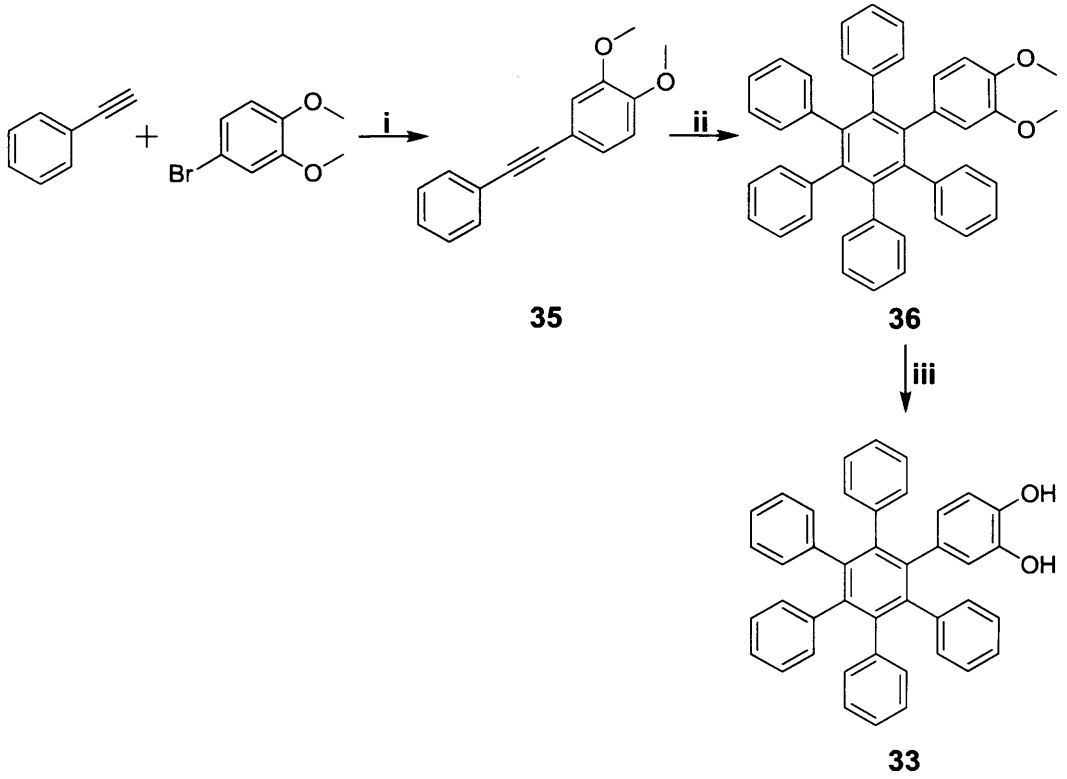

Scheme 3.1.3. Synthesis of 1,2-dihydroxy-4-(phenylethynyl)benzene. Reagents and conditions: i. $[P(Ph)_3]_2PdCl_2$, CuI, Et_3N, DMF, 90 °C, 15hrs; ii. 2,3,4,5-tetraphenylcyclopenta-2,4-dienone, EtOH, KOH, 80 °C; iii BBr_3, DCM.

Monomer **33** was then reacted with 2,2',3,3',5,5',6,6'-octafluorobiphenyl-4,4'-dicarbonitrile in DMF using K_2CO_3 as base. After purification using column chromatography, the resulting compound **34** was obtained in good yield (73%). The model compound was confirmed by MALDI MS (**Figure 3.1.4**). Nitrogen adsorption analysis gave a BET surface area of 406 m^2/g (**Isotherm 3.1.5**). Although this value is slightly smaller than that of OMIM-1 it is still significant for a discrete molecule of modest molecular mass. Using the conventional Brunauer-Deming-Teller classification, this is a Type IV isotherm. This suggests that there are both microporosity and mesoporosity within the material, the latter suggested by the hysteresis loop between adsorption and desorption, which closes at $p/p_o = 0.5$. An alternative explanation for this unusual shaped isotherm is swelling of the material at higher relative pressures. An examination of a molecular model of **34** (**Figure 3.1.4**) shows the awkward shape of **34**

which provides its intrinsic microporosity. In view of this encouraging result, the incorporation of the hexaphenylbenzene unit into polymers of intrinsic microporosity was considered worth pursuing.

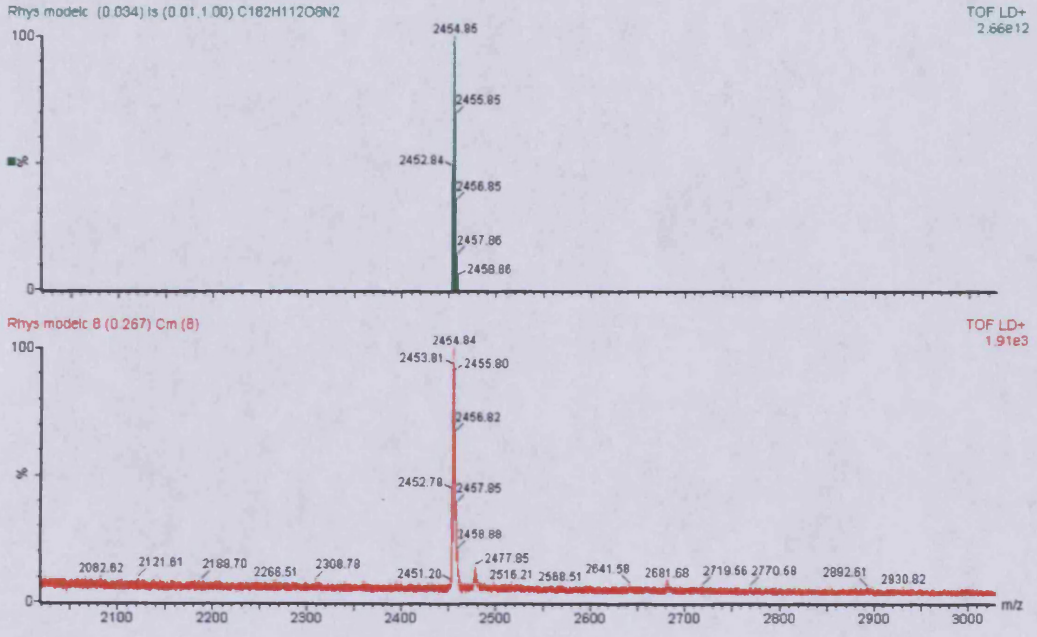

Figure 3.1.4. MALDI MS of OMIM, **34.** (note: isotope model shown above)

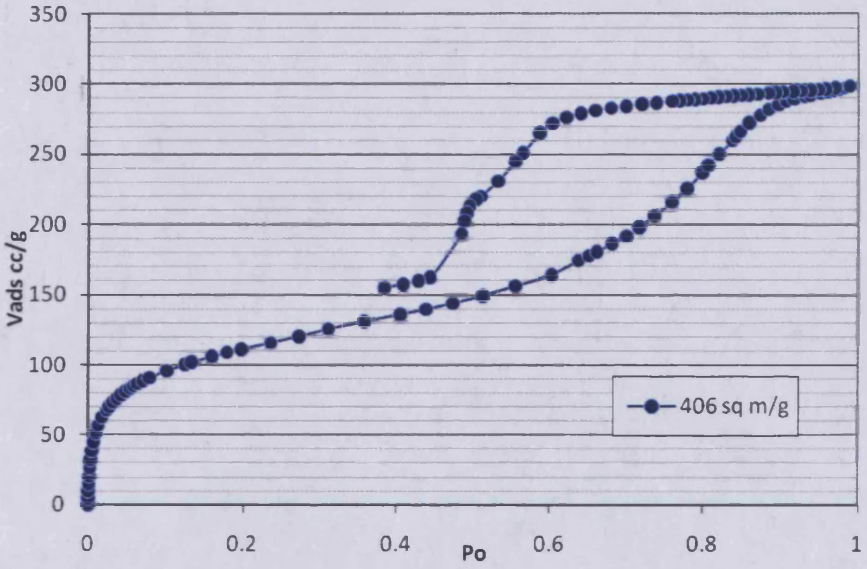

Isotherm 3.1.4. BET isotherm of model compound **34**

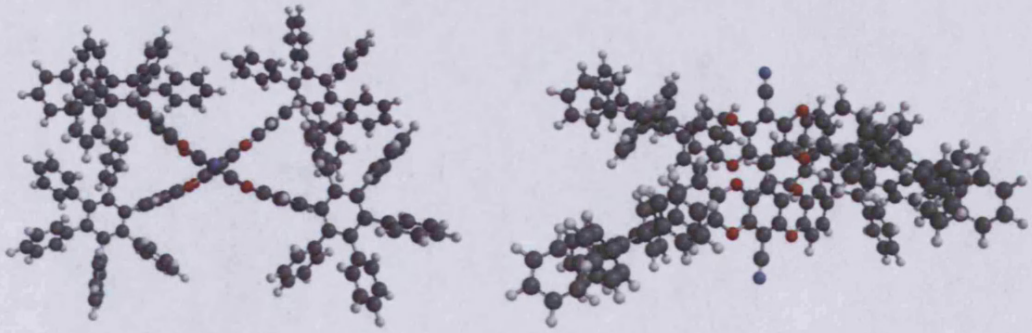

Figure 3.1.5. Two views of the molecular model of **34** showing its awkward shape that leads to intrinsic microporosity.

3.2 Synthesis of hexaphenylbenzene based ladder polymers.

Following the success of the hexaphenybenzene-based OMIM, the synthesis of derivatives that contain two catechol units was desirable as these would be precursors to ladder polymers

(i.e. non-network) when reacted with 2,3,5,6-tetrafluoroterephthalonitrile. It was anticipated that such polymers would be soluble in common organic solvents, which could allow the casting of a membrane film, to be used for gas permeation experiments.

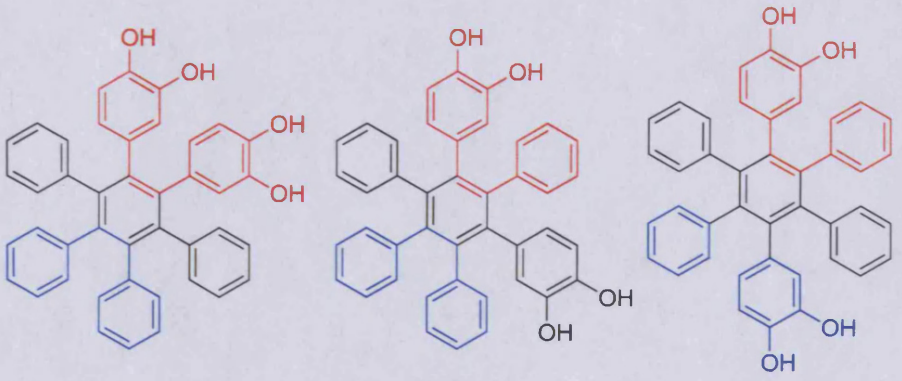

Figure 3.2.1. The three regioisomers of di(3',4'-dihydroxyphenyl)pentaphenylbenzene. In addition there could be conformers due to restricted rotation about the aryl-aryl C-C bonds. The colour coding represent the origin of the phenyl units from the precursors used to build the hexaphenylbenzene unit

There are three potential regioisomers of di(3',4'-dihydroxyphenyl)tetraphenylbenzene, arising from the possibility of *ortho*- (1,2), *meta*- (1,3) or *para*- (1,4) substitution of the central benzene ring as shown in **Figure 3.2.1**. Due to the method of assembly of the hexaphenylene core (as represented by the colour-coding in **Figure 3.2.1**), the only isomers that can be prepared as a single regioisomer is the ortho-derivative **31** and, therefore, this was the initial target.

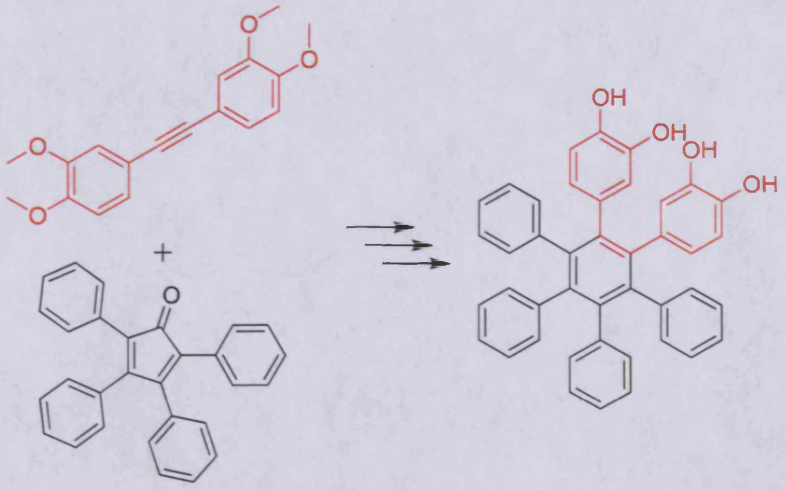

Figure 3.2.2. Precursors used in the unsuccessful attempt at preparing **31.**

3.2.1 Preparation of 1,2-di(3',4'-dihydroxyphenyl)-3,4,5,6-tetraphenylbenzene.

The reaction scheme successfully used previously for compound **33** was modified in order to attempt the synthesis of **31** (**Figure 3.2.2**). Firstly, 4-ethynyl-1,2-dimethoxybenzene **38** had to be prepared via a literature route[88] as it is not commercially available. This was achieved using the Corey-Fuchs reaction as outlined in **Scheme 3.2.1.1**. The Corey-Fuchs reaction is related to the Wittig reaction and involves the synthesis of a dibromoalkene **37** from the aldehyde. This was then treated with BuLi followed by aqueous work-up to eliminate the bromine moieties to obtain the required terminal alkyne. This precursor was then reacted with 4-bromoveratrole, *via* a Sonogashira coupling reaction.

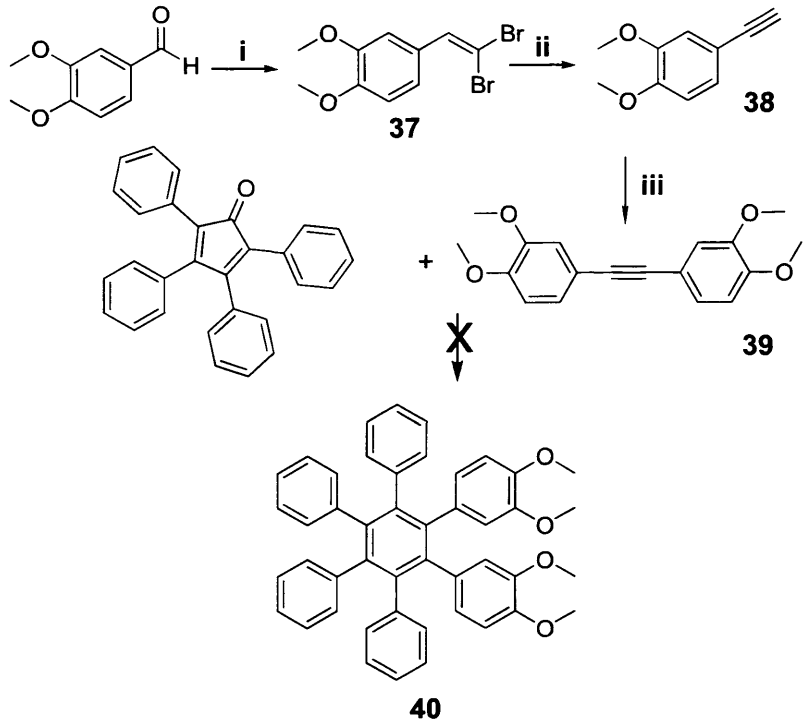

Scheme 3.2.1.1. Attempted synthesis of Monomer **40.** Reagent and Conditions: i. CBr_4, PPh_3, DCM, 30 min; ii. BuLi, DCM; iii. $[P(Ph)_3]_2PdCl_2$, CuI, Et_3N, DMF, 90 °C, 15hrs.

Unfortunately, the attempted Diels-Alder reaction between **39** and 2,3,4,5-tetraphenylcyclopenta-2,4-dienone in refluxing diphenyl ether failed (**Scheme 3.2.1.1**). The reason for this failure is thought to be due to the strong electron donating methoxy groups present on the diphenylacetylene. Classically, for a Diels-Alder reaction the dienophile is electron-deficient and the diene electron-rich, which decreases the energy of the LUMO of the diene, therefore, allowing better overlap with the HOMO of the dienophile.

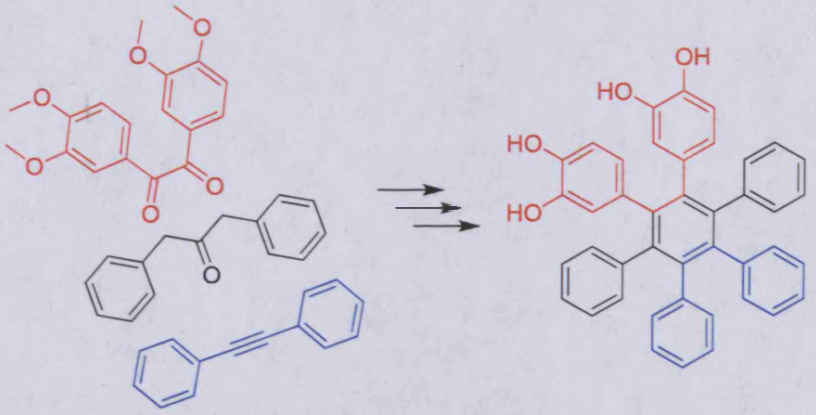

Figure 3.2.1.2. Precursors used in the successful synthesis of **31**

Due to the failure of this synthetic route, another route was devised which incorporated the methoxy groups on the diene, which it was anticipated would enhance the electronic configuration of the Diels-Alder reaction (**Scheme 3.2.1.1**). Literature revealed an apparently straightforward method of making the required dione and is shown in **Scheme 3.2.1.3**.[89] However, the use of the toxic reagent KCN and the long reaction time of 50 hrs prompted us to find an alternative method of preparing **31**.

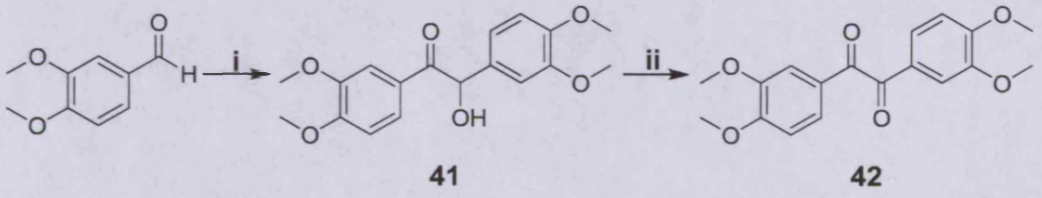

Scheme 3.2.1.3. Literature synthesis of **42**. Reagent and conditions: i. KCN, EtOH, H_2O, reflux, 50 hrs; ii. $CuSO_4.5H_2O$, pyridine, H_2O, 8 hrs.

The first step of the alternative approach involved making the acyl chloride of (3,4-dimethoxyphenyl)acetic acid which was achieved smoothly with thionyl chloride in DCM in very high yield **45** (94%). The resulting acid chloride was successfully reacted with veratrole in a classical Friedel-Crafts acylation, using aluminium trichloride as the Lewis acid, also in

very high yield (81 %). The ketone **44** was then oxidised by selenium dioxide to form the dione **45** (**Scheme 3.2.1.4**).

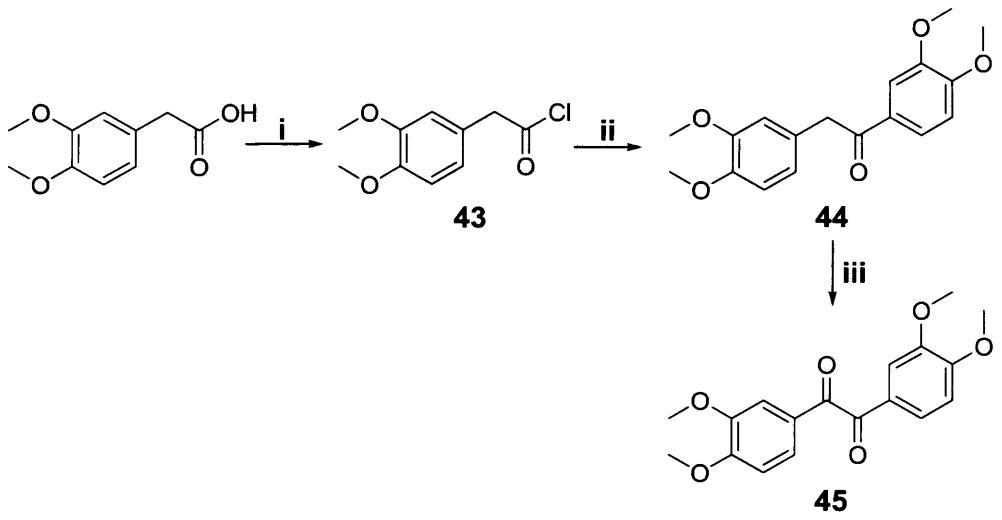

Scheme 3.2.1.4. Synthesis of 1,2-bis(3,4-dimethoxyphenyl)ethane-1,2-dione **45**. Reagent and conditions: i. $SOCl_2$, DCM, 1 hr; ii. Veratrole, $AlCl_3$, DCM, 3 hrs; iii. SeO_2, Dioxane, H_2O, 15 hrs.

This dione **45** was reacted with 1,3-diphenylacetone in an attempt to form the cyclopentadienone derivative **46**. Unfortunately, dione **45** is not soluble in EtOH even when heated. This seemed to have an adverse effect on the reaction, which was monitored by TLC. Although a TLC spot of the expected colour (purple) started to appear, over time it faded and a different red spot appeared of greater polarity. The compound associated with the red TLC spot was isolated by column chromatography but its ^1H NMR spectrum was very difficult to interpret. In an attempt to see if this product was derived from a self-condensation of 1,3-diphenylacetone, a reaction was set up in the absence of the dione. TLC analysis of the product mixture showed an absence of the unknown red spot. In an attempt to increase the speed of the reaction so to avoid the formation of the compound associated with the red TLC spot, a mixture of THF and EtOH was used as solvent to ensure the solubility of **45**. However, this reaction failed and only starting material was observed by TLC. Therefore the choice of the base was examined. However, the use of NaOH or potassium *t*-butoxide did not yield any of the desired dione. The effect of different stoichiometries of KOH was explored. Firstly,

0.5 molar equilvalent of KOH was used and this was left for 1hr; TLC analysis showed that the product spot was slowly appearing, so another 0.5 molar equilvalents of KOH of base was added. After a further hour, TLC analysis showed a strong product spot but also that the unwanted red spot had started to appear. So the reaction was stopped and the resulting precipitate filtered. The black powder was washed with EtOH and gave the required cyclopentadienone **46** in a good yield of 67%. This route became the preferred method for the preparation of tetraphenylcyclopentadienone derivatives as it gave the product in a pure and readily isolated form.

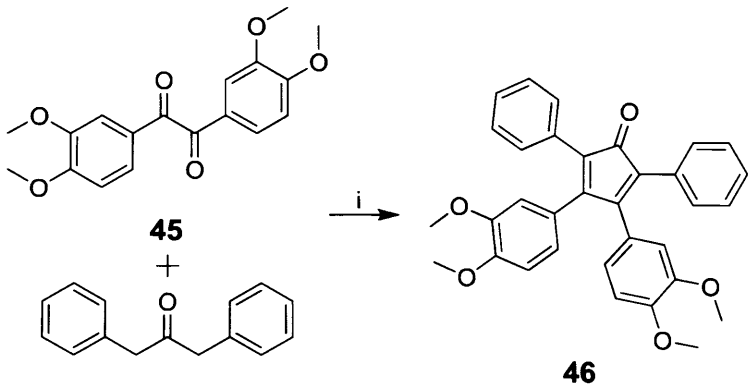

Scheme 3.2.1.5. Synthesis of **46**. Reactions and conditions: i. KOH, EtOH, 80 °C.

Once the desired cyclopentadienone derivative **46** was obtained, the coupling of the two molecules via a Diels-Alder reaction was attempted. The reaction proved successful, presumably due to the more appropriate electronic configuration of the diene and dienophile, and gave the direct precursor to the desired monomer **40** in good yield (65%) after purification by column chromatography. To convert this into monomer **31** ready for polymerisation, it was treated with boron tribromide in DCM and recrystallised from hexane and DCM (**Scheme 3.2.1.6**)

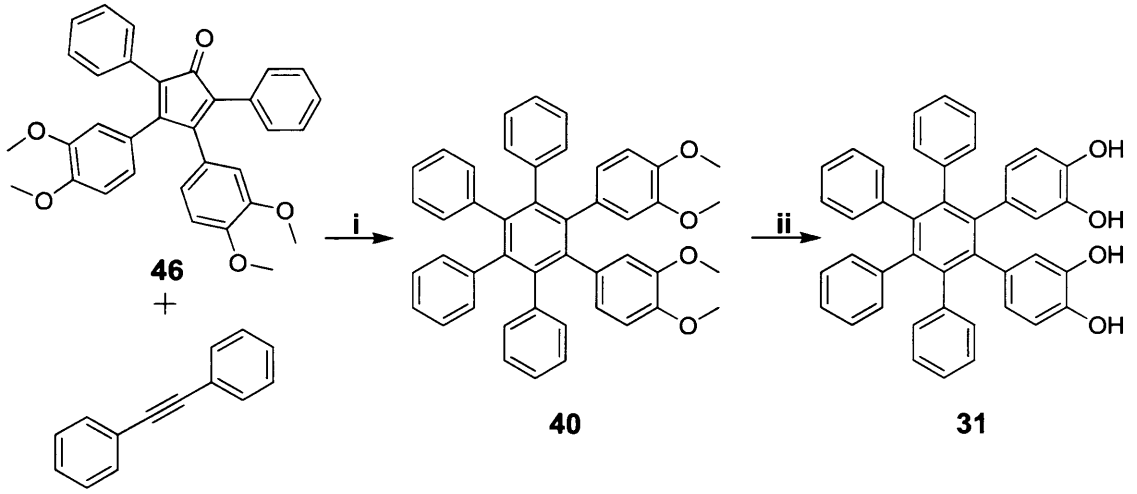

Scheme 3.2.1.6. Synthesis of monomer 1, **31**. Reagents and conditions: i. Ph_2O, reflux, 15 hrs; ii. BBr_3, DCM, 1 hr.

3.2.2 Polymerisation of 1,2-di(3',4'-dihydroxyphenyl)-3,4,5,6-tetraphenylbenzene.

Once the monomer **31** had been purified and carefully dried under vacuum, it was polymerised. This involved reacting **31** with an exact stoichiometric amount of 2,3,5,6-tetrafluoroterephthalonitrile and K_2CO_3 in DMF, which was left for 72 hours at 60 °C (**Scheme 3.2.2.1**). Being a step-growth polymerisation, the stoichiometric ratio of **31** to that of 2,3,5,6-tetrafluoroterephthalonitrile is very important to ensure a reasonable molecular mass of polymer.

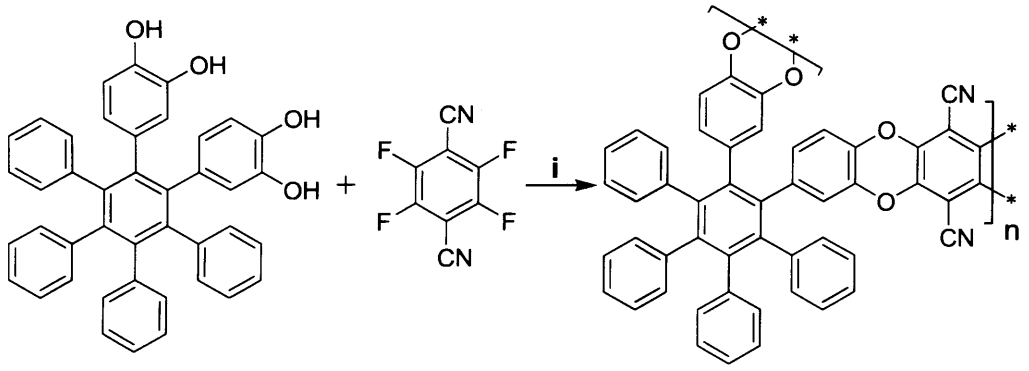

31 **47**

Scheme 3.2.2.1. Synthesis of polymer, **47**, from hexaphenyl monomer. Reactions and conditions: i. DMF, K_2CO_3, 65 °C, 96 hrs.

When the reaction was over the product mixture was quenched with water and treated with a few drops of 2M HCl to remove unreacted K_2CO_3. Normal procedure for isolating a PIM such as PIM-1 involves collecting the solid by filtration under suction then washing the solid with acetone and then methanol to remove small oligomers, which are generally more soluble than a polymer of higher molecular mass. However, washing with acetone led to almost complete dissolution of the solid. This suggested that the polymerization produced mostly oligomers rather than high molecular weight polymer. The polymer was re-dissolved completely and dried in a vacuum oven to remove any traces of solvent and analysed without further purification. The material obtained was tested for nitrogen adsorption and gave an apparent BET surface area of 425 m^2/g (**Isotherm 3.2.2.2**) a result not very dissimilar from OMIM **34** that gave a value of 406 m^2/g. The significant adsorption at $p/p^o < 0.01$ indicates the microporosity of the material, though the apparent surface area is significantly lower than the value of 780 m^2/g obtained for PIM-1.

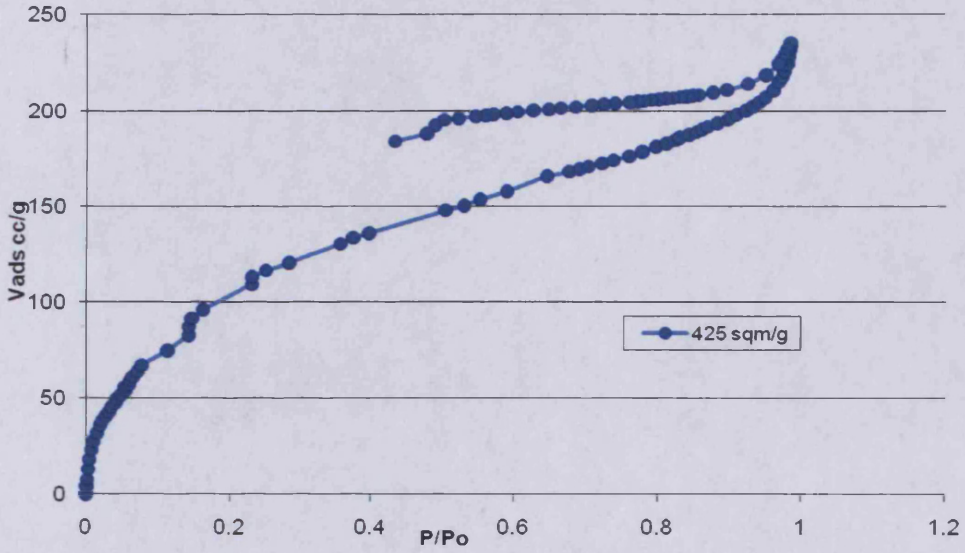

Isotherm 3.2.2.2. Nitrogen adsorption isotherm for polymer, **47**.

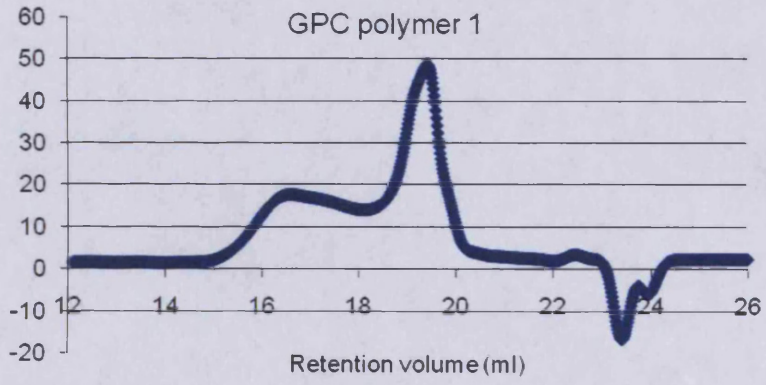

Figure 3.2.2.3. A GPC plot of the product mixture from the polymerisation of **31.**

From the GPC trace (**Figure 3.2.2.3**) shows two main peaks. The broad peak at retention volume = 16.5 ml corresponds to a reasonable polymer mass (*Mn* = 20,000 and *Mw* = 33,000 mol/g). Another peak at retention volume of 19.5 ml corresponds to small oligomers mostly dimer and trimer (*Mp* = 1500; *Mn* = 2,400 and *Mw* = 3,000). Despite its modest average

molecular mass, formation of a self-standing film was attempted for this polymer, by dissolving it in $CHCl_3$ and allowing the solvent to evaporate slowly in a suitable Petri dish. However, no film was formed, which is most likely due to the low molecular mass of the polymer and consequent lack of chain entanglements. Although failing to form solvent cast films, the material is still of interest due to its intrinsic microporosity. In particular, the large proportion of cyclic oligomers (n = 2-9) produced in the polymerisation, as identified in the MALDI-MS (**Figure 3.3.2.4**) allowed the isolation of the cyclic dimer and this material is discussed in chapter 4.4.

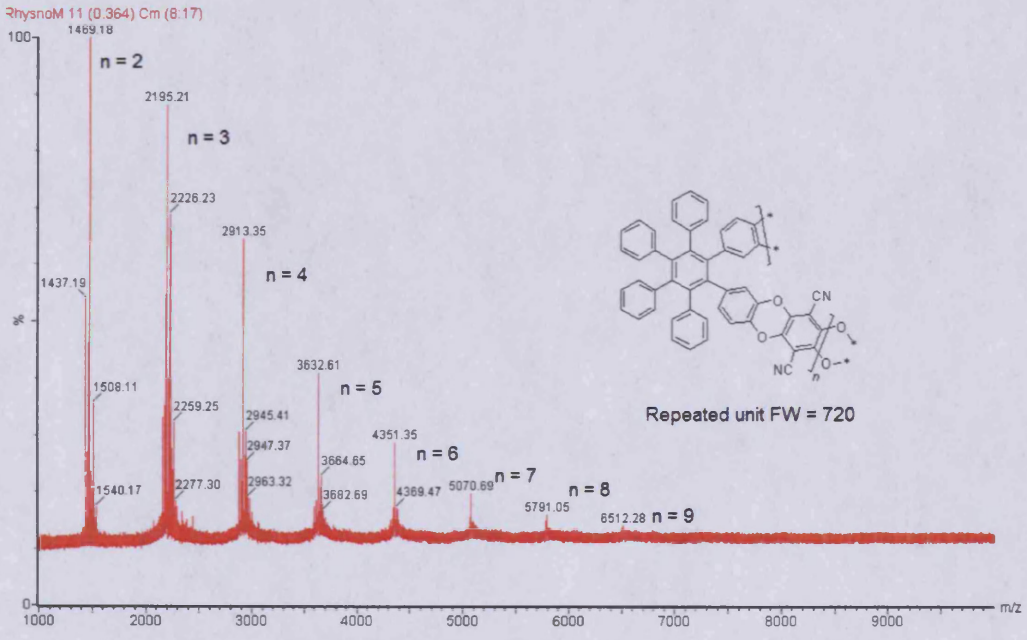

Figure 3.1.2.10. MALDI-TOF showing oligomers present from the polymerisation of **31.**

3.2.3 Preparation of 1,3(4)-di(3',4'-dihydroxyphenyl)-3,4,5,6-tetraphenylbenzene.

The main reason that we attributed the formation of very low molecular weight oligomers during the polymerization of monomer **31** with tetrafluoroterephthalonitrile, was that the two catechol moieties were adjacent to each other on the hexaphenylbenzene unit. This appeared

to encourage the formation of cyclic dimers of relatively low molecular mass. Therefore, our target was to obtain catechols units in *meta* or *para* positions of the central benzene ring.

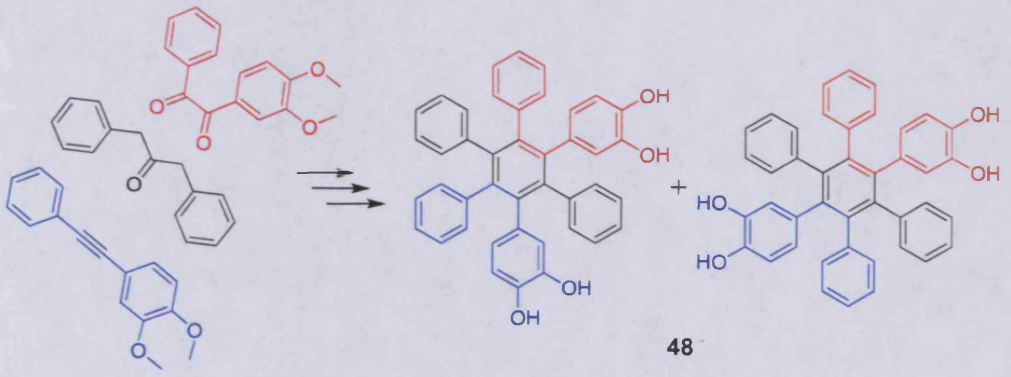

Figure 3.2.3.1. The precursors used to prepare monomer **48** which is formed as a 50:50 mixture of regioisomers.

In order to prepare the desired monomer we aimed to modify the hexaphenylbenzene-forming reaction to have one set of methoxy groups on the dione **50** and another set of methoxy groups on the acetylene **35** so as to place the two set of methoxy groups on opposite sides of the monomer (**Figure. 3.2.3.1**). Using this synthetic strategy, there would be no way of controlling the regioselectivity of the Diels-Alder reaction so that a mixture of isomers would result. Our first attempt at making the dione **50** involved a direct Freidel-Crafts reaction between veratrole and the acyl chloride derived from oxo(phenyl)acetic acid (**Scheme 3.2.3.2**). However, after purification and analysis using ^{13}C NMR, we noticed that only one carbonyl group was present not the two different carbonyl groups that were expected. Mass spectrometry confirmed the absence of the second carbonyl. This reactivity appeared analogous to the decomposition of oxalyl chloride to form $COCl_2$ or $COCl^{\bullet}$ which then performs chlorocarbonylation on an aromatic substrate.[90]

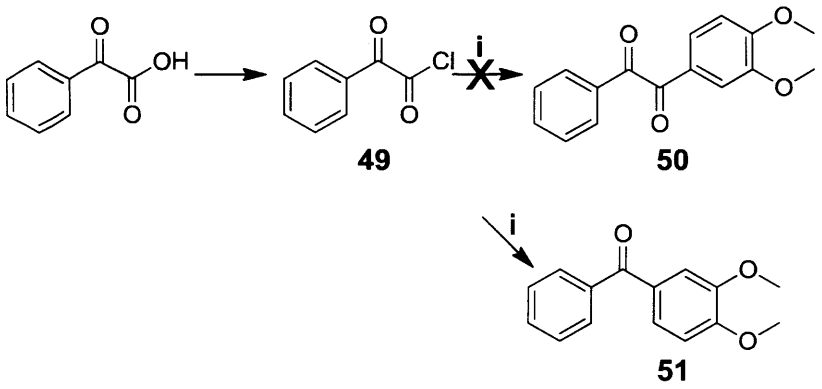

Scheme 3.2.3.2. Attempted synthesis of **50** from oxo(phenyl)acetic. Reagents and conditions: i. Veratrole, $AlCl_3$, DCM, 3 hrs.

As a result of this problem, it was decided to return to a similar synthetic methodology to that used for the preparation of **45** (**Scheme 3.2.1.4**). Firstly, 2-phenylacetic acid and $SOCl_2$ were reacted to form the acyl chloride and then this precursor was used in a Friedel-Craft reaction with veratrole and $AlCl_3$ to give the ketone **52** (68 % yield). Oxidation with SeO_2 proceeded smoothly to give the desired dione **53** in (97 % yield). Dione **53** reacted with 1,3-diphenylacetone, under the previously optimised conditions used for the formation of monomer **31**, to give cyclopentadienone **54** in 65 % yield. The Diels-Alder reaction of **54** with the previously prepared (3,4-dimethoxy)diphenylacetylene **35** gave the tetra-methoxy precursor, which was purified using column chromatography. The last step of this synthesis was the usual demethylation using BBr_3, which gave the desired new monomer **48**.

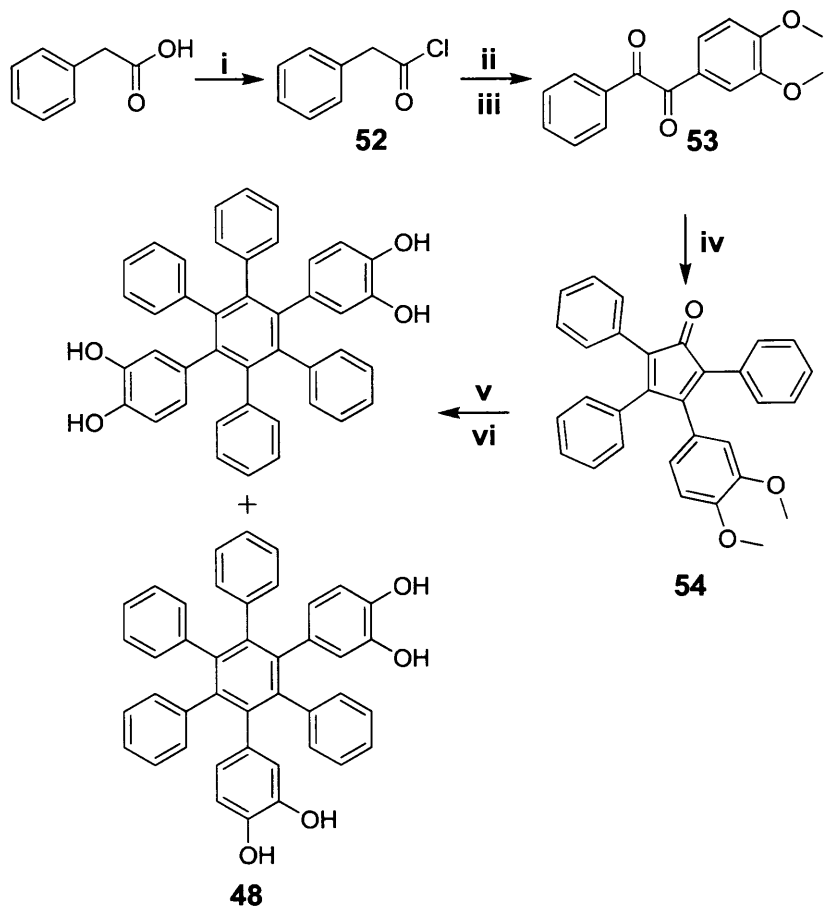

Scheme 3.2.3.3. Synthesis of monomer **48**. Reaction and conditions: i. $SOCl_2$, DCm, 1 hrs; ii. Veratrole, DCM, $AlCl_3$, 3 hrs; iii. Dioxane, H_2O, SeO_2 15 hrs; iv. KOH, EtOH, 80 °C; v. Ph_2O, reflux, 15 hrs; vi. BBr_3, DCM, 1 hr.

With the reaction illustrated in **Scheme 3.2.3.3**, we initially expected no preference for the formation of the 1,3- (meta-) or 1,4- (para-) regioisomers during the Diels-Alder reaction. However in the ^1H NMR of the methoxy analogue of **48**, there are only two singlets corresponding to the methoxy groups, suggesting that there is only one isomer present. This conclusion is supported up by the presence of only the para-isomer in the crystal structure (Figure 4.3.1). This could be due to the reaction having a preference for placing the dimethoxyphenyl groups in the *para* position due to a significant electronic perturbation of the Diels-Alder electrocyclic transition state. After the successful synthesis of the monomer it was dried in a vacuum oven and polymerised using the same conditions as used previously for

monomer **31**, using an exact stoichiometric amount of tetrafluoroterephthalonitrile, K_2CO_3 as base and DMF as solvent for 3 days at 60 °C. **(Scheme 3.2.3.4)**

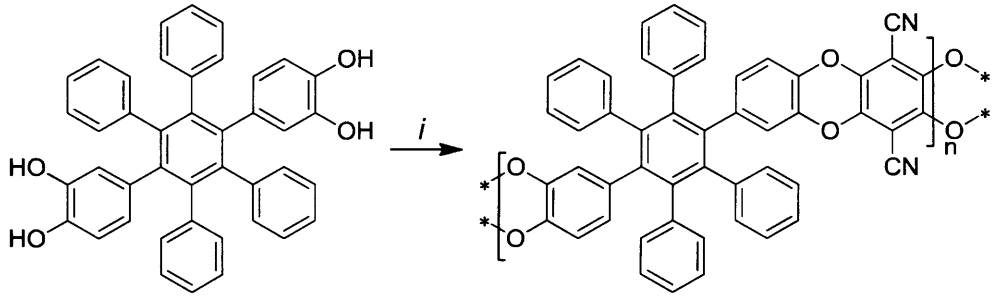

48 **55**

Scheme 3.2.3.4. Polymerisation of monomer **48** (note only one isomer is shown).Reagent and conditions: i. DMF, K_2CO_3, 65 °C, **23**, 96 hrs.

Following the usual work-up procedure for PIMs, the reaction was quenched with water and a few drops of 2M HCl added. This was filtered and, this time, when washed with acetone, only a small amount of solid was dissolved. This is an indication that only a small amount of oligomers was formed during the reaction, in favour of longer chain polymer. After washing with acetone, the polymer was repeatedly washed with MeOH. The polymer was then dissolved in the minimum amount of $CHCl_3$ and reprecipitated by adding the solution dropwise to a mixture of acetone and MeOH (2/1, 80 ml) and collected by filtration. Before attempting the surface area analysis, the material was refluxed in MeOH and put in a vacuum oven, to eliminate the last traces of trapped solvent, which could influence the measurement. The result of this analysis showed an apparent BET surface area of 537 m^2/g. The isotherm obtained is shown below **(Isotherm 3.2.3.5)**

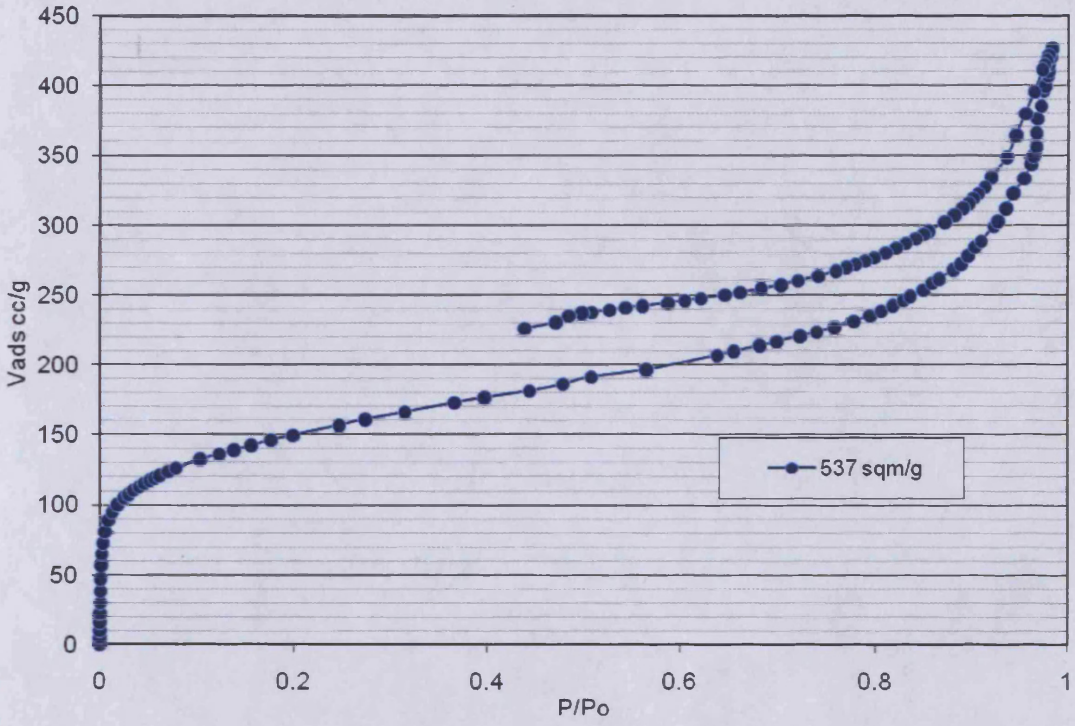

Figure 3.2.3.5. Nitrogen Isotherm of polymer, **55**.

The change of position of the catechol moieties within the monomer has a positive effect on the surface area of polymer **55** by increasing it by over 100 m^2/g relative to that of Polymer **47**. The N_2 isotherm also has a more conventional appearance with significant uptake at low relative pressure. Although the surface area is less than the value obtained for PIM-1, and other soluble non-network PIMs,[62] it is still an interesting result due to the lack of any formal site of contortion (e.g. spirobisindane) contained within the polymer structure. However, the most pleasing feature of polymer **55** was the high molecular mass indicated by GPC analysis,(*Mn* = 57,000 and *Mw* = 105,000), which is a very significant improvement on that obtained for Polymer 1 and supports the idea that the relative position of the catechol units on the hexaphenylbenzene is of crucial importance to the formation of high molar mass polymer. This result supports the earlier observation that the low molecular mass obtained consistently for Polymer **47** is due to the adjacent positions of the catechol units within monomer **31**

favouring the formation of cyclic oligomers. Film formation was successfully achieved by dissolving the polymer in the smallest possible amount of $CHCl_3$ and placing it in a small, flat round Petri dish and allowing slow evaporation of the solvent. The resulting robust self-standing film enabled gas permeation measurements for this type of polymer (**See section 3.2.5**).

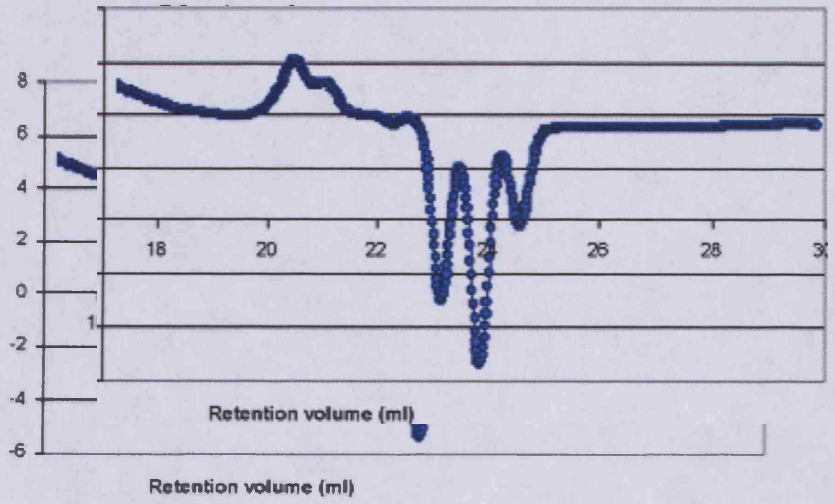

Figure 3.2.3.6. GPC of polymer, **55**.

3.2.5 Gas permeability measurements.

A film of polymer **55** was sent to Dr. Detlev Fritsch of the Polymer Research Institute, GKSS, Geesthacht, Germany, for gas permeability measurements. These were performed using time-lag methodology using specially constructed equipment. The results are presented in **Table 3.2.5.1**. The best term of comparison for evaluating the potential performance of Polymer 2 as the selective layer within a membrane is the data for PIM-1 obtained under the same conditions as for polymer **55** (**Table 3.2.5.1**).[91] As noted previously (**Section 2.7.4**), PIM-1 is a rigid, glassy spirobisindane-based polymer with a high excess free volume,[92] which makes it one of the most permeable polymers known. Probably the most remarkable feature of PIM-1 is

that it possesses high gas permeability coupled with good gas selectivity. This behaviour can be contrasted with the acetylene-based class of polymer that displays greater permeability but far less selectivity.

GAS	**Diffusivity** ($cm^2/sec \times 10^8$)	**Solubility** ($cm^3(STP)/cm^3\ cmHg \times 10^3$)	**Permeability** (Barrer) $cm^3(STP)cm/(cm^2\ s\ cmHg) \times 10^{10}$	**Perm.-Selectivity** PX/PN2
O_2	65.168	17.446	113.689	3.42
N_2	25.269	13.175	33.291	1
He	2362.256	0.855	201.842	6.06
H_2	1193.009	3.167	377.857	11.35
CO_2	31.803	280.499	892.056	26.8
CH_4	10.132	61.201	62.012	1.86
	CO_2/CH_4 3.14	CO_2/CH_4 4.58	CO_2/CH_4 14.39	
	H_2/CH_4 117.74	H_2/CH_4 0.05	H_2/CH_4 6.09	
	CO_2/H_2 0.03	CO_2/H_2 88.56	CO_2/H_2 2.36	

Table 3.2.5.1. Permeability data for polymer **55**

GAS	**Diffusivity** ($cm^2/sec \times 10^8$)	**Solubility** ($cm^3(STP)/cm^3\ cmHg \times 10^3$)	**Permeability** (Barrer) $cm^3(STP)cm/(cm^2\ s\ cmHg) \times 10^{10}$	**Perm.-Selectivity** PX/PN2
O	81	46	370	4
N_2	22	42	92	1
He	2700	2.4	660	7.2
Xe	0.46	1200	55	0.6
H_2	1700	7.6	1300	14
CO_2	26	880	2300	25
CH_4	6.8	180	125	1.4
	CO_2/CH_4 3.8	CO_2/CH_4 4.9	CO_2/CH_4 18.4	
	H_2/CH_4 250	H_2/CH_4 0.04	H_2/CH_4 10.4	
	CO_2/H_2 0.02	CO_2/H_2 115	CO_2/H_2 1.8	

Table 3.2.5.2. Permeability data for PIM-1.[87]

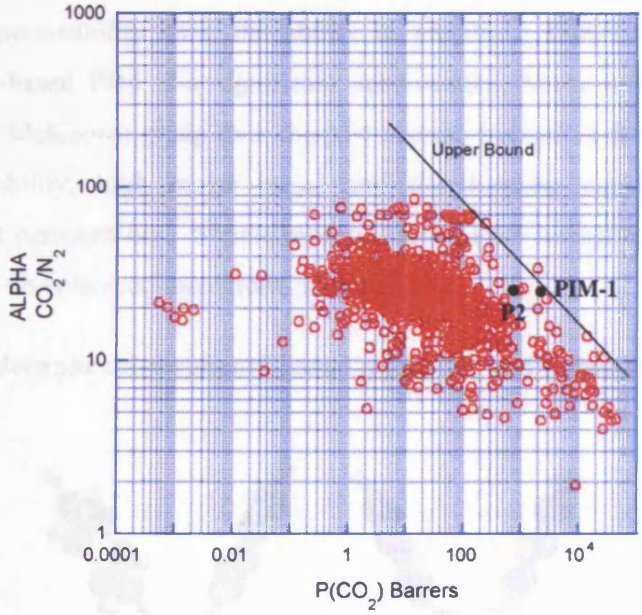

Figure. 3.2.5.3 A typical Robeson plot.[70] This example is for the gas pair CO_2/N_2 and has the data points for PIM-1 and polymer **55 (P2)** added for comparison.

As noted earlier, the performance of polymers with regards the trade-off between selectivity for one gas over another versus permeability has been quantified by the use of Robeson *plots.[70] For most gas pairs PIM-1 helped to define the updated 2008 upper bound which represent the current best 'compromise' between selectivity and permeability. An example of a Robeson plot is give in **Figure 3.2.5.3** which is based upon the accumulated permeability data for all reported polymers for the gas pair CO_2/N_2 – of current interest for the development of gas separation membranes for CO_2 capture. The data for PIM-1 lies on the upper-bound whereas that for polymer **55** lies slightly below because polymer **55** has only slightly higher selectivity for CO_2 over N_2 (27 versus 25 for PIM-1) but significantly lower permeability for CO_2 (900 versus 2200 for PIM-1). Robeson plots for other gas pairs of commercial importance in membrane applications (e.g. CO_2/CH_4, O_2/N_2 or CO_2/H_2) show similar relative behaviour. Thus, we can conclude that polymer **55** has less attractive fundamental gas separation data than PIM-1, although further investigation of its gas permeability properties may reveal other

advantages (e.g. greater stability of flux over extended time periods). Despite the slightly disappointing gas permeability data, the ability to prepare a film-forming example of a hexaphenylbenzene-based PIM is a significant achievement. Many novel PIMs have been prepared within the McKeown group over the past decade, but only a few have demonstrated the necessary solubility, high molar mass, and film-forming capability to allow the measurement of gas permeability. Simple modifications of the hexaphenylbenzene unit may produce polymers with enhanced membrane potential.

3.2.6. Synthesis of decaphenyl-terphenyl-based monomer and Polymer 58.

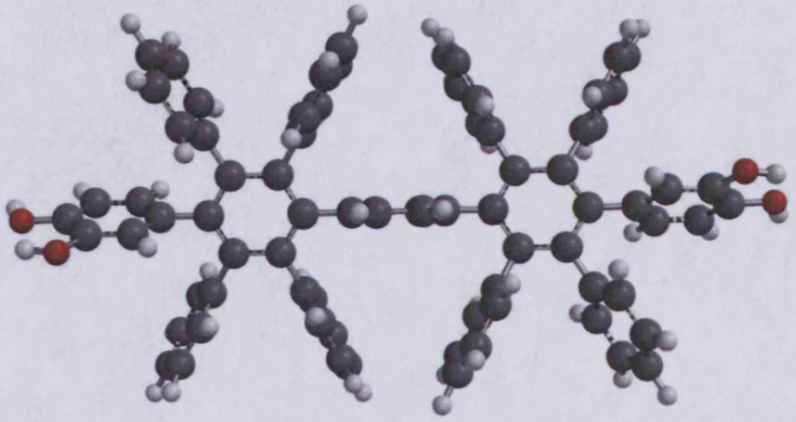

Figure 3.2.6.1 A molecular model of the extended monomer **58**.

Following the success of Polymer 2 it was decided to extend the concept of using polyphenylene-based structural units for the synthesis of PIMs to see if this would have a greater effect on the microporosity of the resulting polymer by creating larger pores (**Figure 3.2.6.1**). After reviewing the literature, it was concluded that the easiest way to prepare such an extended monomer was to use the Diels-Alder reaction between the previously prepared cyclopentadienone derivative **54** and 1,4-bis(phenylethynyl)benzene **56**, which was readily obtained from the Songashira coupling reaction between 1-bromo-4-iodobenzene and phenylacetylene The methylated precursor was then purified using standard methods and demethylated to give the desired monomer **58 (Scheme 3.2.6.3).**

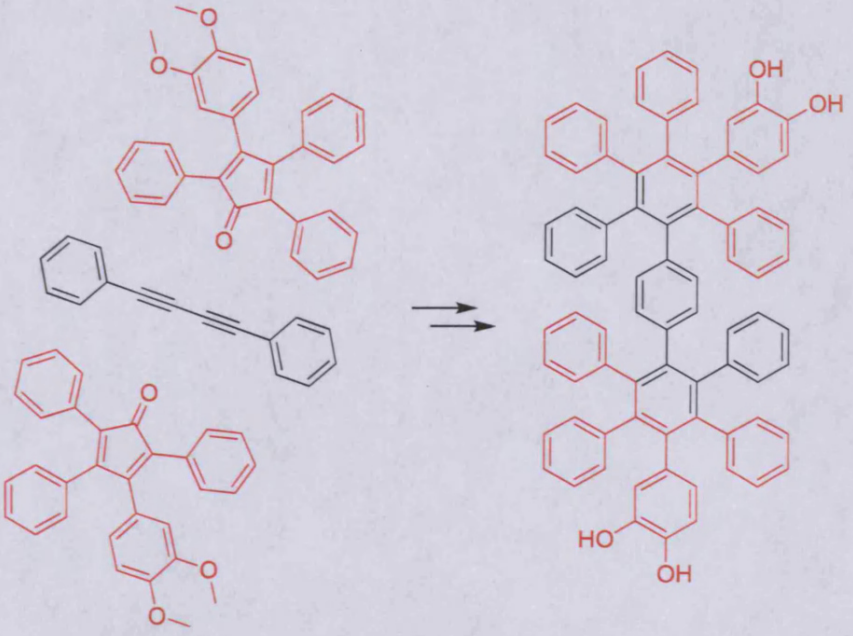

Figure 3.2.6.2. The precursors used for the extended monomer **57**. Note that only one of the four statistical regioisomers is shown.

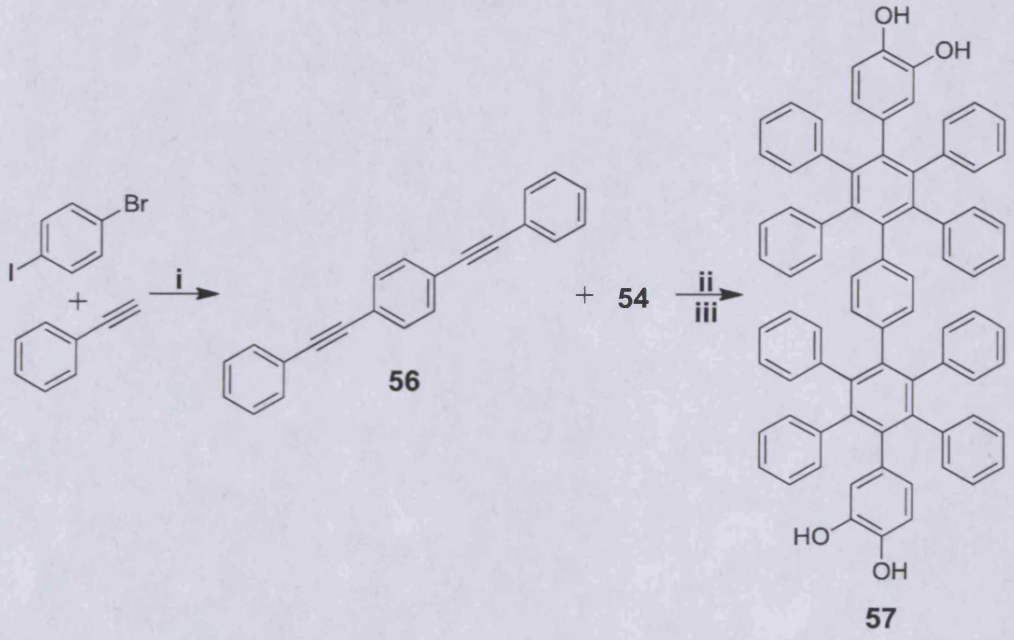

Scheme 3.2.6.3. Showing synthetic route to monomer 3, **57**. Reagents and conditions: i. $[P(Ph)_3]_2PdCl_2$, CuI, Et_3N, DMF, 90 °C; ii. Ph_2O, reflux, 15 hrs. iii. BBr_3, DCM, 1 hr.

Monomer **57** was then polymerised using the same method as the other polymerisations using tetrafluoroterephthalonitrile in DMF with K_2CO_3 for a period of 3 days (**Scheme 3.2.6.4).**

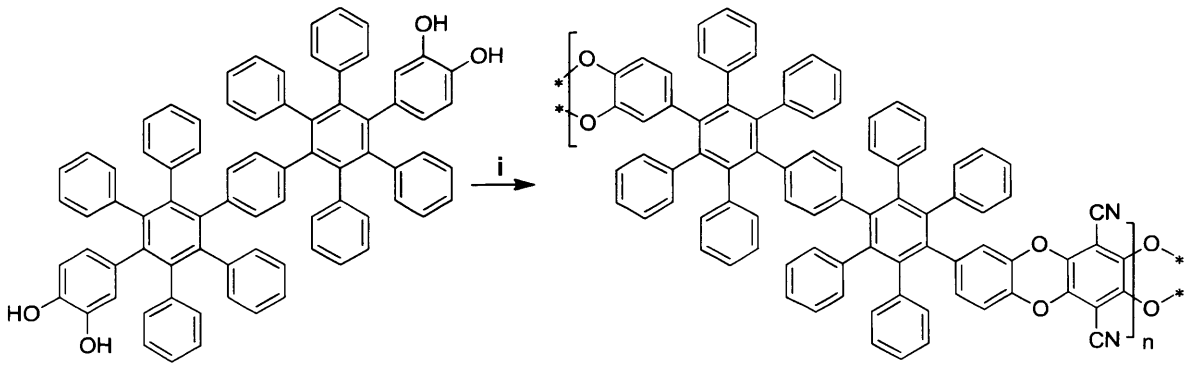

57 **58**

Scheme 3.2.6.4. Preparation of polymer **58** from Monomer **57**. Reagent and conditions: i. DMF, 65 °C, K_2CO_3, **23**, 96 hrs. (Note only one regioisomer is represented).

Once the polymerisation was complete the reaction was quenched with water, filtered and washed with acetone. Interestingly, as with Polymer 1, the resulting polymer **58** was soluble in large amounts with acetone which suggested that only low mass polymer had been formed. This may be due to the large size of monomer **57** and the correspondingly small amount of the tetrafluoroterephthalonitrile required which would reduce the concentration and hence rate of reaction. Despite this, the crude polymer was collected and refluxed in MeOH to remove low mass impurities. The BET surface area was then measured to give a value of 355 m^2/g (**Isotherm 3.2.6.5**). The isotherm is of an unconventional shape with very strong N_2 adsorption at high relative pressure but with minimal hysteresis. Further analysis of this polymer is required in order to interpret this data fully.

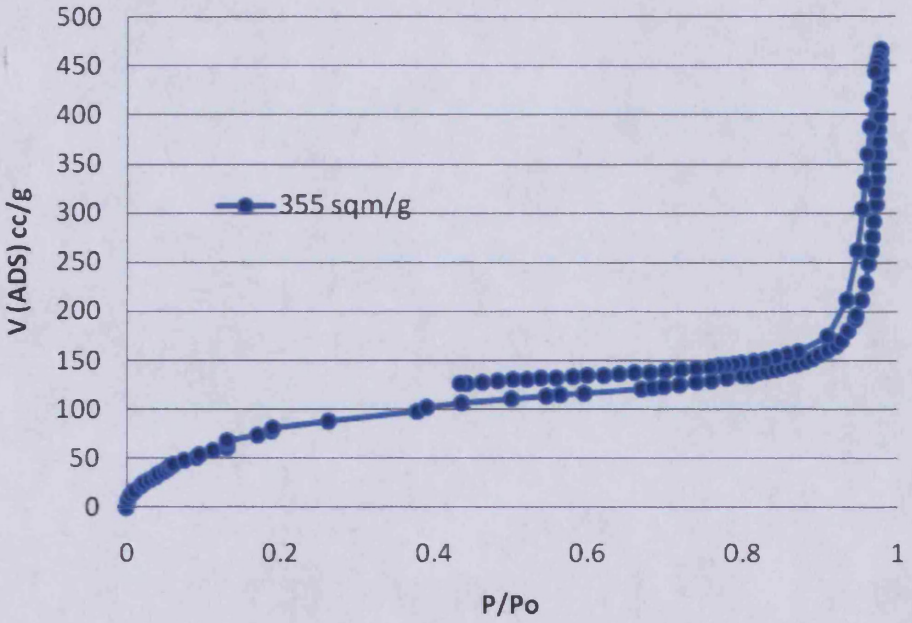

Isotherm 3.2.6.5. Isotherm of polymer **58**.

Chapter 4

Chapter 4. Crystal structures of hexaphenylbenzene-based compounds.

4.1. Introduction.

In order to understand any geometrical differences between the catechol monomers **31** and **48** that lead to the formation of the dimer **59**, whose presence was shown in **Figure 3.1.2.10** and structure in **Figure 4.4.1** and to the larger molecular weight polymer **55**, respectively, crystals were grown suitable for single crystal XRD analysis. Recently, the hexaphenylbenzene unit has been used in 'crystal engineering' by the groups of Wuest[93,94,95] and Kobayashi.[96,97] Therefore, these crystal structures might add useful information to this active field of research.

Crystals derived from the [2+2] cyclic oligomer obtained from the attempted polymerisation of 2,3,5,6-tetrafluoroterephthalonitrile and monomer **31** were also studied by XRD. The cavity within this macrocycle, combined with its highly fluorescent nature also prompted an investigation to establish its potential for optical sensing of nitrated aromatics.

4.2 Crystals of monomer 31.

In general, the crystals of catechol-containing compounds tend to include solvent molecules[98] which can lead to a more difficult growth of the crystal and a more challenging structure solution than those of the analogous methoxy-containing precursors. However, crystals of **31** were grown readily by the slow diffusion of n-hexane into a solution of the monomer in THF. The crystal of monomer **31**, the precursor to the cyclic dimer **59**, grew in the monoclinic space group C2/c with cell dimensions of [a = 11.0423(6), b = 17.9462(10), c = 28.7533(16) Å] and cell angles [α = 90, β = 95.604(3), γ = 90°].); cell volume = 5670.73 Å3. It contained four molecules per unit cell with six molecules of included THF per monomer unit The solid state structure of the molecule is shown in **Figure 4.2.1.** It is worth noting the disorder of the catechol moieties, one in the "ortho" position relative to the other, so that the oxygen atoms were difficult to be located exactly leading to half occupancies. This disorder and the presence

of highly disorder solvent molecules within the crystal contributed to a high R_f (~30%, from an unoptimised analysis), however the basic geometry of the molecule is not in doubt. The hexaphenylbenzene unit adopts the well-established propeller-like conformation due to the mutual steric interactions between neighbouring phenyl groups.

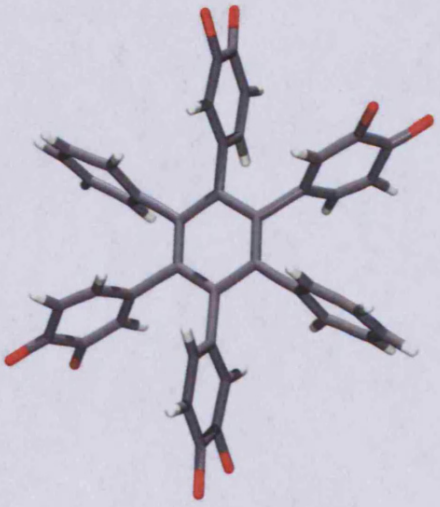

Figure 4.2.1. ORTEP projection of the solid-state structure of monomer 31. Note that the hydroxygroups are disorded with a 50% occupancy.

An analysis of the packing within the crystal, illustrated in (**Figure 4.2.2, left**), shows the expected presence of intermolecular hydrogen-bonding between adjacent catechol moieties (highlighted with the red and blue dotted lines in **Figure 4.2.2, right**). Essentially there is a near-planar arrangement of the molecules within the *a-b* plane of the crystal within which there appears to be a two-dimensional network of hydrogen-bonds (note that this network is in reality incomplete as each of the two catechol units is hydrogen-bonded only to one other catechol).

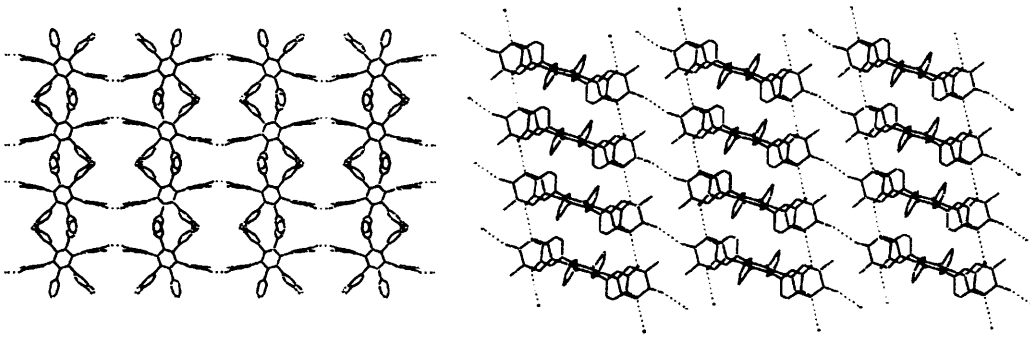

Fig 4.2.2. Packing within the crystal of the monomer **31**. Along c axis (left) and b axis (right).

4.3 Crystal structure of monomer 48.

The crystals from the monomer 48 grew with a very similar unit cell to that of the crystal of the isomeric monomer **31** [monoclinic *C2*; a = 28.468(3); b = 17.9373(17); c = 11.0443(8) Å and angles [α = 90.00; β = 96.119(5); γ = 90.00°]; cell volume = 5607.52 Å^3. It was not possible to locate any included solvent molecules due to the poor quality of the data set. The absence of disordered oxygen in the other phenyl rings, despite the poor data, showed us that this crystal structure is composed solely of the *para* isomer of **48** in which the catechol moieties are in the *para-* (1,4) sites of the central phenyl ring (**Figure 4.3.1**). This result is initially surprising as the product mixture for the formation of **48** should also contain an equal amount of the *meta*-(1,3) isomer. This result implies the reduced solubility of the more symmetrical 1,4-isomer and, therefore its preferential crystallisation.

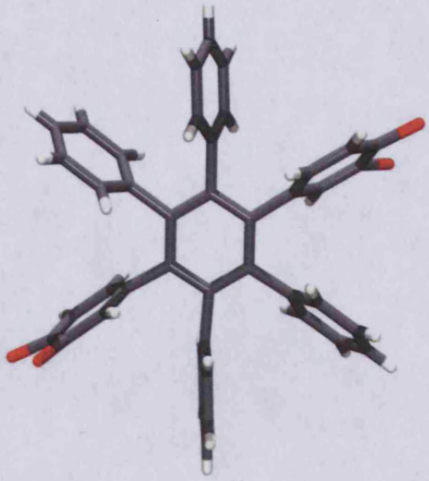

Figure 4.3.1. ORTEP projection of the crystal structure of monomer **48**.

The packing of the monomer **48** (Figure 4.3.2), shows a very similar arrangement and hydrogen-bonding arrangement as that within the crystal of monomer 31.

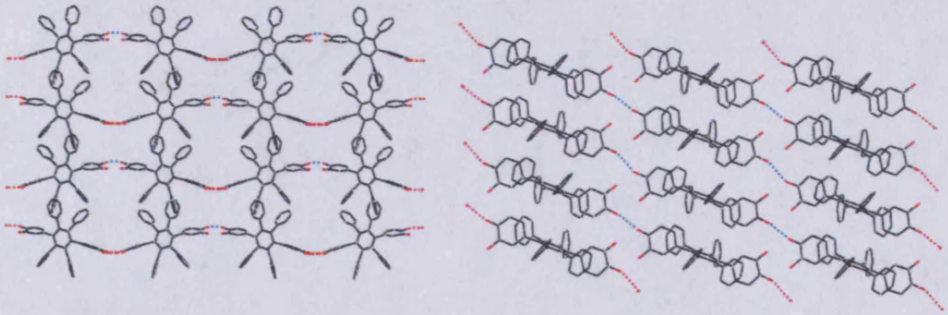

Figure 4.3.2. Packing of the monomer **48**. Along c axis (left) and b axis (right)

4.4 Isolation of the [2+2] cyclic dimer of Polymer 47.

As previously mentioned, one of the outcomes of the polymerisation of monomer **31** was the formation of small oligomers, particularly [2+2], [3+3]....[8+8] cyclic oligomers as characterised by MALDI MS (**Chapter 3; Figure 3.1.2.10**). Monitoring the progress of the polymerization by TLC, there was an isolated spot at relatively low polarity (i.e. high R_f), which looked easy to separate from the large smear at lower R_f. It was anticipated that this spot was the [2 + 2] cyclic dimer formed from two molecules of hexaphenyl monomer **31** and two of tetrafluorophthalonitrile. The isolation of this dimer and its full characterization was of interest, especially because a molecular model of this dimer (**Figure 4.4.1**) suggested it could act as a good macrocyclic host for small aromatics such as benzoquinone and nitrobenzene. The extremely intense fluorescence of PIMs and the presence of the void, suggested its possible application as a material for use in optical sensors.

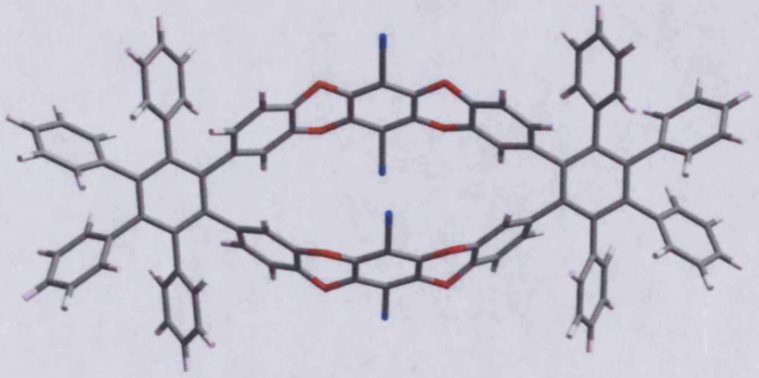

Figure 4.4.1. Model of possible dimer formed in the polymerisation of monomer **31** (Spartan08 molecular modelling software).

The first goal was to isolate the compounds that gave rise to the isolated TLC spot and fully characterise it. The crude reaction mixture from the attempted synthesis of polymer **47** was first purified by flash chromatography on silica (hexane : ethyl acetate) from which we isolated a mixture which gave a number of spots by TLC which ran close to the solvent front. These were isolated from the bulk of the polymer and again passed through a silica column.

By the careful application of a polarity gradient of solvent for the second elution, starting from non-polar (hexane) and gradually increasing in polarity (hexane : ethyl acetate) the desired compound was isolated. NMR and mass spectrometry both confirmed that the compound was the desired cyclic dimer. However, the dimer was isolated only in a very small quantity insufficient for further study. Therefore, we tried to modify the synthesis in order to increase the amount of dimer formed. (**Scheme 4.4.2**)

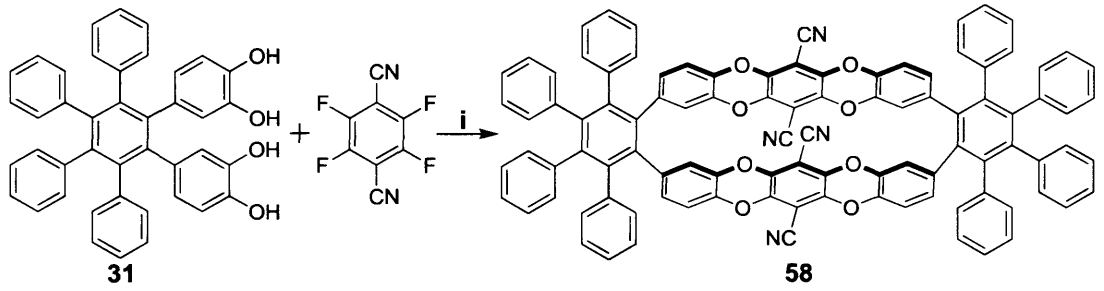

31 **58**

Scheme 4.4.2. Synthetic route to the dimer **58**. Reagents and conditions: i. DMF, K_2CO_3, 65 °C, 15 hrs.

There were a number of factors to be considered; first was the molar ratio of monomer **31** compared to 2,3,5,6,-tetrafluorotrephthalonitrile used in the reaction. Previous studies on cyclic oligomer formation during PIM formation, within the McKeown group, suggest that this can be enhanced by an excess of biscatechol monomer as the anion of the catechol units can back-bite to cause chain scission via an intramolecular reaction to form cyclics. The second factor to be taken into account was the concentration of monomers during the polymerisation reaction. It is generally the case that higher dilution increases the formation of smaller cyclics rather than larger linear polymers. The final factor that was taken into consideration was temperature although it was unknown how this might affect the reaction. Due to the number of different factors to be taken into account, a series of different reactions were set up to try and optimise cyclic dimer formation and these are outlined below (**Table 4.4.3**)

Molar ratio **31:23**	Temperature /°C	Volume of DMF/ml	Yield
1	65	40	8%
2	65	40	14%
2	40	40	6%
2	65	80	4%
2	80	40	< 1%
2	100	40	< 1%
3	65	40	< 1%
4	65	40	< 1%

Table 4.4.3. Showing different conditions in the synthesis of the dimer **59**.

Unfortunately, the yield of cyclic dimer formation in all reactions was very low. However, as shown in the above table, changing the different reaction conditions does have an effect on the yield. Increasing the molar ratio of the biscatechol monomer **31** by a factor of two had the greatest effect on the yield, doubling the amount of dimer formed. Increasing the molar ration further decreased dimer yield as did raising the temperature of the reaction or lowering concentration of the reactants. It is possible that raising the temperature or decreasing concentration allowed competitive reactions (e.g. oxidation of catechol units) to occur. Therefore, the reaction was scaled up, using the optimised conditions so that sufficient quantity was obtained for further study. Evaluation by N_2 adsorption gave a modest but significant value for the surface area of 162 m^2/g (**Isotherm 4.4.4).**

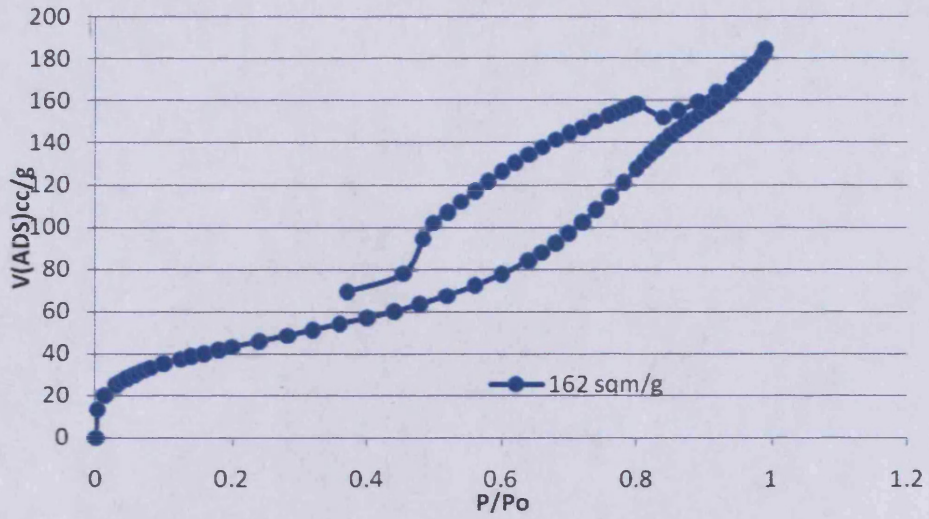

Isotherm 4.4.4. Isotherm of [2+2] cyclic oligomer **59.**

4.5 Solid state crystal structure of the [2+2] cyclic oligomer 59.

Following the successful isolation of a sufficient quantity of the [2 + 2] cyclic oligomer, crystals were grown by the slow diffusion of methanol into chloroform solution. These crystals proved highly unstable to solvent evaporation and a number of attempts at XRD data collection failed due to crystal collapse. Data analysis confirmed the molecular structure of the cyclic oligomer (**Figure 4.5.1**) and proved remarkably similar to the predicted molecular model (**Figure 4.4.1**). Unusually, the dibenzodioxane rings deviate from planarity to relieve ring strain. In all examples of crystal structures of compounds that contain the dibenzodioxane ring held by the Cambridge Structural Database (CSD), the three fused rings are essentially planar relative to one another.[99] The dimension of the macrocyclic cavity is 14.0 x 5.1 Å.

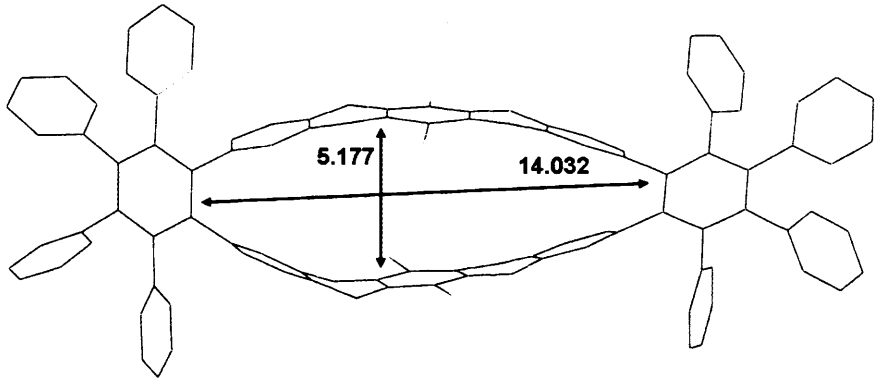

Figure 4.5.1. Solid state crystal structure of the [2+2] cyclic oligomer **59** showing the dimensions of its macrocyclic cavity.

The molecule packs in the monoclinic space group C2/C. The unit cell is large (a = 49.3119(12) Å, b = 25.9637(8) Å, c = 15.3295(4) Å; V = 19558 Å ^{3} and angles α =90; β = 94.7630(10) γ = 90°), with eight [2+2] cyclic oligomer molecules per unit cell. The packing arrangement within the crystal is shown in **Figure 4.5.2**. A large amount of included, highly disordered and poorly defined solvent molecules are included within the crystal (not shown for clarity), and this accounts for its instability and affected the apparent quality of the solution of the crystal structure resulting in a high error factor (Rf = 19.3). The interaction between nitrile groups of two neighbouring molecules within the crystal is typical of nitrile-nitrile dipole-dipole interactions which are often encountered in crystal (and liquid crystal) structures. Investigation of the packing within the crystal structure reveals wide, solvent-filled channels which run along the crystal c axis (**Figure 4.5.3**). Although the observed microporosity of an amorphous powder of the [2 + 2] cyclic oligomer cannot be directly linked to the crystal structure, the large quantity of included solvent within these channels demonstrates the inefficient molecular packing that leads to intrinsic microporosity.

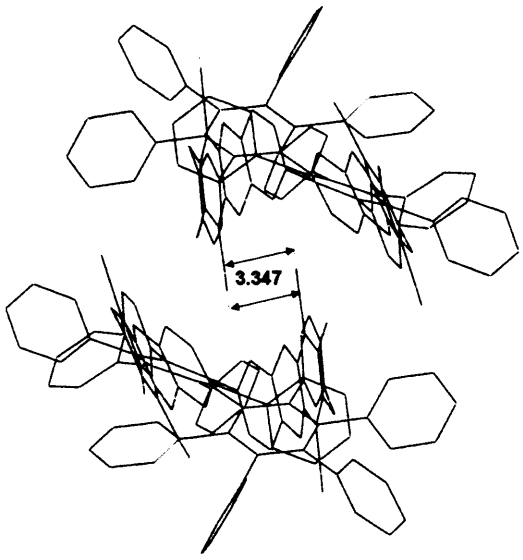

Figure 4.5.2 Solid state crystal structure, interaction of two nitriles groups.

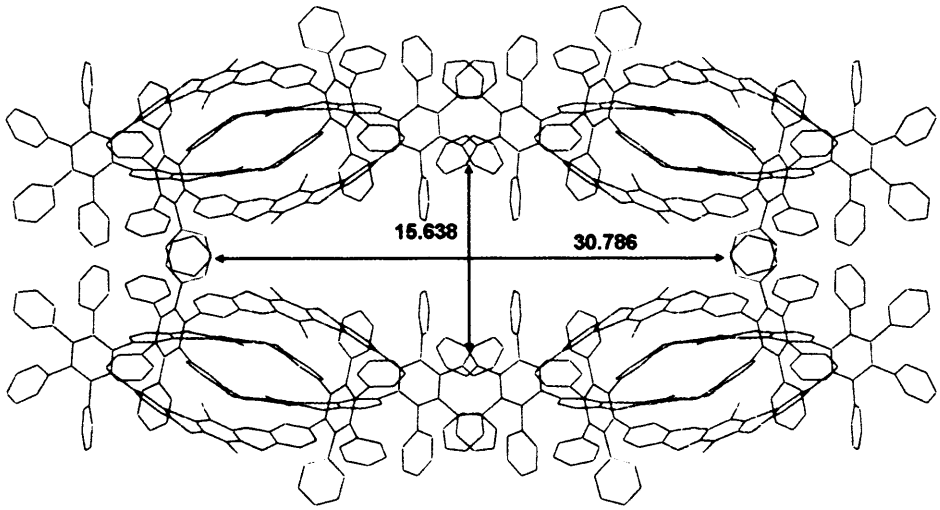

Figure 4.5.3 Solid state crystal structure of the [2 + 2] cyclic dimer, cavity formed by the aromatic moieties during the packing.

4.6 Fluorescence studies on [2+2] cyclic oligomer.

The possible exploitation of the dimer **59** as a fluorescent sensor, for example, in the detection of explosives based on nitrated aromatics, was considered. The dimer is clearly highly emissive in solution and its molecular structure, as shown by XRD analysis, contains a cavity of modest size which might lead to the formation of complexes with aromatic molecules (**Scheme 4.6.1**).

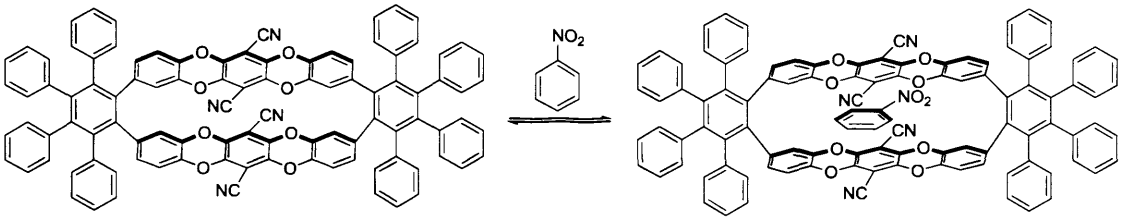

Scheme 4.6.1. Formation of adduct between dimer **59** and nitrobenzene

Fluorescence quenching is one of the sensing methodologies applied for explosives detection.[100] This technique is based on the decrease of the intensity of light emitted from a fluorophore in the presence of an analyte (quencher). Quenching could be static or dynamic, whereas the first involves the formation of a ground-state fluorophore-quencher adduct, and depends on the binding constant of these two species, the second involves momentary collisional interaction between an excited fluorophore with a ground state quencher, and depends on the fluorescence lifetime and the rate of the collision between quencher and fluorophore. In both cases the quenching is generally due to photoinduced electron transfer between the excited state of the fluorophore and the ground state of the quencher.[101] In order to evaluate its potential application as a fluorescent sensor, [2+2] cyclic oligomer **59** was photophysically characterized and some preliminary experiments involving fluorescence quenching were carried out. Absorption, emission, excitation spectra and luminescent lifetimes were measured in different solvents such as THF, DCM, acetone, acetonitrile at room temperature, in order to assess possible solvatochromic effects (**Table 4.6.2**).

SOLVENT	λ_{abs}(log ε)/nm	λ_{em}/nm	λ_{ex}/nm	τ/ns
THF	418 (3.78), 251 (3.61)	476	414	10.7
DCM	421 (3.95), 256 (4.35)	484	417	11.7
Acetone	412 (3.77), 259 (3.32)	480	413	10.3
Acetonitrile	418 (3.60), 242 (4.03)	487	414	9.9

Table 4.6.2. The effect of solvent on the UV/visible absorption spectrum and photophysical properties of dimer **59**.

As it is possible to see from the data reported in **Table 4.6.2** the different solvents did not appear to influence significantly the photophysical behaviour of **59**. The UV-vis spectra showed two absorption bands at *ca.* 250 nm and at *ca.* 420 nm, the first one could be assigned to $\pi \rightarrow \pi^*$ transitions and the one with lower energy probably to charge transfer (CT) deriving from oxygens (n) in the dioxane rings to the nitriles (π^*).[102] The dimer exhibited similar emission and moderate Stokes shifts (about 3500 cm^{-1}) following irradiation at the lowest energy absorption (λ_{ex} 420 nm) in all the solvents (**Figure 4.6.3**) with emission lifetimes (9.9-11.7 ns) typical of a fluorescence event.

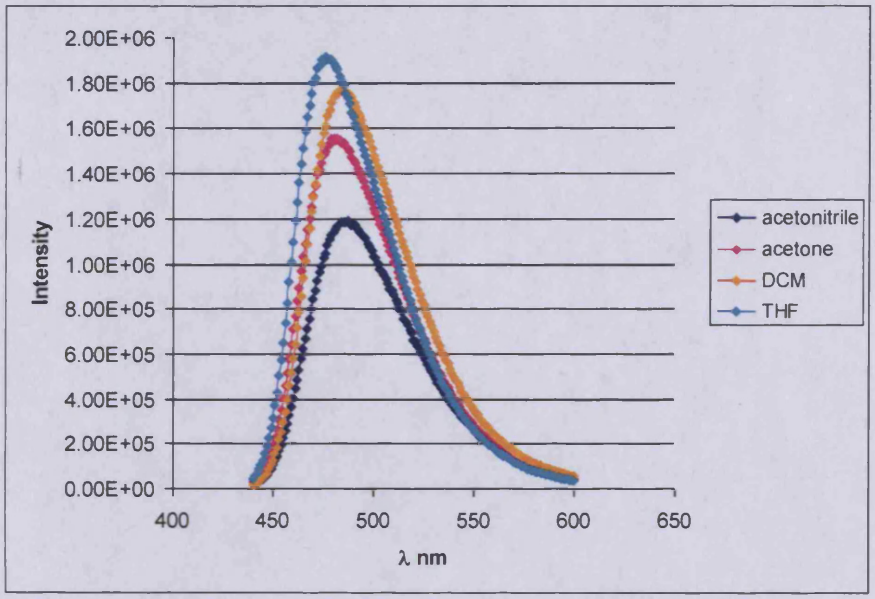

Figure 4.6.3. Fluorescence emission spectra of the [2+2] cyclic oligomer **59** in different solvents with λ_{ex} = 420 nm.

After the assessment of the photophysical properties of the dimer in various solvents, preliminary evaluation of fluorescence quenching was performed using nitrobenzene, which can be considered a model compound for a nitrated aromatic explosive. The experiments were carried out by adding known amounts of the quencher (from *ca.* 10^{-4} to 10^{-2} M in the analysed solutions) to a dilute solution of the fluorophore **59**, *ca.* 10^{-5} M in THF and in THF/H_2O, so that the concentration of the fluorophore was kept almost constant and emission spectra were then measured (**Figure 4.6.4, Figure 4.6.5**). Even a large molar ratio of nitrobenzene to **59** (1000:1) was insufficient to wholly quench the fluorescence.

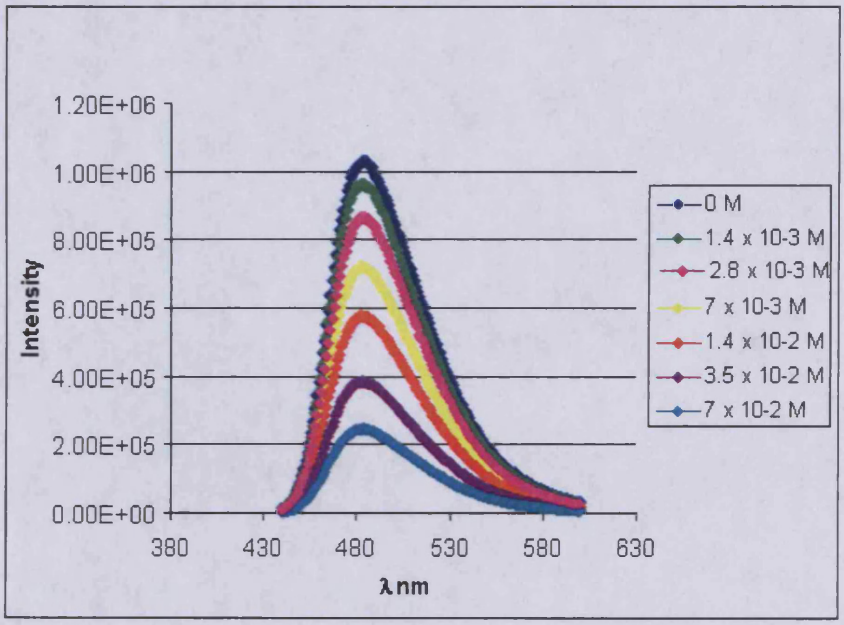

Figure 4.6.4. Fluorescent emission spectra of **59** 7 x 10^{-5} M in THF/H_2O with the addition of various amounts of nitrobenzene.

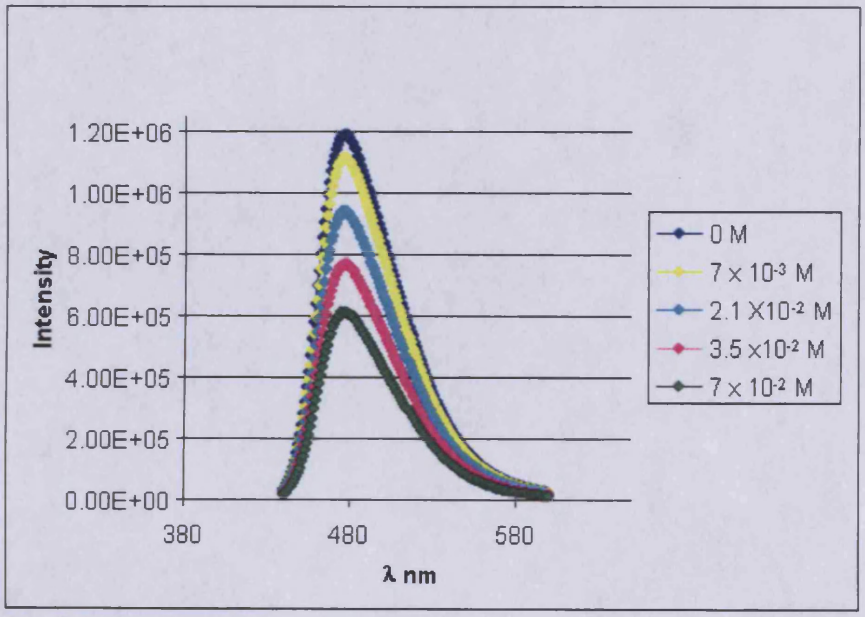

Figure 4.6.5. Fluorescent emission spectra of **59** 7 x 10^{-5} M in THF with the addition of various amounts of nitrobenzene

Furthermore, fluorescence lifetimes for the dimer before and after addition of quencher were measured in both solvent systems. In THF the excited sate lifetime decreased from 10.7 ns, in absence of quencher, to 4.1 ns when the quencher concentration was 1 x 10^{-1} M and in THF/H_2O from 10.1 to 3.3 ns when the concentration of the quencher was 7 x 10^{-2} M. The addition of H_2O is likely to enhance the hydrophobic interactions between the dimer and the quencher and also enhance the possibilities of formation of a complex. From the emission spectra (**Figure 4.6.4** and **Figure 4.6.5**) it is possible to observe that quenching, as expected, was more effective in the presence of H_2O. From these preliminary results it seems probably that quenching is predominantly working through a dynamic mechanism, as suggested by the decrease in lifetime of the excited state. Generally for static quenching, the lifetime does not change since only the free fluorophore molecules are observed and they have the unquenched lifetime τ_0. Instead, dynamic collisional quenching is characterized by an equivalent decrease in fluorescence intensity and excited state lifetime, which is described by the equation $I_0/I = \tau_0/\tau$ where I_0 and I are respectively the emission intensities in the absence or presence of quencher (and τ_0 and τ are the respective lifetimes).[103] Further studies are necessary to understand if simultaneous static quenching is occurring and to determine the sensitivity and selectivity to different quenchers.

Chapter 5

Chapter 5. Future work

5.1 Further membrane forming hexaphenylbenzene-based polymers.

Polymer 2 shows that PIMs of high molecular mass can be prepared from monomers based on hexaphenylbenzene so long as the reactive units are placed on non-adjacent phenyl groups. Our collaborator, Dr. Detlev Fritsch of GKSS, believes that polymers with more polar substituents provide membranes with higher selectivity as compared to related non-polar polymers. Therefore, it will be of interest to make derivatives of polymer **55** that contain polar substituents on the phenyl groups (**Figure 5.1.1**).

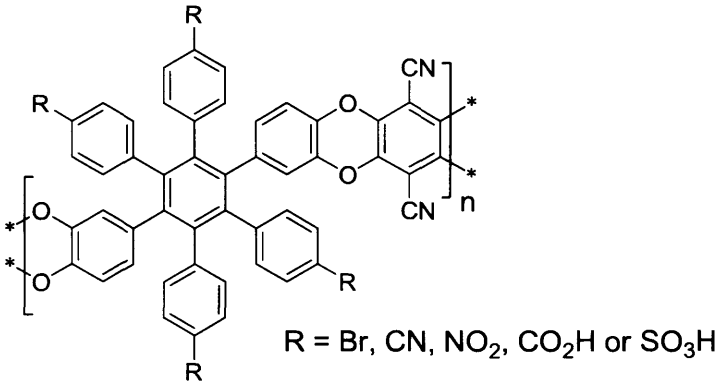

Figure 5.1.1. Potential hexaphenylbenzene-based PIMs

The 4-position of the phenyl susbtituents is activated towards electrophilic substitution so the addition of bromine, nitro- or sulfonate groups should be straightforward. Substitution reactions with CuCN will provide the nitrile substituents and hydrolysis of these nitrile groups the carboxylic acids. The carboxylate and sulfonate substituents may provide water-soluble PIMs and these materials may also be of interest for proton transport membranes for use within fuel cells.

5.2 Large shape resistant catalysts for PIM-based flow chemistry.

There has been recent interest in using PIMs as a nanofiltration membrane, for the application in flow chemistry. Dr. Detlev Fritsch of GKSS in collaboration with Evonik (Germany) have demonstrated the high level of retention (> 98%) of the bulky model compound 1,2,3,4,5,6-hexaphenylbenzene (diameter = 1.4 nm) when using PIM-1 as a membrane materials for nanofiltration (**Figure 5.2.1**)

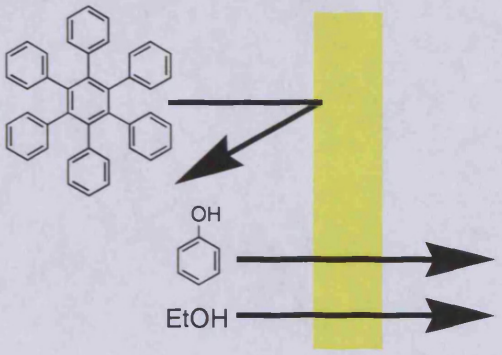

Figure 5.2.1. Schematic of nanofiltration using PIM-1 as the membrane.

Therefore, it is of interest to design homogeneous catalysts based on hexaphenylbenzene that would be retained by a PIM-1 membrane. Using similar synthetic strategies to those used previously in this research project, a large catalyst based on the useful S-Phos ligand designed by Buchwald, which has been used for a number of reactions including Suzuki Couplings.[104,105,106]

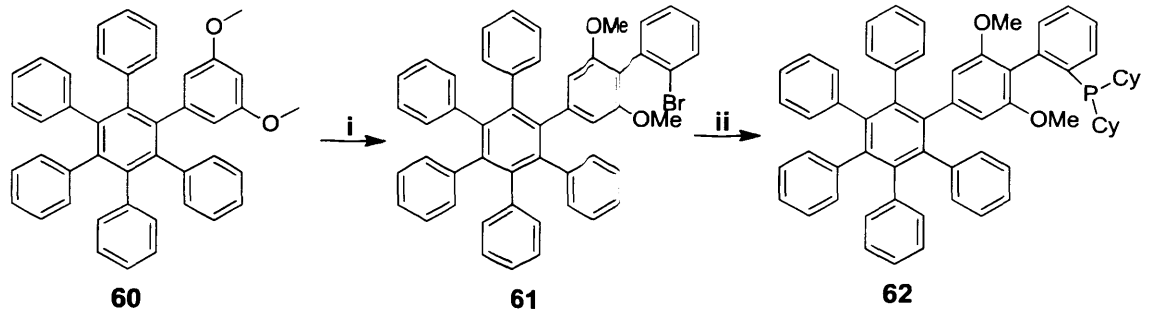

Figure 5.2.2. Proposed synthesis of large ligand based on that of Buchwald's S-Phos ligand. Reagents and conditions: i. *n*-BuLi, 1-bromo-2-chlorobenzene: ii. *n*-BuLi, dicyclohexylchlorophosphine

The starting material for the synthesis of this ligand, as shown in **Figure 5.2.2**, is 1-(3',5'-dimethoxyphenyl)-2,3,4,5,6-pentaphenylbenzene **60**, which was prepared in the course of the research project by employing a Sonogashira coupling reaction between phenylacetylene and 1-bromo-3,5-dimethoxybenzene to give 1,3-dimethoxy-5-(phenylethynyl)benzene (yield = 74%), followed by the Diels-Alder reaction with 2,3,4,5-tetraphenylcyclopentadienone. Due to time constraints the synthesis of the ligand was not completed but it would be of interest for future work.

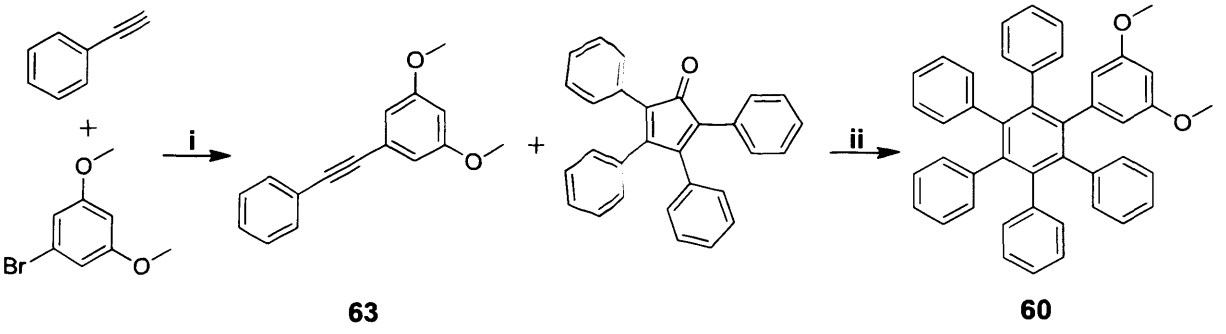

Figure 5.2.3. The synthesis of 1-(3',5'-dimethoxyphenyl)-2,3,4,5,6-pentaphenylbenzene **60**. Reagents and conditions: $[P(Ph)_3]_2PdCl_2$, CuI, Et_3N, DMF, 90 °C; ii. Ph_2O, reflux, 15 hrs.

Chapter 6

Chapter 6. Experimental techniques.

6.1 General techniques and materials

Commercially available reagents were used without further purification. Anhydrous dichloromethane was obtained by distillation over calcium hydride under nitrogen atmosphere. Dry THF was obtained by pre-drying commercially available THF over sodium in presence of sodium benzophenone as indicator. Anhydrous *N,N*-dimethylformamide was bought from Aldrich. All reactions using air/moisture sensitive reagents were performed in oven-dried or flame-dried apparatus, under a nitrogen atmosphere. TLC analysis refers to analytical thin layer chromatography, using aluminum-backed plates coated with Merck Kieselgel 60 GF_{254}. Product spots were viewed either by UV fluorescence, or by staining with a solution of Cerium Sulfate in aqueous H_2SO_4. Flash chromatography was performed on silica gel 60A (35-70 micron) chromatography grade (Fisher Scientific). Under vacuum refers to evaporation at reduced pressure using a rotary evaporator and diaphragm pump, followed by the removal of trace volatiles using a vacuum oven. Melting points were recorded using a Gallenkamp Melting Point Apparatus and are uncorrected.

InfraRed spectra (IR). Infrared spectra were recorded in the range 4000-600 cm^{-1} using a Perkin-Elmer 1600 series FTIR instrument either as a thin film or as a nujol mull between sodium chloride plates. All absorptions are quoted in cm^{-1}.

Nuclear Magnetic Resonance (NMR). ^1H NMR spectra were recorded in $CDCl_3$ (unless otherwise stated) using an Avance Bruker DPX 400 instrument (400 MHz) or an Avance Bruker DPX 500 (500 MHz), with ^{13}C NMR spectra recorded at 100 MHz or 125 MHz respectively. Chemical shifts (δ_H and δ_C) were recorded in parts per million (ppm) from tetramethylsilane (or chloroform) and are corrected to 0.00 (TMS) and 7.26 ($CHCl_3$) for ^1H NMR and 77.00 ($CHCl_3$), centre line, for ^{13}C NMR. The abbreviations s, d, t, q, m and br. denote singlet, doublet, triplet, quartet, multiplet and broadened resonances; all coupling constants were recorded in hertz (Hz).

Mass spectrometry. Low-resolution mass spectrometric data were determined using a Fisons VG Platform II quadrupole instrument using electrospray ionisation (ES) unless otherwise stated. High-resolution mass spectrometric data were obtained in electrospray (ES) mode unless otherwise reported, on a Waters Q-TOF micromass spectrometer.

MALDI-TOF analysis was performed with a Waters MALDI Micro MX spectrometer.

Nitrogen adsorption/desorption. Low-temperature (77 K) N_2 adsorption/desorption measurements of PIM powders were made using a Coulter SA3100. Samples were degassed for 800 min at 120 °C under high vacuum prior to analysis.

Thermo-Gravimetric Analysis (TGA). The TGA was performed using the device Thermal Analysis SDT Q600 at a heating rate of 20 °C/min from room temperature to 1000 °C.

X-Ray crystal structure determination were made in Cardiff using a Bruker-Nonius Kappa CCD area-detector diffractometer equipped with an Oxford Cryostream low temperature cooling device operating at 150(2) K (λ = 0.71073 Å).

Gel permeation chromatography was carried out at Cardiff University using a GPC MAX variable loop equipped with two KF-805L SHODEX columns in THF, with a RI(VE3580) detector using a GPC MAX pump operating at flow rate of 1 ml/min. Calibration was achieved using a series of Viscotek polystyrene standards up to Mw = 9.4* 10^5.

Photophysical data were obtained on a JobinYvon-Horiba Fluorolog spectrometer fitted with a JY TBX picoseconds photodetection module. Luminescence lifetime profiles were obtained using the JobinYvon-Horiba FluoroHub single photon counting module and the data fits yielded the lifetime values using the provided DAS9 deconvolution software.

6.2. Synthesis of materials.

6.2.1 Diethyl 3,3-bis(4-hydroxyphenyl)pentanedioate 1.

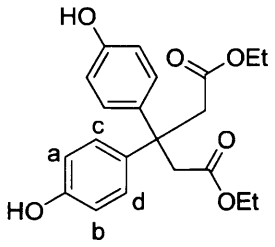

In a round bottom flask diethyl 3-oxopentanedioate (1.00 g, 4.95 mmol) and sulfuric acid (5 ml) where stirred in a round bottom flask for 1 hr. This was then quenched with water (50 ml) and extracted using DCM (2 x 50 ml) and washed again with water (3 x 30 ml). The organic solvent was evaporated under vacuum to give a light yellow powder of diethyl 3,3-bis(4-hydroxyphenyl)pentanedioate **1** (1.14 g, 62%). M.p. 138 – 142 °C; IR (nujol)/cm^{-1} 1673.9, 1451.6, 1377.8, 1346.5, 1264.5, 1152.7, 1071.7, 1026.9; ^{1}H NMR (400 MHz; $CDCl_3$) δ 6.98 (s, 2H, H_a) 6.96 (s, 2H, H_b) 6.65 (s, 2H, H_c) 6.63 (s,2H, H_d) 3.38 (q, 4H, J = 7.1 Hz, C**H**$_2$CH$_3$) 3.45 (s, 4H, CH_2) 1.01 (t, 6H, C**H**$_3$CH$_2$); ^{13}C NMR (100 MHz; $CDCl_3$) 171.8, 154.0, 138.3, 128.5, 114.7, 60.2, 45.8, 42.8, 13.9, LRMS, (EI$^+$), *m/z*: (M$^+$ 373, 100%).

6.2.2 Diethyl 3,3-bis(4-(3,4-dicyanophenoxy)phenyl)-pentanedioate 2

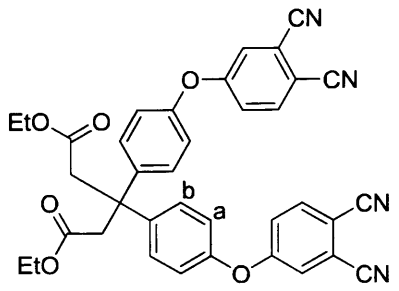

In a round bottom flask 3,3-bis(4-hydroxyphenyl)pentanedioate **1** (1.00 g, 2.69 mmol) was stirred under nitrogen with 4-nitrophthalonitrile (1.40 g, 8.07 mmol) and heated to 120 °C. Once at temperature, K_2CO_3 (1.49 g, 10.76 mmol) was added. The reaction was left for 15 hrs and quenched with water (50 ml). This was then filtered to give the product as an off white powder. (1.04 g, 62%). M.p. 150 – 152 °C; IR (film)/cm^{-1} 3945.6, 3675.1, 3056.6, 2984.3, 2685.3, 2593.3, 2305.9, 2233.6, 1901.4, 1732.7, 1592.9, 1564.9, 1486.3, 1422.7, 1370.1, 1265.5, 1177.3, 1119.9, 1088.6, 1016.3, 990.2, 953.6, 895.7, 838.4, 734.2, 524.5; ^{1}H NMR (400 MHz; $CDCl_3$) 7.70 (d, 2H, J = 8.1 Hz, H_a) 7.36 (m, 8H, H_{Ar}) 6.80 (d, 4H, J = 8.1, H_b) 3.58 (q, 4H, CH_2CH_3) 3.51 (s, 4H, CH_2) 1.02 (t, 6H, CH_2CH_3); 13C NMR (100 MHz; $CDCl_3$) 171,2; 161,8; 152,5; 144,3; 135,8; 130,2; 122,1; 121,7; 120,5; 118,0; 115,7; 115,3; 109,5; 60,8; 47,0; 42,9; 14,5; LRMS, (EI^+), *m/z*: (M^+ 625, 100%).

6.2.3. 3,4-Bis(4-methoxyphenyl)-2,5-diphenylcyclopenta-2,4-dienone 11

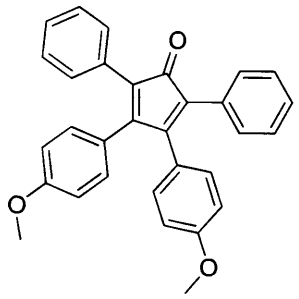

In a round bottom flask 1,2-bis(4-methoxyphenyl)ethane-1,2-dione (2.70g , 10.00 mmol) and 1,3-diphenylpropan-2-one (2.10 g, 10.00 mmol) were heated in EtOH (50 ml) to 80 °C. KOH was added (0.56 g, 10.00 mmol) and the reaction left for 20 min. The reaction was filtered and the dark purple solid washed with EtOH and dried to give the desired product **11** (3.81 g, 83%). M.p. 208 – 211 °C; IR (film)/cm^{-1} 3054.2, 2986.7, 2305.4, 1707.6, 1606.9, 1511.4, 1421.7, 1265, 1177.3, 1029.3, 896.2, 842.2, 737.1, 705.3; ^{1}H NMR (400 MHz, $CDCl_3$) δ 7.22 (m, 10H, H_{Ar}), 6.84 (m, 4H, H_{Ar}), 6.68 (m, 4H, H_{Ar}). ^{13}C NMR (100 MHz, $CDCl_3$) 158.6, 158.6, 152.9, 130.1, 129.0, 126.9, 126.1, 126.0, 124.1, 123.6, 112.3, 54.1. LRMS, *m/z*, ($APCl^+$) 445 (M^+, 100%).

6.2.4 1,2-(1-Methoxyphenyl)-3,4,5,6-tetraphenylbenzene 12

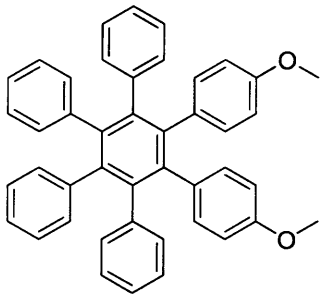

In a round bottom flask 3,4-bis(4-methoxyphenyl)-2,5-diphenylcyclopenta-2,4-dienone **11** (3.00 g, 6.75 mmol) and diphenylacetylene (1.32 g, 7.43 mmol) were stirred in Ph_2O (10 ml) and refluxed for 15 hrs. This was then allowed to cool and poured into cold MeOH. Hexane (50 ml) was added to dissolve up most of the Ph_2O. This was then filtered and purified by column chromatography (hexane : ethyl acetate, 7 : 3) to give a light orange powder of the desired product **12** (3.39g, 73%). M.p. 276 – 278 °C; IR(film)/cm^{-1} 3054.2, 2986.7, 2685.3, 2305.4, 1610.2, 1515.7, 1441.4, 1421.7, 1265.5, 1176.8, 1030.2, 895.7, 843.7, 737.1; ^{1}H NMR (400 MHz; $CDCl_3$) δ 6.85 (m, 20H, H_{Ar}) 6.71 (m, 4H, H_{Ar}) 6.41 (m, 4H, H_{Ar}) 3.61(s, 6H, OMe). ^{13}C NMR (100 MHz; $CDCl_3$) δ157.3, 141.2, 141.1, 140.9, 140.5, 140.5, 133.5,

132.8, 131.8, 127.0, 126.9, 125.5, 125.4, 119.3, 112.5, 55.3. LRMS, *m/z*, (EI^+) 594 (M, 100%).

6.2.5 Synthesis of 1,2-Di-(4'-hydroxyphenyl)-3,4,5,6-tetraphenylbenzene 13

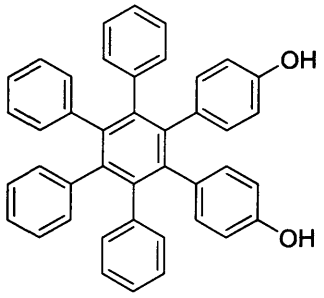

In a two-necked round bottom flask was added 1,2-(1-methoxyphenyl)-3,4,5,6-tetraphenylbenzene **12** (1.00 g, 1.68 mmol) to dry dichloromethane (30 ml) was added under a dry nitrogen atmosphere that was maintained throughout the reaction. This mixture was cooled to 0 °C then boron tribromide (1.05 g, 4.21 mmol) was added dropwise and the reaction stirred at room temperature for a further 30 min. The reaction was poured into ice and left under vigorous stirring allowing the evaporation of excess dichloromethane. The precipitate was filtered off, washed with water and dried. Recrystallization from dichloromethane/hexane (1/1) gave the desired compound as an off-white solid **13** (0.4 g, 89%) M.p. + 360 °C; IR(film)cm^{-1} 3521.3, 3055.1, 1611,7, 1516.7, 1440.0, 1265.5, 1177.3, 1073.1, 1029.8, 896.2, 802.7, 739.5, 704.3; ^1H NMR (400 MHz; Acetone d^6) δ 6.79 (m, 20H, H_{Ar}) 6.54 (m, 4H, H_{Ar}) 6.23 (m, 4H, H_{Ar}); ^{13}C NMR (100 MHz; Acetone d^6) δ 148.2, 144.2, 143.2, 143.1, 142.9, 142.6, 141.1, 139.0, 138.7, 136.2, 133.9, 128.7, 119.4, 116.1; LRMS, (EI), *m/z*: 566 (M, 100%).

6.2.6. 1,2-Di(4'-(3'',4''-dicyano)phenoxy)-3,4,5,6-tetraphenyl-benzene 14.

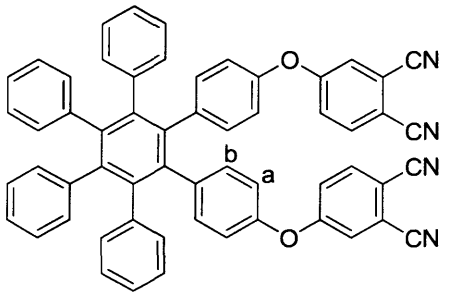

In a round bottom flask 1,2-(1-hydroxyphenyl)-3,4,5,6-tetraphenylbenzene **13** (1.00 g, 1.80 mmol) was stirred under nitrogen with 4-nitrophthalonitrile (0.93 g, 5.40 mmol) and heated to 120 °C. Once at temperature K_2CO_3 (1.00 g, 7.20 mmol) was added. The reaction was left for 15 hrs and quenched with water (50 ml). This was then filtered to give the product as an off-white powder. (1.04 g, 62%). M.p. 150 – 153 °C; IR (film)/cm^{-1} 3055.1, 2435.6, 1625,7, 1547.8, 1443.2, 1283.5, 1179.4, 1067.9, 1034.8, 3.2, 812.6, 754.6, 726.5; ^{1}H NMR (400 MHz; $CDCl_3$) δ 7.65 (d, 4H, J = 8.7 Hz, H_a) 7.08 (d, 4H, J = 8.7 Hz, H_b) 6.96 (m, 20H, H_{Ar}) 6.61 (m, 6H, H_{Ar}); ^{13}C NMR (100 MHz; $CDCl_3$) 162,6; 151,3; 141,4; 141,0; 140,5; 140,3; 139,8; 139,2; 135,6; 134,0; 131,7; 131,6; 127,3; 127,2; 126,3; 126,0; 122,1; 120,4; 120,1; 117,8; 115,8; 115,3; 108,9; LRMS, (EI), *m/z*: (M^+ 818, 100%).

6.2.7. 5,6-Dichloroisobenzofuran-1,3-dione 5

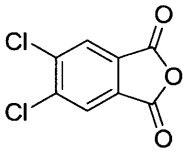

4,5-Dichlorophthalic acid (90 g, 381 mmol) and acetic anhydride (150 ml) were heated under gentle reflux for 5 h with slow distillation of solvent (20 ml). After cooling, the off-white solid was filtered, washed with petroleum ether and dried under vacuum (77.8 g, 95%). M.p.184-

186 (lit m.p. 184-186°C); IR (film)/cm^{-1} 1830, 1786, 1378, 1310, 1248, 1094, 915, 733; ^{1}H NMR (400 MHz; $CDCl_3$) δ 8.44 (s, 2H, H_{Ar}); ^{13}C NMR (100 MHz; $CDCl_3$) δ 161.1, 139.1, 131.1, 127.0; LRMS, (EI), *m/z*: (M^+ 216, 35%).

6.2.8. 5,6-Dichloroisoindoline-1,3-dione 6

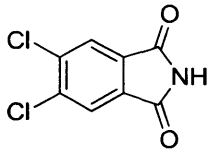

5,6-Dichlorobenzofuran-1,3-dione ***5*** (77 g, 356 mmol) in formamide (100 ml) was heated at reflux for 3 h, under stirring. After cooling, the precipitate off-white formed was filtered, washed with water and dried under vacuum (75.36 g, 98%). M.p. 202-203 (lit[20] m.p. 193-195°C); IR 3225, 1711, 1345, 1059, 906, 742 cm^{-1}; ^{1}H NMR (400 MHz; $CDCl_3$) δ 8.05 (s, 2H, H_{Ar}); ^{13}C NMR (100 MHz; $CDCl_3$) δ 167.0, 136.9, 132.4, 124.9; LRMS, (EI), *m/z*: 215 (M^+, 100%).

6.2.9. 4,5-Dichlorobenzene-1,2-diamide 7

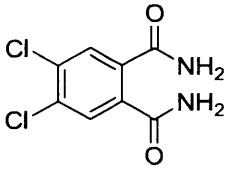

5,6-Dichloroisoindoline-1,3-dione **6** (75 g, 347 mmol) was stirred for 24 h in 25% NH_4OH (900 ml) then 33% NH_4OH was added and stirring was continued for another 24 h. The precipitate was filtered, washed with water and dried under vacuum (60 g, 70%). M.p. 235-237 °C (lit[20] m.p. 245-247 °C); IR (nujol)/cm^{-1} 3426, 3296, 3131, 1667, 1608, 1173, 1121, 916, 897; ^{1}H NMR (400 MHz; $CDCl_3$) δ 7.84 (s, 2H, NH_2), 7.71 (s, 2H, H_{Ar}), 7.46 (s, 2H,

NH_2); ^{13}C NMR (100 MHz; $CDCl_3$) δ 167.3, 136.2, 131.4, 129.3; LRMS, (EI), *m/z:* 232 ($M^{\bullet+}$, 100%).

6.2.10. 4,5- Dichlorophthalonitrile 8

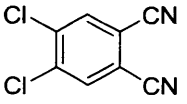

At 0 °C, $SOCl_2$ (200 ml) was added under stirring and under N_2 to anhydrous DMF (300 ml). After 2 h, 4,5-dichlorobenzene-1,2-diamide 7 (60 g, 257 mmol) was added and the mixture was stirred at 0 °C for 5 h then at r.t. for 20 h. The mixture was slowly added to ice water to quench the excess of $SOCl_2$. The light green product was collected by filtration and washed with water, then recrystallized twice from methanol (38 g, 75%). M.p. 180-183 °C (litref m.p. 182-184°C); IR (film)/cm^{-1} 2916, 2237, 1815, 1467, 1348, 1262, 1217, 1132, 917, 683; ^1H NMR (400 MHz; $CDCl_3$) δ 7.91 (s, 2H, H_{Ar}); ^{13}C NMR (100 MHz; $CDCl_3$) δ 139.0, 134.9, 114.9, 113.6; LRMS, (APCI), *m/z*: 197 (MH^+, 100

6.2.11. 4-(2,6-Diisopropylphenoxy)phthalonitrile 4

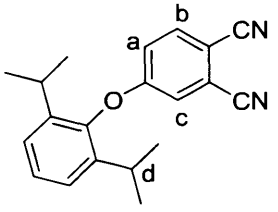

In a round bottom flask, 4-nitrophthalonitrile (1.00 g, 5.70 mmol) and 2,6-diisopropylphenol (1.21 g, 6.80 mmol) in DMF (10 ml) was stirred in nitrogen. K_2CO_3 was added and the reaction monitored by TLC. Once the reaction was complete water (300 ml) was added and then the product was extracted with ethyl acetate (3 x 100 ml). The combined organic layer was washed with NaOH solution (100 ml), washed with (3 x 75 ml) and dried with $MgSO_4$. The solvent was removed under reduced pressure to give white needle like crystals (1.32

g,76%) .M.p. 115 – 116 °C; ^{1}H NMR (400 MHz, $CDCl_3$) δ 7.74 (d, 1H, J = 8.1 Hz, H_a), 7.33 (m, 3H, H_{Ar}), 7.23 (br s, 1H, H_b), 7.13 (br d, J = 8.1 Hz, H_c) 2.87 (sept, J = 7.0 Hz, H_d) 1.18 (d, 12H J = 7.0 Hz, CH_3); ^{13}C NMR (100 MHz, $CDCl_3$) δ 162.3, 146.8, 140.8, 135.4 127.3, 125.1, 119.8, 119.4, 117.7, 115.4, 114.9, 108.2, 27.1, 23.2; LRMS(APCI$^+$), *m/z*: 305.

6.2.12. 4,5-Bis(2',6'-di-iso-propylphenoxy)phthalonitrile31 9

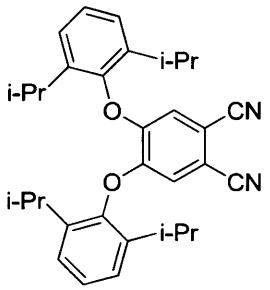

Anhydrous potassium carbonate (26.24 g, 190.0mmol) was added to a solution of 2,6-di-*iso*-propylphenol (25.40 g, 142.5 mmol) and 4,5-dichlorophthalonitrile 8 (9.35 g, 47.5 mmol) in anhydrous dimethylformamide, this was monitored by TLC until all the starting material was consumed. Once consumed the reaction was quenched with water and filtered to give the crude compound which was purified by recrystallization from methanol (14.69 g, 65%). Mp 161-163 °C; IR (nujol)/cm^{-1} 3080, 2228, 1589, 1503, 1332, 1096, 881, 795; ^{1}H NMR (400 MHz; $CDCl_3$) δ 7.26 (m, 6H, Ar*H*), 6.69 (s, 2H, Ar*H*), 2.87 (sept, 4H, J = 6.7 Hz, CH_3CHCH_3), 1.18 (d, 12H, J = 6.7 Hz, CH_3CHCH_3), 1.10 (d, 12H, J = 6.7 Hz, CH_3CHCH_3); ^{13}C NMR (100 MHz; $CDCl_3$) δ 151.4, 147.0, 140.6, 127.3, 125.1, 117.7, 115.3, 109.1, 27.4, 24.1, 22.4; LRMS, (APCI), m/z: 481 (M^+, 100%); HRMS $C_{32}H_{36}O_2N_2$ requires 480.2777 found 480.2796.

6.2.13. 2,2',3,3',5,5',6,6'-Octafluorobiphenyl-4,4'-dicarbonitrile 32

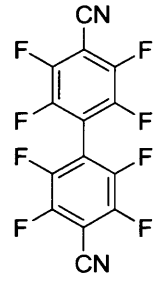

Pentafluorobenzonitrile (4.79 g, 0.025 mol) was dissolved in dry diethylether (30 mL) and stirred under nitrogen for 10 mins. Hexaethylphosphoroustriamide (3.07 g, 0.0125 mol) was then added dropwise and the reaction stirred under nitrogen at room temp. After 3 hrs the deep-red solution was neutralised with hydrochloric acid and concentrated under reduced pressure. The resultant red/brown solid was purified via column chromatography using 70 % dichloromethane and 30 % hexane as the mobile phase. The pure product was eluted first, concentrated under reduced pressure and recrystallized from methanol to give 2,2',3,3',5,5',6,6'-octafluorobiphenyl-4,4'-dicarbonitrile (1.23 g, 14.2 %) as white needle-like crystals. ^{19}F NMR (300 MHz, $CDCl_3$, ppm) -129.5 (1F, s), -133.3 (1F, s); ^{13}C NMR (100 MHz, $CDCl_3$, ppm) 97.6, 106.9, 112.2, 143.1, 145.7, 146.4, 149.1. Mp 109-111 °C (MeOH)

6.2.14. 1,2-Dimethoxy-4-(phenylethynyl)benzene 35

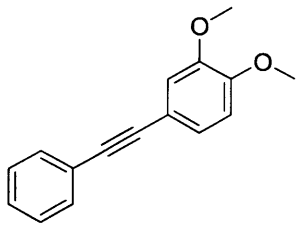

A mixture of 4-bromoveratrole (0.61 g, 2.82 mmol) Et_3N (4 ml) and DMF (4 ml) were deoxygenated in a round bottom flask under a nitrogen atmosphere. 4-Ethynyl-1,2-

dimethoxybenzene (0.32 g, 3.10 mmol) was added and the reaction heated to 90 °C to which CuI (53.7 mg, 0.28 mmol) and $[P(Ph)_3]_2PdCl_2$ (0.198g, 0.28 mmol) were added and the reaction left for 15 hrs. The reaction was then quenched with water (40 ml) and allowed to stir for 1hr. This was then extracted using DCM (3 x 30ml), the organic layers were combined washed with water (3 x 20 ml) and dried with $MgSO_4$. The solvent was removed under reduced pressure and purification by column chromatography gave the desired product as a yellow solid (0.47, 70%) M.p 94 - 95 °C (lit m.p 93 - 95 °C)ref IR(film)/cm^{-1} 2362.8, 1594.3, 1512.3, 1465.1, 1327.7, 1251, 1225, 1138.2, 1124.3, 1024.5, 849, 810.4, 763.6, 692.8; ^1H NMR (400 MHz; $CDCl_3$) δ 7.98 (m, 1H, H_{Ar}), 7.96 (m, 1H, H_{Ar}), 7.64 (m, 2H, H_{Ar}), 7.50 (m, 3H, H_{Ar}), 6.89 (d, 1H, H_{Ar}), 3.96 (s, 3H, OMe) 3.95 (s, 3H, OMe). ^{13}C NMR (100 MHz; $CDCl_3$) δ 149.4, 148.5, 131.4, 128.3, 127.9, 124.8, 123.3, 115.3, 114.1, 110.9, 89.415, 87.9, 55.8, 55.8. LRMS, *m/z*, ($APCl^+$) 239 (M^+, 100%) 240 (M^{2+}, 20%)

6.2.15. 1-(1,2-Dimethoxyphenyl)-2,3,4,5,6-pentaphenylbenzene 36

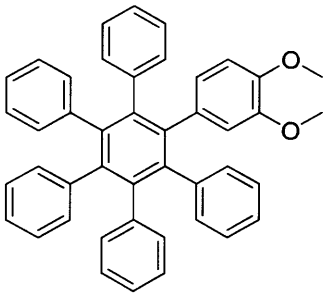

In a round bottom flask 2,3,4,5-tetraphenylcyclopenta-2,4-dienone (3.00 g, 7.81 mmol) and 1,2-dimethoxy-4-(phenylethynyl)benzene **35** (2.23 g, 9.37 mmol) were stirred in Ph_2O (8 ml) and refluxed for 15 hrs. This was then allowed to cool and poured into cold MeOH. Hexane (50 ml) was added to dissolve up most of the Ph_2O. This was then filtered and purified by column chromatography (hexane : ethyl acetate, 7 : 3) to give a light orange powder of the desired product (3.39g, 73%). M.p. 264 – 266 °C; IR (film)cm^{-1} 3062.3, 2895.8, 2735.4, 2467.3, 1535.8, 1476.8, 1436.8, 1264.6, 1041.3, 887.9, 745.6 ^1H NMR (500 MHz; $CDCl_3$) δ 6.84 (m, 25H, H_{Ar}) 6.35 (m, 3H, H_{Ar}) 3.68 (s, 3H, OMe) 3.42 (s, 3H, OMe). ^{13}C NMR

(125 MHz; $CDCl_3$) δ 147.2, 146.4, 144.3, 140.8, 140.6, 140.6, 140.4, 140.4, 140.2, 139.8, 133.0, 132.9, 131.4, 131.4, 131.3, 131.2, 126.7, 126.6, 126.5, 124.2, 115.6, 109.5, 55.5, 55.4. LRMS, *m/z*, (EI^+) 594 (M, 100%).

6.2.16. 1-(1,2-Dihydroxyphenyl)-2,3,4,5,6-pentaphenylbenzene 33

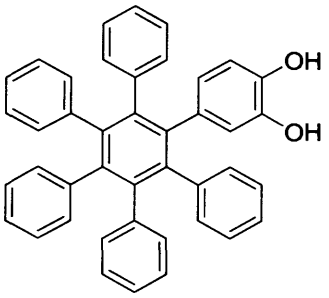

In a two-necked round bottom flask was added **36** (1.00g, 1.68 mmol) to dry dichloromethane (30 ml) under a dry nitrogen atmosphere that was maintained throughout the reaction. This mixture was cooled to 0 °C then boron tribromide (1.05 g, 4.21 mmol) was added dropwise and the reaction stirred at room temperature for a further 30 min. The reaction was poured into ice and left under vigorous stirring allowing the evaporation of the excess dichloromethane. The precipitate was filtered off, washed with water and dried. Recrystallization from dichloromethane/hexane (1/1) gave the desired compound as an off-white solid (0.83 g, 87 %). M.p. 354 – 356 °C; IR (film)cm^{-1} 3533.4, 3041.2, 1621,8, 1508.9, 1401.2, 1259.6, 1142.6, 1012.8, 1023.8, 876.2, 812.8, 745.7; ^1H NMR (500 MHz; Acetone d^6) δ 6.82 (m, 25H, H_{Ar}) 6.39 (d, 1H, J = 2.0 Hz, H_a) 6.32 (d, 1H, J = 8.1 Hz, H_b) 6.22 (dd, 1H, J = 2.0, 8.1 Hz, H_c). ^{13}C NMR (500 MHz; Acetone d^6) 145.2, 144.2, 142.8, 142.7, 142.7, 142.4, 142.2, 142.1, 141.8, 134.3, 133.2, 133.1, 133.1, 128.3, 126.9, 126.9, 125.1, 120.4, 118.5, 118.3, 118.0, 115.4; HRMS Calc.for $C_{42}H_{30}O_2$ 566.2246 , found 566.2249.

6.2.17. OMIM 34 from 32 and 33

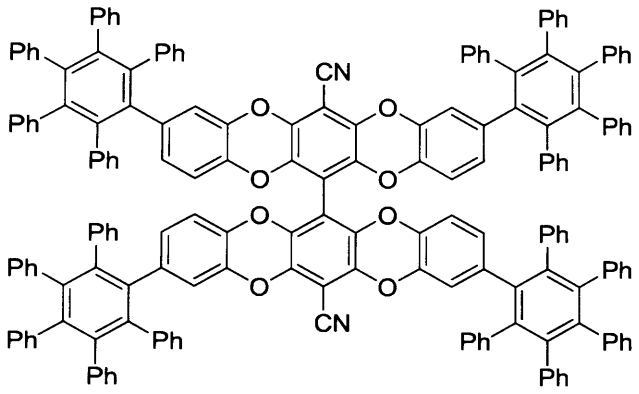

In a two neck flask under a nitrogen atmosphere 2,2',3,3',5,5',6,6'-octafluorobiphenyl-4,4'-dicarbonitrile **32** (334 mg, 0.56 mmol) and 1-(1,2-dihydroxyphenyl)-2,3,4,5,6-pentaphenylbenzene **33** (46.2 mg, 0.13 mmol) were stirred in DMF (5 ml) at 65 °C. K_2CO_3 was added (1.94g, 14.11 mmol) and the reaction left for 18hrs. The reaction was then quenched by pouring into water (100 ml); this was left to stir and then filtered. The filtered solid was purified by column chromatography, (hexane : ethyl acetate, 6 : 4) and the OMIM fraction was collected and the solvent removed under reduced pressure and the solid dried in the oven. This gave the desired compound as a pale yellow powder **34** (252 mg, 73%) M.p > 360 °C MS IR (nujol)cm^{-1} 2339.3, 1302.9, 1054.6, 1025.8, 834.1, 733.2, 702.6, 696.8; ^1H NMR (400 MHz, $CDCl_3$) δ 6.58 (m, 100H, H_{Ar}) 6.49 (m, 12H, H_{Ar}); ^{13}C (100 MHz,$CDCl_3$) δ 141,0; 140,9; 140,9; 140,8; 140,7; 140,6; 140,5; 138,6; 131,8; 131,8; 131,7; 131,6; 131,6; 131,5; 131,5; 131,4; 131,4; 131,4; 131,3; 127,5; 127,4; 127,3; 127,2; 127,1; 127,1; 127,0; 126,1; 125,9; 125,7; 125,7; (MALDI-TOF): cluster centered at *m/z* 2454.9 (M^+).

6.2.18. 4-(2,2-Dibromovinyl)-1,2-dimethoxybenzene 37

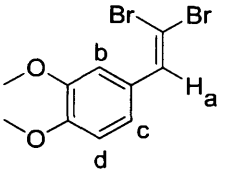

In a round bottom flask 3,4-dimethoxybenzaldehyde (4.00 g , 24.07 mmol) was added to a solution of CBr_4 (9.58 g , 28.88 mmol) and PPh_3 (15.16 g , 57.77 mmol) in dry DCM (40 ml) at room temperature. After stirring for 60 min the reaction was quenched by pouring into water (50 ml) and extracted with DCM (3 x 30 ml). The organic layers were combined washed with water and dried using $MgSO_4$ and the solvent removed under vacuum. The crude was purified by column chromatography (hexane : ethyl acetate, 8 : 2) to give the desired product as a colourless oil **37** (7.99g, 67%). IR (nujol) 1599.8, 1513.1, 1462.2, 1266.3, 1142.8, 1025.6, 871.1 cm^{-1}; ^1H NMR(400 MHz, $CDCl_3$) δ 7.41 (s, 1H, H_a), 7.19 (d, J = 2.0 Hz, 1H, H_b), 7.10 (dd, J = 2.0, 8.4 Hz, 1H, H_c), 6.86 (d, J = 8.4 Hz, 1H, H_d), 3.90 (s, 3 H), 3.89 (s, 3 H); ^{13}C NMR (100 MHz, $CDCl_3$) δ 149.3, 148.6, 136.5, 128.0, 122.0, 111.1, 110.8, 87.4, 55.9. LRMS, *m/z*, ($APCI^+$) 321 (M, 100%).

6.2.19. 4-Ethynyl-1,2-dimethoxybenzene 38

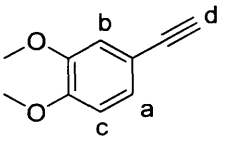

In a two necked round bottom flask, dry THF (30 ml) and 4-(2,2-dibromovinyl)-1,2-dimethoxybenzene (2.50 g, 7.53 mmol) were stirred under a nitrogen atmosphere at -78 °C. To this BuLi (6.33 g, 15.81 mmol) was added drop wise and allowed to stir for 1.5 hrs. After this time the reaction was allowed to warm to room temperature and was then quenched using NH_4Cl (100 ml) and the product extracted using DCM (2 x 100 ml). The organic layers were combined and the solvent removed under vacuum, and purified using column

chromatography (hexane : ethyl acetate, 2 : 1) to give the desired product as a white solid (0.75 g, 61 %). M.p. 64 – 66 °C (lit m.p[87] 65 -67 °C); IR (film) 3284.6, 2916.4, 2849.8, 1579.3, 1599.2, 1511.2, 1462.6, 1409.7, 1322.1, 1263.3, 1239.4, 1152.8, 1136.6 ,1023. 7, 851.3, 807.5, 479.6 cm-1; ^{1}H NMR (400 MHz, $CDCl_3$) δ 7.10 (dd, J = 1.9, 8.3 Hz, 1 H, H_a), 6.99 (d, J = 1.9 Hz, 1 H, H_b),6.80 (d, J = 8.3 Hz, 1 H, H_c), 3.89 (s, 3 H, OMe), 3.88 (s, 3 H, OMe), 3.00 (s, 1 H, H_d); 13C NMR (100 MHz, $CDCl_3$) δ 149.8, 148.5, 125.4, 114.6, 114.1, 110.9, 83.8, 75.7, 55.8. LRMS, *m/z*, (EI^+) 162 (M, 100%).

6.2.20. 1,2-Bis(3,4-dimethoxyphenyl)ethyne 39

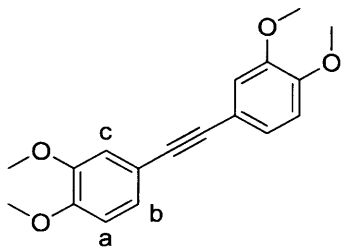

A mixture of 4-bromoveratrole (0.61 g, 2.82 mmol) Et_3N (4 ml) and DMF (4 ml) were deoxygenated in a round bottom flask under a nitrogen atmosphere. 4-Ethynyl-1,2-dimethoxybenzene **38** (0.50 g, 3.10 mmol) was added and the reaction heated to 90 °C to which CuI (53.7 mg, 0.28 mmol) and [$(Ph_3P)_2PdCl_2$] (0.198g, 0.28 mmol) were added and the reaction left for 15 hrs. The reaction was then quenched with water (40 ml) and allowed to stir for 1hr. This was then extracted using DCM (3 x 30 ml), the organic layers were combined washed with water (3 x 20 ml) and dried with $MgSO_4$. The solvent was removed under reduced pressure and purification by column chromatography gave the desired product as a yellow solid (0.64, 76%). Mp 162 – 164 °C; IR (Nujol) 1588.2, 1573.3, 1544.9, 1463.6, 1449.2, 1441.5, 1410.5, 1329.5 cm^{-1}. ^{1}H NMR (400 MHz, $CDCl_3$) δ 7.22 (d, J = 8.0 Hz, 2H, H_a), 7.10 (dd, J = 8.0, 1.9 Hz, 2H, H_b), 6.83 (d, J = 1.9 Hz, 2H_c), 3.96 (s, 12H, OMe); 13C (100 MHz,$CDCl_3$) δ 149.4, 148.7, 124.7, 115.7, 114.2, 111.1, 88.0, 55.9; LRMS, *m/z*, ($APCI^+$) 299 (M^+, 100%).

6.2.21. 1,2-Bis(3,4-dimethoxyphenyl)ethanone 42

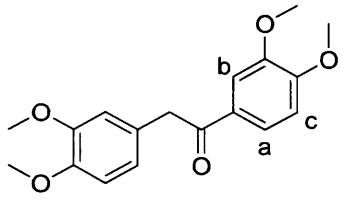

To a dry two-necked round bottom flask 2-(3,4-dimethoxyphenyl)acetic acid (16.50 g, 84.10 mmol) was stirred in dry DCM (30 ml). Thionyl Chloride (18.58 g, 156.14 mmol) was added drop wise. Once added the reaction was heated to reflux for 1 hr. Once completed the reaction was distilled firstly to remove any DCM and thionyl chloride. Then the temperature was increased to distil off the acid chloride, which was an orange oil. This oil (16.80g, 78.38 mmol) was transferred to another two-necked round bottom flask containing dry DCM (150 ml) and veratrole (16.01g, 117.58 mmol). Aluminium trichloride (15.68 g, 117.58 mmol) was added carefully to the mixture and once added the mixture was refluxed for 3 hrs. After refluxing the reaction was quenched by pouring into iced water (100 ml) containing 6M HCl (30 ml). The product was extracted using DCM (3x20 ml) and the combined organic layers reduced under vacuum. Recrystallisation from EtOH gave the desired product as a yellow solid (19.71g 79%). M.p. 103 – 105 °C (lit m.p.[88] = 104 – 106 °C); IR (nujol)cm^{-1} 1679.2, 1152.2, 1018.2, 721.2; ^{1}H NMR (400 MHz; $CDCl_3$) δ 7.66 (dd, 1H, J= 8.4, 1.9 Hz, H_a), 7.56 (d, 1H, J= 1.9 Hz H_b), 6.88 (d, 1H, J= 8.4 Hz, H_c) 6.81 (m, 3H, H_{Ar}), 4.83 (s, 2H, CH_2), 3.94 (s, 3H, OMe), 3.92 (s, 3H, OMe), 3.86 (s, 3H, OMe), 3.85 (s, 3H, OMe). ^{13}C NMR (100 MHz; $CDCl_3$) δ 196.4, 153.1, 148.9, 148.8, 147.7, 129.5, 127.3, 123.3, 121.3, 112.2, 111.1, 110.4, 109.8, 77.3, 76.9, 76.6, 55.9, 55.8, 55.7, 55.7, 44.6. LRMS, *m/z*, (APCI$^+$): 317 (MH^+, 100%), 318 (20%).

6.2.22. 1,2-Bis(3,4-dimethoxyphenyl)ethane-1,2-dione 45

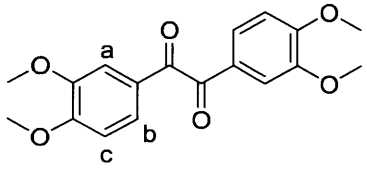

A round bottom flask containing 1,4-dioxane (150 ml), water (5 ml) and 1,2-bis(3,4-dimethoxyphenyl)ethanone **42** (14.50 g, 45.84 mmol) was stirred. Selenium dioxide (5.09 g, 45.84 mmol) was added and the reaction heated to reflux for 15 hr. Once the reaction was cooled to room temperature it was filtered. The solid was washed with 1,4-dioxane to remove any traces of starting material. Once dry the filtrate was washed with DCM to leave behind the selenium residue. The DCM was reduced under vacuum to leave a green fluffy solid (12.32 g, 81%). M.p. 222 – 225 °C (lit m.p.[88] = 223 – 224 °C)ref; IR (nujol)cm^{-1} 1651.7, 1460.3, 1417.4, 1376.9, 1351.8, 1271.3, 1227.9, 1188.9, 1173.4, 1145, 1067.4, 1027.8, 1010, 971.4, 869.7, 816.2, 791.1; ^{1}H NMR (400 MHz; $CDCl_3$) δ 7.59 (d, 2H J = 1.9 Hz, H_a), 7.46 (dd, 2H, J = 8.4, 1.9 Hz, H_b), 6.87 (d, 2H, J = 8.4 Hz, H_c) 3.95 (s, 6H, OMe) 3.94 (s, 6H, OMe). ^{13}C NMR (100 MHz; $CDCl_3$) δ 193.9, 155.2, 150.0, 149.9, 126.8, 110.7, 110.6, 56.7, 56.6. LRMS, *m/z*, (APCI$^+$) 331 (MH^+, 100%)

6.2.23. 3,4-Bis(3,4-dimethoxyphenyl)-2,5-diphenylcyclopenta-2,4-dienone 46

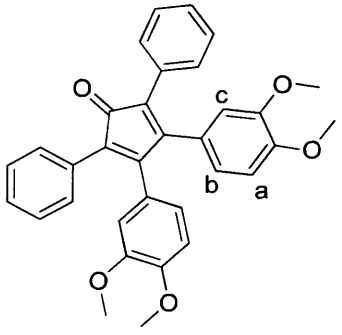

In a round bottom flask 1,2-bis(3,4-dimethoxyphenyl)ethane-1,2-dione (2.00 g, 6.06 mmol) diphenylacetone (1.40 g, 6.67 mmol) and EtOH (12 ml) was stirred at 85 °C; KOH (0.17 g, 3.03 mmol) was added and the reaction left for 1 hr. After 1 hr a further 0.5 eq of KOH (0.17g, 3.03mmol) was added and then left for a further hour. The reaction was then filtered hot and washed with water and then EtOH; this gave the desired product as a black powder (2.02 g, 67%) M.p. 171 – 173 °C; IR (nujol)cm^{-1} 1696.5, 1377.4, 1236.1, 1140.2, 1020.6, 963.2, 864.4, 827.3, 813.8, 781, 763.6; ^{1}H NMR (400 MHz; $CDCl_3$) δ 7.21 (m, 10H, H_{Ar}), 6.67 (d, 2H, J = 8.3 Hz, H_a), 6.49 (dd, 2H, J = 8.3, 1.9 Hz, H_b), 6.43 (d, 2H, J = 1.9 Hz, H_c), 3.83 (s, 6H, OMe), 3.42 (s, 6H, OMe); ^{13}C NMR (100 MHz; $CDCl_3$) δ 200,6; 154,6; 154,4; 149,6; 148,3; 133,9; 131,6; 131,1; 130,5; 129,8; 128,8; 128,5; 128,4; 127,8; 127,7; 126,0; 125,4; 124,8; 123,3; 113,3; 110,7; 56,1; 55,8; LRMS, *m/z*, (EI$^+$) 444 (M, 100%).

6.2.24. 1,2-(1,2-Dimethoxyphenyl)-3,4,5,6-tetraphenylbenzene 40

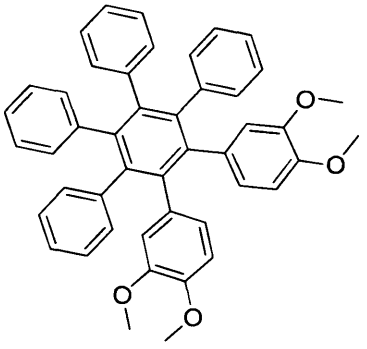

In a 50 ml round bottom flask Ph_2O (8 ml), 3,4-bis(3,4-dimethoxyphenyl)-2,5-diphenylcyclopenta-2,4-dienone **46** (2.00 g, 3.96 mmol) and diphenylacetylene (0.91 g, 4.76 mmol) were refluxed in a mantle for 15 hrs. The reaction mixture was then allowed to cool and poured into cold MeOH. Hexane (50 ml) was added to dissolve up most of the Ph_2O. This was then filtered and purified by column chromatography (hexane : ethyl acetate, 7 : 3). Further purification by recrystalisation in MeOH gave a cream powder (1.7g, 65%). M.p. 204 – 206 °C; IR (nujol)cm^{-1} 1600.1, 1517.7, 1312.8, 1255.4, 1176.8, 1135.8, 1070.7, 1026.4, 914.5, 857.6, 795.4, 770.9, 697.6; ^{1}H NMR (400 MHz; $CDCl_3$) δ 6.87 (m, 20H, H_{Ar}) 6.39

(m, 6H, H_{Ar}) 3.71 (s, 6H, OMe) 3.70 (s, 6H, OMe). ^{13}C NMR (100 MHz; $CDCl_3$) δ 147.7, 146.8, 141.3, 141.1, 140.8, 131.9, 131.8, 131.7, 131.7, 127.1, 127.0, 125.6, 125.6, 124.4, 115.9, 115.7, 109.9, 56.1, 55.9. LRMS, *m/z*, (EI^+) 654 (M, 100%).

6.2.25 .1,2-(1,2-Dihydroxyphenyl)-3,4,5,6-tetraphenylbenzene 31

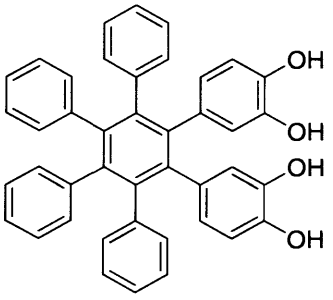

In a two-necked round bottom flask was added **40** (0.50 g, 0.76 mmol) to dry dichloromethane (30 ml) was added under a dry nitrogen atmosphere that was maintained throughout the reaction. This mixture was cooled to 0 °C then boron tribromide (0.60 g, 2.29 mmol) was added dropwise and the reaction stirred at room temperature for a further 30 min. The reaction was poured into ice and left under vigorous stirring allowing the evaporation of the excess dichloromethane. The precipitate was filtered off, washed with water and dried. Recrystallisation from dichloromethane/hexane (1/1) gave the desired compound as an off-white solid (0.4 g, 89%) M.p. + 360 °C; IR (film)cm^{-1} 3055.1, 2305.4, 1599.1, 1517.2, 1439.6, 1265, 1109.8, 1071.7, 1019.1, 896.2, 739, 425.2; ^1H NMR (400 MHz; Acetone d^6) δ 7.46 (dd, 4H, OH) 6.84 (m, 20H, H_{Ar}) 6.35 (m, 2H, H_{Ar}) 6.22 (m, 2H, H_{Ar}). ^{13}C NMR (100 MHz; $CDCl_3$) 145.2, 144.2, 143.0, 142.9, 142.4, 141.7, 134.5, 133.1, 128.2, 126.8, 126.7, 125.0, 124.9, 120.3, 120.2, 115.0. HRMS Calc.for $C_{42}H_{30}O_4$ requires 598.2144 , found 598.2158.

6.2.26. 1-(3,4-Dimethoxyphenyl)-2-phenylethanone

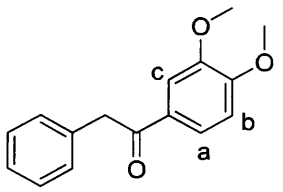

To a dry two-necked round bottom flask containing 2-phenylacetic acid (5.00 g, 36.72 mmol) was added to dry DCM (20 ml). Thionyl chloride (13.80 g, 73.42 mmol) was added drop wise. Once added the reaction was heated to reflux for 1 hr. Once completed the reaction was distilled firstly to remove any DCM and unreacted thionyl chloride. Then the temperature was increased to distil of the acid chloride **43**, which was a reddish oil. This oil (5.50 g, 35.62 mmol) was transferred to another two necked round bottom flask containing dry DCM (150 ml) and veratrole (7.35 g, 53.20 mmol). Aluminium trichloride (7.09g, 53.20 mmol) was added carefully to the mixture and once completed added the mixture was refluxed for 3 hrs. After refluxing the reaction was quenched by pouring into iced water (100 ml) containing 6M HCl (30 ml). The product was extracted using DCM (3x20 ml) and the combined organic layers reduced under vacuum. Recrystallisation from EtOH gave the desired product as a yellow solid **45** (6.23g 68%). M.p. 85 – 87 °C (lit m.p.[107] = 86 – 88 °C); IR (nujol)cm^{-1} 1673.9, 1451.6, 1377.8, 1346.5, 1264.5, 1152.7, 1071.7, 1026.1; ^1H NMR (400 MHz; $CDCl_3$) 7.59 (dd, 1H, H_a, J = 8.3, 2.0 Hz), 7.48 (d, 1H, H_b, J = 2.0 Hz), 7.21 (m, 6H, H_{Ar}), 6.83 (d, 1H, H_c, J = 8.3 Hz), 4.16 (s, 2H, CH_2), 3.86 (s, 3H, OMe), 3.83 (s, 3H, OMe). 13C NMR (100 MHz; $CDCl_3$) δ 196.3, 153.2, 149.0, 135.0, 129.6, 129.2, 128.6, 126.7, 123.4, 110.5, 109.9, 56.0, 55.9, 45.2, LRMS, *m/z*, ($APCl^+$): 257 (MH^+, 100%), 258 (20%).

6.2.27. 1-(3,4-Dimethoxyphenyl)-2-phenylethane-1,2-dione 50

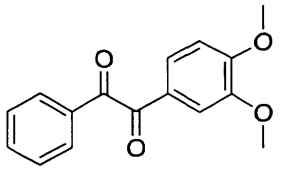

A round bottom flask containing 1,4-dioxane (150 ml), water (5 ml) and 1-(3,4-dimethoxyphenyl)-2-phenylethanone (2.00 g, 7.80 mmol) was stirred. Selenium dioxide (0.86 g, 7.80 mmol) was added and the reaction heated to reflux for 15 hr. Once the reaction was cooled to room temperature it was filtered. The solid was washed with 1,4-dioxane to remove any traces of starting material. Once dry the filtrate was washed with DCM to leave behind the selenium residue. The DCM was reduced under vacuum and the solid dried in the oven to remove traces of dioxane to give a light red solid (2.05g, 97%). M.p. 113-136 °C (lit m.p.[106] = 114 – 115 °C) ; IR (nujol)cm^{-1} 1663.3, 1460.31418.8, 1376.9, 1303.6, 1283.8, 1240, 1146.4, 1022, 932.8, 875, 834.5, 809.4, 787.2, 764.6, 749.2, 716.9, 683.6, 673.1; ^{1}H NMR (400 MHz; $CDCl_3$) δ 7.98 (m, 1H, H_{Ar}), 7.96 (m, 1H, H_{Ar}), 7.64 (m, 2H, H_{Ar}), 7.50 (m, 3H, H_{Ar}), 6.89 (d, 1H, H_{Ar}), 3.96 (s, 3H, OMe), 3.95 (s, 3H, OMe). ^{13}C NMR (100 MHz; $CDCl_3$) δ194.6, 193.2, 154.8, 149.5, 134.7, 133.1, 129.9, 128.8, 126.3, 126.1, 110.2, 110.0, 56.2, 56.0,. LRMS, *m/z*, (APCI$^+$) 271 (MH^+, 100%) 272 (20%)

6.2.28. 3-(3,4-Dimethoxyphenyl)-2,4,5-triphenylcyclopenta-2,4-dienone 54

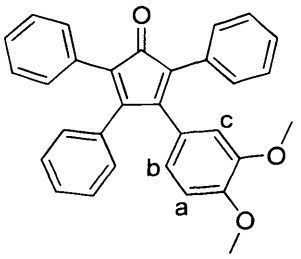

In a round bottom flask a mixture of 1-(3,4-dimethoxyphenyl)-2-phenylethane-1,2-dione **50** (1.00 g, 2.25 mmol), diphenylacetone (0.52 g, 2.48 mmol) and EtOH (12 ml) was stirred at 85 °C, KOH (0.06 g, 1.13 mmol) and left to react for 1 hr. After 1 hr a further 0.5 eq of KOH (0.06 g, 1.13 mmol) was added and then left for a further hour. The reaction was filtered hot and washed with water and then EtOH; this gave the desired product as a black powder. M.p. 180 – 184 °C; IR (nujol)cm^{-1} 1700.4, 1597.7, 1576.5, 1510.4, 1490.7, 1412.6, 1377.4, 1353.7, 1316.6, 1301.7, 1275.6, 1253, 1233.2, 1186.9, 1161.9, 1139.2, 1116.1, 1090, 1077, 1019.1, 1002.3, 971.9, 937.7, 917.4, 871.6, 841.2, 817.1, 803.2, 790.6, 769.4, 760.7, 744.3, 735.2, 714, 691.3, 638.3, 625.7, 616.1; ^{1}H NMR (400 MHz; $CDCl_3$) δ 7.18 (m, 13H, H_{Ar}) 6.90 (m, 2H, H_{Ar}) 6.57 (d, 1H, J = 8.3 Hz, H_a) 6.45 (dd, 1H, J = 8.3, 2.0 Hz, H_b) 6.24 (d, 1H, J = 2.0 Hz, H_c) 3.77 (s, 3H, OMe) 3.29 (s, 3H. OMe); ^{13}C NMR (100 MHz; $CDCl_3$) δ 200,6; 154,6; 154,4; 149,6; 148,3; 133,9; 131,6; 131,1; 130,5; 129,9; 129,8; 129,1; 128,8; 128,5; 128,4; 127,8; 127,7; 126,0; 125,4; 124,8; 123,3; 113,3; 110,7; 56,1; 55,8; LRMS, *m/z*, (EI^+) 444 (M, 100%).

6.2.29 . 1,3(4)-Di(3',4'-dimethoxyphenyl)-2,3,5,6-tetraphenylbenzene

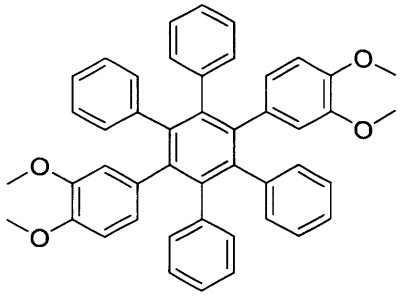

In a 50 ml round bottom flask Ph_2O (8 ml), 3-(3,4-dimethoxyphenyl)-2,4,5-triphenylcyclopenta-2,4-dienone **54** (1.55 g, 3.50 mmol) and 1,2-dimethoxy-4-(phenylethynyl)benzene (1.00g, 4.20 mmol) were refluxed in a mantle for 15 hrs. This was then allowed to cool and the mixture poured into cold MeOH. Hexane (50 ml) was added to dissolve up most of the Ph_2O. This was then filtered and purified by column chromatography (hexane : ethyl acetate). Further purification by recrystallisation in MeOH gave a cream powder (1.46g, 61%). M.p. 204 – 208 °C; IR (nujol)cm^{-1} 1584.2, 1518.1, 1417.4, 1377.4,

1330.1, 1313.7, 1254.4, 1231.3, 1176.3, 1136.8, 1071.2, 1028.3, 910.2, 892.3, 856.2, 808, 768, 699.5, 665.8, 634.4; ^{1}H NMR (400 MHz; $CDCl_3$) δ 6.86 (m, 20H, H_{Ar}) 6.32 (m, 6H, H_{Ar}) 3.68 (s, 6H, OMe) 3.40 (s, 6H, OMe). ^{13}C NMR (100 MHz; $CDCl_3$) δ147.2, 146.4, 140.9, 140.5, 139.7, 132.9, 131.5, 131.4, 131.3, 131.2, 126.8, 126.7, 126.7, 126.6, 126.5, 125.1, 124.2, 115.4, 109.3, 55.5, 55.4,. LRMS, *m/z*, (EI^+) 654 (M, 100%).

6.2.30. 1,4-Di(3',4'-dihydroxyphenyl)-2,3,5,6-tetraphenylbenzene 48

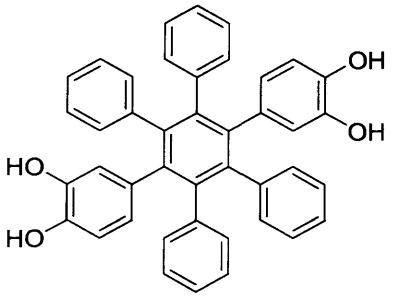

In a two-necked round bottom flask was added 1,3(4)-di(3',4'-dimethoxyphenyl)-2,3,5,6-tetraphenylbenzene (1.00 g, 1.52 mmol) to dry dichloromethane (30 ml) was added under a dry nitrogen atmosphere that was maintained throughout the reaction. This mixture was cooled to 0 °C then boron tribromide (1.50 g, 3.80 mmol) was added dropwise and the reaction stirred at room temperature for a further 30 min. The reaction was poured into ice and left under vigorous stirring allowing the evaporation of the excess dichloromethane. The precipitate was filtered off, washed with water and dried. Recrystallization from dichloromethane/hexane (1/1) gave the desired compound as an off-white solid (0.82 g, 91%) M.p. 352 – 355 °C; IR (film)cm^{-1} 3054.6, 1598.7, 1520.1, 1265, 896.2, 738.6; ^{1}H NMR (400 MHz; Acetone d^6) δ 7.40 (m, 4H, OH) 6.87 (m, 20H, H_{Ar}) 6.29 (m, 6H, H_{Ar}). ^{13}C NMR (100 MHz; $CDCl_3$). 145.3, 144.3, 143.0, 142.5, 142.3, 142.1, 141.8, 134.4, 133.2, 133.1, 128.2, 126.8, 125.1, 120.4, 115.5. HRMS Calc.for $C_{42}H_{30}O_4$ requires 598.2144, found 598.2136.

6.2.31. 1,4-Bis(phenylethynyl)benzene 56

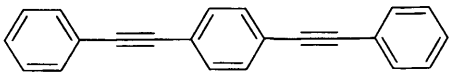

To a round bottom flask under a nitrogen atmosphere was added 1-bromo-4-iodobenzene (0.28 g, 1.00 mmol), piperidine (1.70 g, 2.00 mmol), $PdCl_2$ (11 mg, 5 mol%), water (3.00 g) and acetone (3.00 g). After 5 min of stirring phenylacetylene (0.12g , 1.2 mmol) was added and the reaction heated at 65 °C for 18hrs. After this time the reaction was cooled and the product extracted with Et_2O and purified using column chromatography (hexane : ethyl acetate, 8 : 2) to give the desired product as a yellow powder (0.14 g, 52%). M.p. 183-186 °C (lit m.p.[108] 184-186 °C); IR (film)cm^{-1} 3054.2, 2360.4, 1515.2, 1439.1, 1265, 1104, 1069.8, 919.3, 896.2, 838.4, 738.6; ^1H NMR (500 MHz; $CDCl_3$) δ 7.54 (m, 4H, H_{Ar}), 7.52 (s, 4H, H_{Ar}), 7.34 (m, 6H, H_{Ar}). ^{13}C NMR (125 MHz; $CDCl_3$) 131.6, 131.5, 128.4, 128.3, 123.1, 123.0, 91.2, 89.1,. LRMS, *m/z*, ($APCl^+$) 279 (M^+, 100%).

6.2.32. 4,4'-Di(3'',4''-dimethoxyphenyl)-2,2',3,3',5,5',6,6'-octaphenyl-*p*-terphenyl

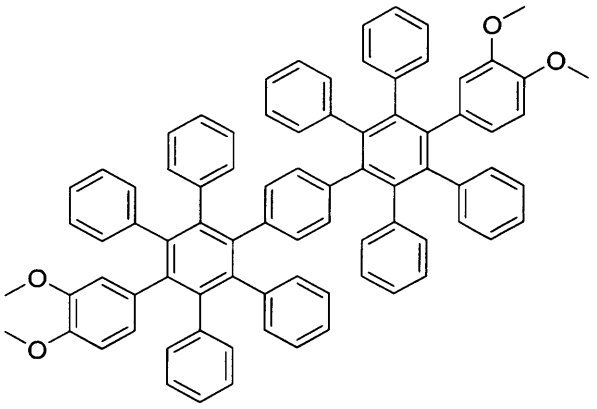

In a 50 ml round bottom flask Ph_2O (8 ml), **54** (2.0 g, 4.49 mmol) and 1,4-bis(phenylethynyl)benzene (0.50g, 1.80 mmol) **56** were refluxed in a mantle for 15 hrs. This was then allowed to cool and poured into cold MeOH. Hexane (50 ml) was added to

dissolve up most of the Ph_2O. This was then filtered and purified by column chromatography (hexane : ethyl acetate). Further purification by recrystallisation in MeOH gave a light orange powder (1.46 g, 61%). M.p. 193 – 195 °C; IR (film)cm^{-1} 3042.6, 2986.7, 2837.7, 2305.4, 1600.6, 1515.2, 1465.1, 1442, 1419.8, 1261.2, 1235.1, 1174.9, 1138.2, 1072.2, 1028.3, 895.7, 849.4, 698.5; ^1H NMR (400 MHz; $CDCl_3$) δ 6.80 (m, 40H, H_{Ar}) 6.28 (m, 10H, H_{Ar}) 3.67 (s, 3H, OMe) 3.66 (s, 3H, OMe) 3.38 (s, 3H, OMe) 3.37 (s, 3H, OMe). ^{13}C NMR (100 MHz; $CDCl_3$) 150.0, 147.5, 146.7, 141.4, 141.2, 141.0, 137.0, 132.2, 131.9, 131.8, 131.7, 130.7, 130.7, 127.1, 127.0, 126.9, 126.8, 125.4, 124.5, 109.7, 55.9, 55.8; LRMS, *m/z*, (ES^+) 1133 ($M+Na^+$, 100%).

6.2.33. 4,4'-Di(3'',4''-dimethoxyphenyl)-2,2',3,3',5,5',6,6'-octaphenyl-*p*-terphenyl 57

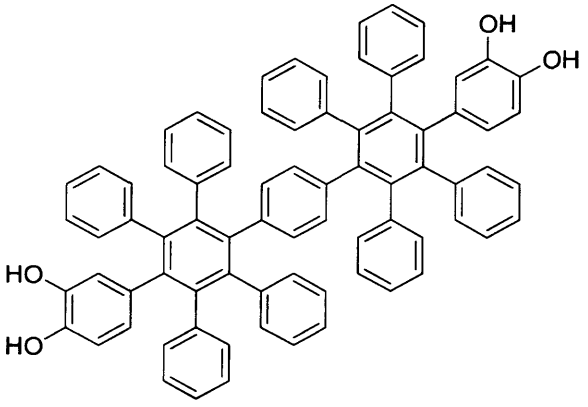

In a two-necked round bottom flask was added 4,4'-di(3'',4''-dimethoxyphenyl)-2,2',3,3',5,5',6,6'-octaphenyl-*p*-terphenyl (1.00 g, 0.90 mmol) to dry dichloromethane (30 ml) under a dry nitrogen atmosphere that was maintained throughout the reaction. This mixture was cooled to 0 °C then boron tribromide (0.56 g, 2.25 mmol) was added dropwise and the reaction stirred at room temperature for a further 30 min. The reaction was poured into ice and left under vigorous stirring allowing the evaporation of the excess dichloromethane. The precipitate was filtered off, washed with water and dried. Recrystallization from dichloromethane/hexane (1/1) gave the desired compound as an off-white solid (0.84 g, 88%). M.p. >360 °C; IR (film)cm^{-1} 3048.5, 1588.1, 1515.1, 1237.3, 986.2, 896.2, 745.8 702.6,

608.3. 598.4; ^{1}H NMR (400 MHz; Acetone d^{6}) δ 7.37 (m, 4H, H_{Ar}) 7.22 (m, 10, H_{Ar}) 6.82 (m, 30, H_{Ar}) 6.46 (m, 6H, H_{Ar}) 6.26 (m, 2H, H_{Ar}) 6.13 (m, 2H, H_{Ar}); ^{13}C NMR (100 MHz; $CDCl_3$) 149.2, 145.6, 144.3, 142.9, 142.3, 141.5, 138.6, 135.1, 132.7, 132.6, 132.0, 131.9, 131.5, 128.9, 128.6, 128.1, 127.9, 127.8, 125.6, 113.6;. HRMS Calc.for $C_{78}H_{54}O_4$ requires 1055.2677, found 1055.1452.

6.2.34. Polymer 1 from 1,2-(3',4'-dihydroxyphenyl)-3,4,5,6-tetraphenylbenzene 47

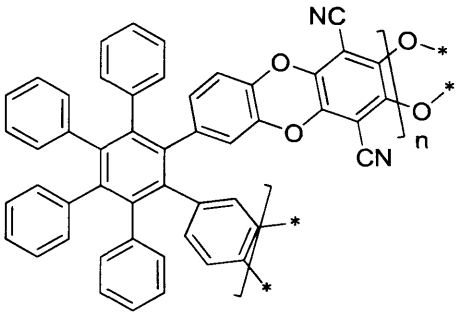

In a two-necked round bottom flask was added under a dry nitrogen atmosphere 1,2-(3',4'-dihydroxyphenyl)-3,4,5,6-tetraphenylbenzene (500 mg, 0.84 mmol), 2,3,5,6-tetrafluoroterephthalonitrile (167 mg, 0.84 mmol) and dry DMF (20 ml). This mixture was heated to 65 °C, until complete dissolution of the two starting materials, then dry K_2CO_3 (0.92 g, 6.68 mmol) was added and the mixture kept to stirring for 96 hrs. The solution was quenched with water (100 ml), filtered and dried in a vacuum oven to remove any traces of solvent, to give a pale yellow product. (654 mg, 86 % based on the molecular weight of the repeated unit). IR (nujol)cm^{-1} 2340.4, 1262.6, 1020.6, 1004.7, 815.7, 721.2, 697.6; ^{1}H NMR (400 MHz; $CDCl_3$) δ 6.57 (br m, 20H, H_{Ar}), 6.40 (br m, 6H, H_{Ar}); BET surface area = 425 m^2/g; total pore volume = 0.36 cm^3/g at (P/P_0) 0.98, adsorption. (nitrogen): 3% loss of weight occurred at ~ 350 °C. Initial weight loss due to thermal degradation commences at ~ 535 °C.

6.2.35. Polymer 2 from 1,4-(3',4'-dihydroxyphenyl)-2,3,5,6-tetraphenylbenzene 55

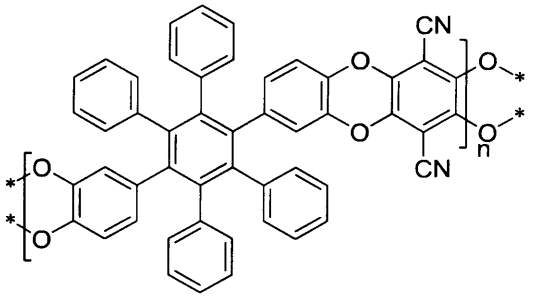

In a two-necked round bottom flask was added under a dry nitrogen atmosphere 1,2-(3',4'-dihydroxyphenyl)-3,4,5,6-tetraphenylbenzene (500 mg, 0.84 mmol), 2,3,5,6-tetrafluoroterephthalonitrile (167 mg, 0.84 mmol) and dry DMF (20 ml). This mixture was heated to 65 °C, and then dry K_2CO_3 (0.92 g, 6.68 mmol) was added and the mixture kept to stirring for 96 hrs. The solution was quenched with water (100 ml), filtered and washed repeatedly with water and acetone. The solid was dissolved in $CHCl_3$ (20 ml) and, throughout filtration by cotton wool, poured in to a flask containing a mixture of acetone/methanol (2/1, 80 ml). The product was dried under high vacuum overnight to give the final product as a pale yellow solid (699 mg, 92 % based on the molecular weight of the repeated unit); IR (nujol)cm^{-1} 1258.4, 1109.5, 998.6, 834.6, 801.9, 768.9, 702.3, 651.3; ^1H NMR (400 MHz; $CDCl_3$) δ 6.58 (br s, 20H, H_{Ar}), 6.40 (br s, 6H, H_{Ar}); BET surface area = 537 m^2/g; total pore volume = 0.65 cm^3/g at (P/P_0) 0.98, adsorption TGA analysis (nitrogen): 1% loss of weight occurred at ~ 350 °C. Initial weight loss due to thermal degradation commences at ~ 525 °C.

6.2.36. Synthesis of polymer from 4,4'-di(3'',4''-dimethoxyphenyl)-2,2',3,3',5,5',6,6'-octaphenyl-*p*-terphenyl 58

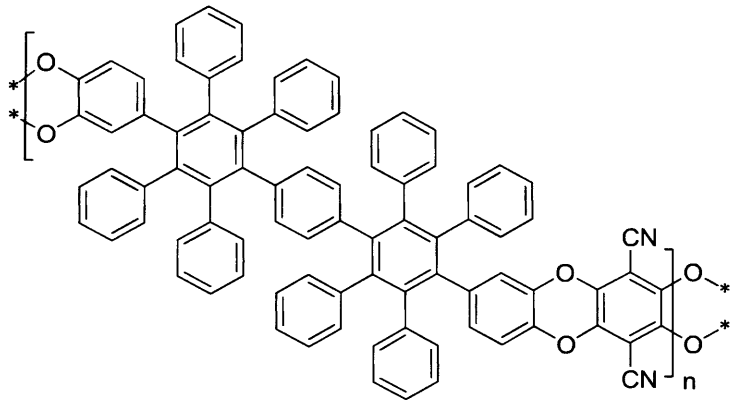

In a two-necked round bottom flask was added under a dry nitrogen atmosphere 4,4'-di(3'',4''-dimethoxyphenyl)-2,2',3,3',5,5',6,6'-octaphenyl-*p*-terphenyl **56** (350 mg, 0.33 mmol), 2,3,5,6-tetrafluoroterephthalonitrile (66.4 mg, 0.33 mmol) and dry DMF (20 ml). This mixture was heated to 65 °C, and then dry K_2CO_3 (0.15 g, 2.64 mmol) was added and the mixture kept to stirring for 96 hrs. The solution was quenched with water (100 ml), filtered and washed repeatedly with water and acetone. The solid was dissolved in $CHCl_3$ (20 ml) and, throughout filtration by cotton wool, poured in to a flask containing a mixture of acetone/methanol (2/1, 80 ml). The product was dried under high vacuum overnight to give the final product as a pale yellow solid (375 mg, 94 % based on the molecular weight of the repeated unit); IR (nujol)cm^{-1} 3054.6, 2986.7, 2359, 1600.6, 1472.8, 1421.7, 1266, 1019.6, 1004.7, 895.7, 702.9; ^1H NMR (400 MHz; $CDCl_3$) δ 6.63 (br m, 29H, H_{Ar}), 6.32 (br m, 6H, H_{Ar}); BET surface area = 355 m^2/g; total pore volume = 0.70 cm^3/g at (P/P_0) 0.98, adsorption TGA analysis (nitrogen): 4% loss of weight occurred at ~ 350 °C. Initial weight loss due to thermal degradation commences at ~ 531 °C.

6.2.37 [2+2] Cyclic oligomer 59

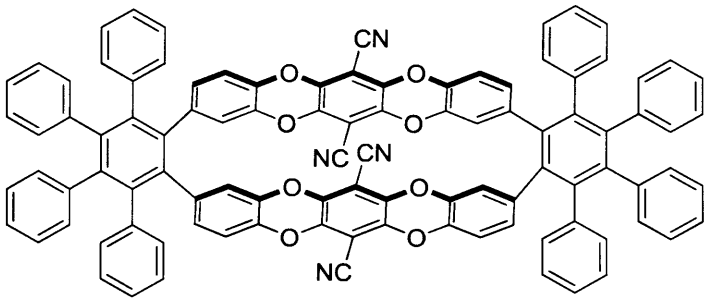

In a two-necked round bottom flask was added under a dry nitrogen atmosphere 1,2-(3',4'-dihydroxyphenyl)-3,4,5,6-tetraphenylbenzene (250 mg, 0.17 mmol), 2,3,5,6-tetrafluoroterephthalonitrile (18 mg, 0.09 mmol) and dry DMF (40 ml). This mixture was heated to 65 °C, until complete dissolution of the two starting materials, then dry K_2CO_3 (76 mg, 1.36 mmol) was added and the mixture kept stirring for 15 hrs. The solution was quenched with water (100 ml). The product was then extracted with DCM (3 x 20 ml) and the organic phases combined, and the solvent removed under vacuum. The crude product was first columned with a hexane : ethyl acetate (8 : 2) solvent eluent and the spots which moved collected and solvent removed again under vacuum. The crude solid was again columned, this time using a more polar mix of hexane : ethyl acetate eluent, (6 : 4). The top spot was collected, solvent removed and the solid dried in a vacuum oven to remove any traces of solvent, to give a yellow powder . (654 mg, 14 %). M.p > 350 °C; IR (nujol)cm^{-1} 2340.4, 1273.4, 1236.7, 1134.5, 1023.8, 901.4, 711.3, 701.9 683.1; ^1H NMR (400 MHz; $CDCl_3$) δ 6.57 (br m, 40H, H_{Ar}), 6.40 (br m, 12H, H_{Ar}); LRMS, *m/z*, (ES^+) 1476 ($M+K^+$, 100%). BET surface area = 162 m^2/g; total pore volume = 0.28 cm^3/g at (P/P_0) 0.98, adsorption, (nitrogen).

3.2.38. 1,3-Dimethoxy-5-(phenylethynyl)benzene 63

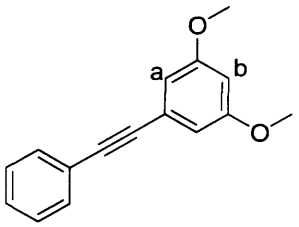

A mixture of 1-bromo-3,5-dimethoxybenzene (1.00 g, 4.20 mmol), Et_3N (4 ml) and DMF (4 ml) were deoxygenated in a round bottom flask under a nitrogen atmosphere. Phenylacetylene (0.32 g, 4.62 mmol) was added and the reaction heated to 90 °C to which CuI (80.0 mg, 0.42 mmol) and $[P(Ph)_3]_2PdCl_2$ (295 mg, 0.42 mmol) were added and the reaction left for 15 hrs. The reaction was then quenched with water (40 ml) and allowed to stir for 1hr. The product was then extracted using DCM (3 x 30ml), the organic layers were combined washed with water (3 x 20 ml) and dried with $MgSO_4$. The solvent was removed under reduced pressure and purification by column chromatography gave the desired product as a light brown oil (1.25 g , 62%); IR(nujol)cm^{-1} 15728.3, 1571.3, 1569.3, 1532.2, 1423.1, 1422.9, 1421.1, 1418.6, 1345.5 ^1H NMR (400 MHz, $CDCl_3$) δ 7.60 (m, 2H, H_{Ar}) 7.39 (m, 3H, H_{Ar}), 6.72 (d, 2H, J = 2.3 H_a), 6.52 (t, 1H, J = 2.3 H_b), 3.82 (s, 6H, OMe); ^{13}C NMR (100 MHz, $CDCl_3$) δ 165.2, 141.9, 132.1, 129.1, 119.2, 118.7, 106.1, 99.8, 93.7, 83.4, 53.8; LRMS, *m/z*, ($APCl^+$) 239 (M^+, 100%).

3.2.39. 1-(3,5-Dimethoxyphenyl)-2,3,4,5,6-pentaphenylbenzene 60

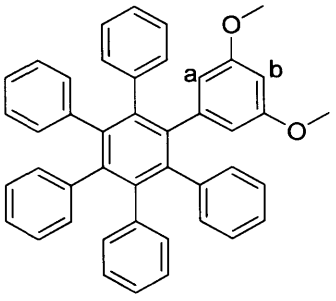

In a round bottom flask 2,3,4,5-tetraphenylcyclopenta-2,4-dienone (2.00 g, 5.21 mmol) and 1,3-dimethoxy-5-(phenylethynyl)benzene **62** (1.48 g, 6.24 mmol) were stirred in Ph_2O (8 ml) and refluxed for 15 hrs. The reaction was then allowed to cool and poured into cold MeOH.

Hexane (50 ml) was added to dissolve up most of the Ph_2O. This was then filtered and purified by column chromatography (hexane : ethyl acetate, 7 : 3) to give a light orange powder of the desired product (2.41 g , 78%). M.p. 224 – 226 °C (lit m.p.[109] 223 – 224 °C); IR (film)cm^{-1} 3012.7, 2878.1, 2873.5 2742.3, 2378.2, 1545.1, 1476.8, 1411.1, 1185.1, 1012.1, 796.9, 745.1; ^1H NMR (400 MHz, $CDCl_3$) δ 6.85 (m, 25H, H_{Ar}), 6.00 (d, 2H, J = 2.3 Hz, H_a), 5.96 (t, 1H, J = 2.3 Hz, H_b), 3.40 (s, 6H, OMe); ^{13}C NMR (100 MHz, $CDCl_3$) δ 160.3, 148.4, 142.5, 141.2, 141.24, 140.9, 139.1, 137.6, 136.7, 134.8, 133.1, 131.7, 128.4, 126.9, 127.1, 124.9, 124.5, 123.6, 112.7, 101.8, 55.7; LRMS, *m/z*, (EI^+) 594 (M, 100%)

References

[1] McKeown, N. B. *Phthalocyanine Materials: Structure, Synthesis and Function*, 1998

[2] Gregory, P. *J. Porphyrins Phthalocyanines* **2000**, *4*, 432.

[3] Cronshaw, C. T. J. *Endeavour* **1942**, *1*, 79.

[4] Dandridge, A. G.; Drescher, H. A. E.; Thomas, J.; (Scottish Dyes, Ltd.). GB, 1928.

[5] Braun, A.; Tscherniac, J. *Ber. Dtsch. Chem. Ges.* **1907**, *40*, 2709.

[6] de Diesbach, H.; von der Weid, E. *Helv. Chim. Acta* **1927**, *10*, 886.

[7] Linstead, R. P. *J. Chem. Soc.* **1934**, 1016.

[8] Byrne, G. T.; Linstead, R. P.; Lowe, A. R. *J. Chem. Soc.* **1934**, 1017.

[9] Linstead, R. P.; Lowe, A. R. *J. Chem. Soc.* **1934**, 1022.

[10] Dent, C. E.; Linstead, R. P. *J. Chem. Soc.* **1934**, 1027.

[11] Linstead, R. P.; Lowe, A. R. *J. Chem. Soc.* **1934**, 1031.

[12] Dent, C. E.; Linstead, R. P.; Lowe, A. R. *J. Chem. Soc.* **1934**, 1033.

[13] Robertson, J. M. *J. Chem. Soc.* **1936**, 1195.

[14] McKeown, N. B. *Porphyrin Handb.* **2003**, *15*, 61.

[15] Hanack, M.; Heckmann, H.; Polley, R. *Methods of Organic Chemistry* fourth ed.; Georg Thieme Verlag: Stuttgart, 1998; Vol. E-9

[16] Guerek, A. G.; Bekaroglu, O. *J. Chem. Soc., Dalton Trans.* **1994**, 1419.

[17] Woehrle, D.; Eskes, M.; Shigehara, K.; Yamada, A. *Synthesis* **1993**, 194-.

[18] McKeown, N. B.; Chambrier, I.; Cook, M. J. *J. Chem. Soc., Perkin Trans* **1990**, *1*, 1169.

[19] de la Torre, G.; Claessens, C. G.; Torres, T. *Chem. Commun.* **2007**, 2000.

[20] Shaabani, A. *J. Chem. Res., Synop.* **1998**, 672.

[21] Kempa, A.; Dobrowolski, J. *Can. J. Chem.* **1988**, *66*, 2553.

[22] Leznoff, C. C.; Lever, A. B. P.; Editors *Phthalocyanines: Properties and Applications*, 1989.

[23] Law, K. Y. *Chem. Rev.* **1993**, *93*, 449

[24] Wang, J.; Wang, H.; Yan, X.; Huang, H.; Jin, D.; Shi, J.; Tang, Y.; Yan, D. *Adv. Funct. Mater.* **2006**, *16*, 824.

[25] Rosenthal, I. *Photochem Photobiol* **1991**, *53*, 859.

[26] Robert, A.; Benoit-Vical, F.; Meunier, B. *Coord. Chem. Rev.* **2005**, *249*,1927.

[27] Leznoff, C. C.; Greenberg, S.; Marcuccio, S. M.; Minor, P.C.; Seymour, P.; Lever, A. B. P.; Tomer. K. B.; *Inorg Chim Acta* **1984**, *89*, L35.

[28] Kobayashi, N.; Lam, H.; Nevin, W. A.; Janda, P.; Leznoff, C.C.; Lever, A. B. P.; *Inorg. Chem.* **1990**, *29*, 3416

[29] Cook, M. J.; Heeney, M. J.; *Chem. Eur. J.* **2000**, *6*, 3958.

[30] Dodsworth, E. S.; Lever, A. B. P.; Seymour, P.: Leznoff, C. C. *J. Phys. Chem.* **1985**, *89*, 5698

[31] Wohrle, D.; Eskes, M.; Shigehara, K.; Yamada, A.; *Synthesis.* **1993**, 194.

[32] Muller, S.; Mullen, K. *Philos. Trans. R. Soc. A-Math. Phys. Eng. Sci.* **2007**, *365*, 1453

[33] Zhao, X. S. *J. Mater. Chem.* **2006**, *16*, 623

[34] Sing, K. S. W.; Everett, D. H.; Haul, R. A. W.; Moscou, L.; Pierotti, R. A.; Rouquerol, J.; Siemieniewska, T. *Pure Appl. Chem.* **1985**, *57*, 603.

[35] Kuznicki, S. M.; B3ell, V. A.; Nair, S.; Hillhouse, H. W.; Jacubinas, R. M.; Braunbarth, C. M.; Toby, B. H.; Tsapatsis, M. *Nature* **2001**, *412*, 720.

[36] Wang, D.; Teo, W. K.; Li, K. *Sep. Purif. Technol.* **2004**, *35*, 125.

[37] Barton, T. J.; Bull, L. M.; Klemperer, W. G.; Loy, D. A.; McEnaney, B.; Misono, M.; Monson, P. A.; Pez, G.; Scherer, G. W.; Vartuli, J. C.; Yaghi, O. M. *Chem. Mater.* **1999**, *11*, 263.

[38] Braunbarth, C.; Hillhouse, H. W.; Nair, S.; Tsapatsis, M.; Burton, A.; Lobo, R. F.; Jacubinas, R. M.; Kuznicki, S. M. *Chem. Mater.* **2000**, *12*, 1857.

[39] Brunauer, S.; Emmett, P. H.; Teller, E. *J. Am. Chem. Soc.* **1938**, *60*, 309-19.

[40] Campos, V.; Buchler, P. M. *Environ. Geol.* **2007**, *52*, 1187.

[41] Sekhon, B. S.; Sangha, M. K. *Resonance* **2004**, *9*, 35.

[42] Hernandez-Maldonado, A. J.; Yang, R. T. *Angew. Chem., Int. Ed.* **2004**, *43*, 2321.

[43] Usui, K.; Kidena, K.; Murata, S.; Nomura, M.; Trisunaryanti, W. *Fuel* **2004**, *83*, 1899.

[44] Tchernev, D. I. *Rev. Mineral. Geochem.* **2001**, *45*, 589.

[45] Tomita, T.; Nakayama, K.; Sakai, H. *Micropor. Mesopor. Mater.* **2004**, *68*, 71.

[46] Areerachakul, N.; Vigneswaran, S.; Ngo, H. H.; Kandasamy, J. *Sep. Purif. Technol.* **2007**, *55*, 206-11.

[47] Cheremisinoff, P. N.; Morresi, A. C. *Carbon Adsorption Handb.* **1978**, 1-53.

[48] Patrick, J. W.; Walker, A. *Porosity Carbons.* **1995**, 195.

[49] Lennon, D.; Lundie, D. T.; Jackson, S. D.; Kelly, G. J.; Parker, S. F. *Langmuir* **2002**, *18*, 4667.

[50] Ferey, G. *Chem. Soc. Rev.* **2008**, *37*, 191.

[51] Wong-Foy, A.G.; Matzger, A. J.; Yaghi, O. M. *J. Am. Chem. Soc.* 2006, *128*, 3494.

[52] El-Kaderi, H. M.; Hunt, J. R.; Mendoza-Cortes, J. L.; Cote, A. P.; Taylor, R. E. O'Keeffe, M.; Yaghi, O. M.. *Science.* **2007**, 316, 268.

[53] Eddaoudi, M. *et al.*, *Accounts of Chemical Research.* **2001**, *34*, 319.

[54] Tozawa, T. *et al. Nat Mater.* **2009**, *8*, 973.

[55] Msayib, K. *et al.*, *Angew. Chem.* **2009,** *121*, 3323.

[56] Tozawa, T.; Jones, J. T. A.; Swamy, S. I.; Jiang, S.; Adams, D. J.; Shakespeare, S.; Clowes, R.; Bradshaw, D.; Hasell, T.; Chong, S. Y.; Tang, C.; Thompson, S.; Parker, J.; Trewin, A.; Bacsa, J.; Slawin, A. M. Z.; Steiner, A.; Cooper, A. I. *Nature Mater.* **2009**, *8*, 973.

[57] Bezzu, C. G.; Warren, J. E.; Helliwell, M.; Allan, D. R.; McKeown, N. B. *Science.* **2010**, *327*, 1627.

[58] McKeown, N. B.; Budd, P. M. *Macromolecules.* **2010**, *43*, 5163.

[59] McKeown, N. B.; Budd, P. M.; Msayib, K. J.; Ghanem, B. S.; Kingston, H. J.; Tattershall, C. E.; Makhseed, S.; Reynolds, K. J.; Fritsch, D. *Chem.-Eur. J.* **2005**, *11*, 2610.

[60] McKeown, N. B. *J. Mater. Chem.* **2000**, *10*, 1979.

[61] McKeown, N. B.; Makhseed, S.; Budd, P. M. *Chem. Commun.* **2002**, 2780.

[62] Budd, P. M.; Elabas, E. S.; Ghanem, B. S.; Makhseed, S.; McKeown, N. B.; Msayib, K. J.; Tattershall, C. E.; Wang, D. *Adv. Mater.* **2004**, *16*, 456-59.

[63] Kestemont, G.; de Halleux, V.; Lehmann, M.; Ivanov, D. A.; Watson, M.; Geerts, Y. H. *Chem. Commun.* **2001**, 2074-75.

[64] Budd, P. M.; Ghanem, B.; Msayib, K.; McKeown, N. B.; Tattershall, C. *J. Mater. Chem.* **2003**, *13*, 2721-26.

[65] McKeown, N. B.; Gahnem, B.; Msayib, K. J.; Budd, P. M.; Tattershall, C. E.; Mahmood, K.; Tan, S.; Book, D.; Langmi, H. W.; Walton, A. *Angew. Chem., Int. Ed.* **2006**, *45*, 1804-07.

[66] Lindsey, A. S. *J. Chem. Soc.* **1965**, 1685-92.

[67] Mckeown, N. B.; *J. Mater. Chem.* **2000**, 10, 1979.

[69] Cordes, A. W.; Fair, C. K. *Acta Crystallogr., Sect. B* **1974**, *30, Pt. 6*, 1621-3.

[70] Horvath, G.; Kawazoe, K. *J. Chem. Eng. Jpn.* **1983**, *16*, 470-5.

[71] Baker, W.; McGowan, J. C. *J. Chem. Soc.* **1943**, 486-7.

[72] Jacob, P., III; Callery, P. S.; Shulgin, A. T.; Castagnoli, N., Jr. *J. Org. Chem.* **1976**, *41*, 3627-9.

[73]Ghanem, B. S.; Msayib, K. J.; McKeown, N. B.; Harris, K. D. M.; Pan, Z.; Budd, P. M.; Butler, A.; Selbie, J.; , Book, D.; Walton, A. *Chem. Commun.*, **2007**, 67.

[74] Robeson, L. M. *J. Membr. Sci.* **1991**, *62*, 165.

[75] Robeson, L. M. *J. Membr. Sci.* **2008**, *320*, 390.

[76] T. Masuda, *J. Polym. Sci., Part A: Polym. Chem.*, 2006, **45**, 165.

[77] J. Jia and G. L. Baker, *J. Polym. Sci., Part B: Polym. Phys.*, 1998, **36**, 959.

[78] Budd, P. M.; McKeown, N. B.; Ghanem, B. S.; Msayib, K. J.; Fritsch, D.; Starannikova, L.; Belov, N.; Sanfirova, O.; Yampol'skii, Y. P.; Shantarovich, V. *J. Membrane Sci.* **2008**, *325*, 851

[79] Budd, P. M.; Msayib, K. J.; Tattershall, C. E.; Ghanem, B. S.; Reynolds, K. J.; McKeown, N. B.; Fritsch, D. *J. Membrane Sci.* **2005**, *251*, 263.

[80] Muller, S.; Mullen, K. *Philos. Trans. R. Soc. A-Math. Phys. Eng. Sci.* **2007**, *365*, 1453.

[81] Maly, K. E.; Gagnon, E.; Maris, T.; Wuest, J. D. *J. Am. Chem. Soc.* **2007**, *129*, 4306.

[82] Gagnon, E.; Halperin, S. D.; Metivaud, V.; Maly, K. E.; Wuest, J. D. *J. Org. Chem.* **2010**, *75*, 399.

[83] Gagnon, E.; Maris, T.; Arseneault, P. M.; Maly, K. E.; Wuest, J. D. *Cryst. Growth Des.* **2010**, *10*, 648.

[84] Jimenez-Garcia, L.; Kaltbeitzel, A.; Pisula, W.; Gutmann, J. S.; Klapper, M.; Mullen, K. *Angewandte Chemie-International Edition* **2009**, *48*, 9951.

[85] Matsumura, S.; Hlil, A. R.; Al-Souz, M. A. K.; Gaudet, J.; Guay, D.; Hay, A. S. *Journal of Polymer Science Part a-Polymer Chemistry* **2009**, *47*, 5461.

[86] Li, Z. A.; Ye, S. H.; Liu, Y. Q.; Yu, G.; Wu, W. B.; Qin, J. G.; Li, Z. *J. Phys. Chem. B* **2010**, *114*, 9101.

[87] Vickery, E. H.; Pahler, L. F.; Eisenbraun, E. J. *J. Org. Chem.* **1979**, *44*, 4444.

[88] Fang, Z.; Song, Y.; Sarkar, T.; Hamel, E; Fogler, W. E.; Agoston, G. E.; Fanwick, P. E.; Cushman, M. *J. Org. Chem.* **2008**, *73*, 4241.

[89] Sengul, A.; Arslan, H.; Bayari , S. H.; Buyukgungor, O. *Struct Chem.* **2008**, *19*, 467.

[90] Mohr, B.; Enkelmann, V.; Wegner. E.; *J. Org. Chem.* **1994**, *59*, 635

[91] Budd, P. M.; Msayib, K. J.; Tattershall, C. E.; Ghanem, B. S.; Reynolds, K. J.; McKeown, N. B.; Fritsch, D. *J. Membrane Sci.* **2005**, *251*, 263.

[92] McKeown. N.B. *Adv. Mater.*, **2004**, *16*, 456.

[93] Gagnon, E.; Halperin, S. D.; Metivaud, V.; Maly, K. E.; Wuest, J. D. *J. Org. Chem.* **2010**, *75*, 399.

[94] Gagnon, E.; Maris, T.; Arseneault, P. M.; Maly, K. E.; Wuest, J. D. *Cryst. Growth Des.* **2010**, *10*, 648.

[95] Maly, K. E.; Gagnon, E.; Maris, T.; Wuest, J. D. *J. Am. Chem. Soc.* **2007**, *129*, 4306

[96] Kobayashi, K.; Kobayashi, N.; Ikuta, M.; Therrien, B.; Sakamoto, S.; Yamaguchi, K. *J. Org. Chem.* **2005**, *70*, 749.

[97] Kobayashi, K.; Shirasaka, T.; Sato, A.; Horn, E.; Furukawa, N. *Angewandte Chemie-International Edition* **1999**, *38*, 3483.

[98] Bjork, J. A.; Brostrom, M. L.; Whitcomb, D. R. *J. Chem. Crystallogr.* **1997**, *27*, 223.

[99] Msayib, K.; Makhseed, S.; McKeown, N. B. *J. Mater. Chem.* **2001**, *11*, 2784.

[100] Mcguffin, V.L. *anal chimica acta.* **2008**, *610* 57.

[101] Germain, M. E. *Chem. Soc. Rev.* **2009**, *38*, 2543.

[102] Bonnichon, F. *J. of Photochem. and Photobiol. A: Chem.* **1998**, *119*, 25.

[103] Lakowicz, J. R. *Principles of Fluorescence Spectroscopy, Third Edition, Plenum Press, New York.* **2006.**

[104] Altman, R. A.; Buchwald, S. L. *Nature Protocols*, **2007**, *2*, 3115.

[105] Billingsley, K. L.; Anderson, K. W.; Buchwald, S. L. *Angew. Chem., Intl. Edn.* **2006**, *45*, 3484.

[106] Walker, S .D.; Barder, T. E.; Martinelli, J. R.; Buchwald, S. L. *Angew. Chem., Intl. Edn.*, **2004**, *43*, 1871.

[107] Faroog, M. O.; Rahman, W.; Ilyas, M. *Chem. Ber.* **1959**, *92*, 2555.

[108] Keshtov, M.; Petrovskii, P.; Stakhanov, A.; Kochurov, A.; Khokhlov, A. *Doklady Chem.* **2009**, *429*, 277.

[109] Gagon, E.; Rochefort, A.; Metivaud, V.; Wuest, J. *Org lett.* **2010**, *12*, 380.